THE REGULATORY ROLE OF MATRIX METALLOPROTEINASES IN T CELL ACTIVATION

Heather Lynette Benson

Submitted to the faculty of the University Graduate School
in partial fulfillment of the requirements
for the degree
Doctor of Philosophy
in the Department of Biochemistry and Molecular Biology
Indiana University

October 2009

Accepted by the Faculty of Indiana University, in partial
fulfillment of the requirements for the degree of Doctor of Philosophy.

_____

David S. Wilkes, M.D., Chair

_____

Janice S. Blum, Ph.D.

Doctoral Committee

_____

Mark G. Goebl, Ph.D.

July 28, 2009

_____

Maureen A. Harrington, Ph.D.

_____

Gerald N. Smith, Ph.D.

DEDICATION

This thesis is dedicated to my husband, Eric “Bunny-bear” Benson, for his love, support and encouragement during the pursuit of my Ph.D. and continually throughout our marriage. I’m an orange moon and I shine so bright cause I reflect the light of my sun.; and to my wonderful parents, Robin and Stan Rayford, for giving me life, always believing in me and imparting strength and wisdom from which I draw from daily. Thank you for getting me off to a great start so that I can fly beautifully, just like Jemima Puddle-Duck.

ACKNOWLEDGEMENTS

I would like to thank “my P.I.” and mentor, Dr. David Wilkes, for his unique ability to always bring out the best in me. Dr. Wilkes, thank you for pushing me to think critically and outside the box, for believing in my abilities, for entertaining my ideas and giving me freedom to explore, for writing grants to fund my projects, for the knowledge that you have imparted and for really investing in me. Thank you for teaching me how to be a scientist.

I would also like to thank the other members of my “All-star Dream Team” research committee: Dr. Janice Blum, Dr. Mark Goebl, Dr. Maureen Harrington and Dr. Gerald Smith. Thank you all for your time, energy, patience, advice, guidance and support. I would not have been able to complete this dissertation project without you. Additionally, I would like to thank Dr. Matthias Clauss and Dr. Alexander Obukhov for lending their advice and expertise in calcium signaling to support the progress of my project.

To the Wilkes lab, thanks for helping out when needed and for always making sure we have fun no matter how hard we’re working. Jeremy “J-Lott” Lott, thanks for being a great friend, lab-mate and lunch-buddy; it’s been fun. Elizabeth “Liz” Mickler, thanks for being a great friend, for always being willing to go everywhere, whether it’s to the gym, riding bikes or just out for a good time. Dr. Ann Kimble-Hill, thanks for being my BFF and for always being willing to talk science. To all of my other school/science friends, you know who you are; thanks for always being willing to sit through my

practice talks, for talking through experiments and other great science with me and for always being supportive.

I thank Dr. Bruce Uhal and Dr. William Martin for sparking my interest in lung research as an undergraduate, allowing me to explore different areas of lung research and for serving as excellent mentors. I am grateful to my life-long mentor Sis. Marion Jeffers, for always being there for me, helping me develop into a great student and for believing in me.

Mom and Dad, thank you for giving me all of the tools I need to be a successful contributor to society. You've taught me to be steadfast, unmovable, always abounding in the work of the Lord. I love you very much! To my husband, "Two are better than one, because they have a good reward for their labor. Two working together to fulfill their divine destiny in the Lord can be a powerful team" Ecclesiastes 4:9. Thank you for being my teammate, I look forward to fulfilling our divine destiny together. Throughout this process, I have come into a deeper understanding that I can do all things through Christ who strengthens me. Thank you God for your divine favor and for all that you've allowed me to accomplish in my life.

ABSTRACT

Heather Lynette Benson

THE REGULATORY ROLE OF MATRIX METALLOPROTENASES IN T CELL ACTIVATION

Introduction: Matrix metalloproteinases (MMPs) are known for their role in extracellular matrix remodeling, but their role in regulating intracellular immune cell function is unknown. We reported that MMP inhibition down regulated T cell proliferation in response to alloantigens and autoantigens; but the direct role of MMP involvement in T cell activation has not been reported.

Methods: MMP deficient or MMP sufficient wild-type $CD4^+$ or $CD8^+$ T cells from C57BL/6 mice were treated with SB-3CT, a specific inhibitor of MMP2 and MMP9, stimulated with anti-CD3 Ab, alone, or with IL-2 or CD28. Cellular activation and cytokine profiles were examined. A mouse model of antigen specific T cell mediated lung injury was used to examine MMP inhibition in antigen-specific T cell mediated lung injury.

Results: SB-3CT (1-25μM) induced dose-dependent reductions in anti-CD3 Ab-induced proliferation ($p<0.0001$). Compared to wild-type, MMP9-/- $CD4^+$ and $CD8^+$ T cells proliferated 80-85% less ($p<0.001$) in response to anti-CD3 Ab. Compared to untreated or wild-type cells, anti-CD3 Ab-induced calcium flux was enhanced in SB-3CT-treated or MMP9-/- $CD4^+$ and $CD8^+$ T cells. Cytokine transcripts for IL-2, TNF-α and IFN-γ

were reduced in both $CD4^+$ and $CD8^+$ MMP9-/- T cells, as well as in SB3CT treated $CD4^+$ T cells. MMP inhibition dampened antigen-specific T cell mediated lung injury.

Conclusions: Although known to be functional extracellularly, the current data suggest that MMPs function inside the cell to regulate intracellular signaling events involved in T cell activation. T cell targeted MMP inhibition may provide a novel approach of immune regulation in the treatment of T cell-mediated diseases.

David S. Wilkes, M.D., Chair

TABLE OF CONTENTS

LIST OF TABLES

LIST OF FIGURES

ABBREVIATIONS

ARRE	Antigen receptor response element
ADAP	Adhesion- and degranulation promoting protein
AP-1	Activator protein 1
APCs	Antigen presenting cells
BAL	Bronchoalveolar lavage
BM	Basement membrane
CD3	Cluster of differentiation 3 molecule
CD4	Cluster of differentiation 4
CD8	Cluster of differentiation 8
CD25	Cluster of differentiation 25
CD28	Cluster of differentiation 28
CD40	Cluster of differentiation 40
CD40L	Cluster of differentiation 40 ligand
CD44	Cluster of differentiation 44

CD62L	Cluster of differentiation 62 L-selectin
CD69	Cluster of differentiation 69
CD80	Cluster of differentiation 80
CD86	Cluster of differentiation 86
cDNA	complementary deoxyribonucleic acid
CC10	Clara cell secretory protein
CF	Cystic fibrosis
COL-3	Chemically modified tetracycline 3
COPD	Chronic obstructive pulmonary disease
CRAC	Calcium released activated calcium
CTL	Cytotoxic T cells
CTLA-4	Cytotoxic T lymphocyte antigen 4
DAG	1, 2, diacylglycerol
DCs	Dendritic cells
ECM	Extracellular matrix

ER	Endoplasmic reticulum
ERK	Extracellular-regulated mitogen activated protein kinase
FOXP3	Forkhead box protein 3
GATA3	GATA binding protein 3
GADs	GRB2-related adaptor protein downstream of Shc
GRB2	Growth factor receptor-bound protein 2
IL-2	Interleukin-2
IL-2Rα	Interleukin-2 receptor alpha
IL-4	Interleukin-4
IL-5	Interleukin-5
IL-6	Interleukin-6
IL-8	Interleukin-8
IL-10	Interleukin-10
IL-1β	Interleukin-1 beta
IL-12	Interleukin-12
IL-13	Interleukin-13

IL-21	Interleukin-21
IL-22	Interleukin-22
IL-23	Interleukin-23
IFN-γ	Interferon gamma
ITK	IL-2 inducible T cell kinase
IP3	Inositol 1, 4, 5 triphosphate
IPF	Idiopathic pulmonary fibrosis
ITAM	Immunoreceptor tyrosine-based activation motifs
KC	IL-8
LAT	Linker for activation of T cells
LCK	Leukocyte-specific protein tyrosine kinase
MAPK	Ras-mitogen activated protein kinase
MCP3	Monocyte chemotactic protein 3
MEK1	Mitogen activated protein kinase-extracellular signal regulated kinase kinase 1
MHC	Major Histocompatability Complex

MMP	Matrix metalloproteinase
MMPI	Matrix metalloproteinase inhibitor
mRNA	Messenger ribonucleic acid
NCK	Non-catalytic region of tyrosine kinase adaptor protein
NE	Neutrophil elastase
NFAT	Nuclear factor of activated T cells
OAD	Obstructive airway disease
OB	Obliterative bronchiolitis
OVA	Ovalbumin
PI3K	Phosphatidylinositol-3 kinase
PIP2	Phosphatidylinositol-4,5,-bisphosphate
PKC	Protein kinase C
PLCγ1	Phospholipase C gamma 1
PTK	Protein tyrosine kinase
RAG	Recombinase activating gene
RORγt	RAR-related orphan receptor gamma t

RT-PCR Quantitative reverse transcription polymerase chain reaction

SCID Sever combined immunodeficiency

SH2 Src homology 2 domain

SHC Src homology 2 domain-containing

SLP-76 Src homology 2 domain containing leukocyte phosphoprotein of 76 kDa

SOCE Store-operated calcium entry

STAT-4 Signal transducer and activator of transcription 4

STAT-6 Signal transducer and activator of transcription 6

T-bet T-box expressed in T cells

TCR T cell receptor

Thy1.1 Thymus cell antigen 1, theta

Thy1.2 Thymus cell antigen 2, theta

TIMP Tissue inhibitor of matrix metalloproteinases

TGF-β Transforming Growth Factor beta

Th1 T helper 1

Th2	T helper 2
Th17	T helper 17
TNF-α	Tumor necrosis factor alpha
Treg	Regulatory T cells
VAV1	Vav 1 guanine nucleotide exchange factor
ZAP-70	zeta chain associated protein kinase 70

I. INTRODUCTION

A. The immune response

The immune response consists of a concerted action of both innate and adaptive immunity that serve to protect the body from infection, disease and foreign antigens. The innate immune system is comprised of a variety of cells and processes that serve in a non-specific manner as the body's first line of defense against invading pathogens. The innate system does not confer long-lasting or protective immunity, therefore the immune system is able to adapt accordingly and activate a second response known as adaptive immunity. It is through the adaptive immune response that the immune system gains the ability to recognize a specific pathogen, and to mount an even stronger attack each time the pathogen is encountered. The basis of adaptive immunity lies in its ability to distinguish between the body's own cells, and those that are foreign. In the adaptive immune system B cells and T cells ($CD4^+$ and $CD8^+$) are the major cell types present. B cells are involved in the humoral immune response, whereas T-cells are involved in cell-mediated immune responses. Cell-mediated immunity involves direct interactions between T cells and antigen presenting cells (APC) that can present antigens that the T cells recognize. $CD8^+$ T cells, also known as cytotoxic T cells (CTLs), are activated when their T-cell receptor (TCR) strongly interacts with a peptide-bound MHC class I molecule. Since all nucleated cells express MHC class I, CTLs have the ability to respond to any virally infected cell. Once activated, the CTL undergoes clonal expansion, in which it gains functionality and rapidly divides to produce an army of "armed" effector cells. When

exposed to these infected cells, effector CTLs release perforin which form pores in the infected cell's plasma membrane and granzyme B, a serine protease,' to cause cell lysis and death.

In contrast, $CD4^+$ T cells, also known as helper T cells, are immune response mediators that play an important role in establishing and maximizing the capabilities of the adaptive immune response. $CD4^+$ T cells express TCRs that recognize antigen bound class II MHC molecules on the cell surface antigen presenting cells (APCs). APCs, which include dendritic cells, tissue macrophages, and B cells, provide a key contact point for the generation of the appropriate adaptive immune response. Dendritic cells have potent antigen-processing capabilities, express abundant class II MHC molecules, and are present at sites that facilitate naïve T cell encounters. Recent studies have suggested that dendritic cells may be the primary, and perhaps exclusive, type of APC involved in presenting alloantigen peptides to naïve T cells (1). Once activated, the $CD4^+$ T cells undergo clonal expansion to produce T helper cells, which release cytokines that influence the activity of many cell types in the local environment.

Three types of helper $CD4^+$ T cell responses can be induced by APCs, designated Th1, Th2 and Th17 [figure 1] (2). The Th1 response is characterized by the production of interferon-gamma (IFN-γ) and interleukin 2 (IL-2). The Th2 response is characterized by the release of interleukin 4 (IL-4), IL-5, IL-6, IL-10 and IL-13. The recently identified Th17 response is characterized by the release of IL-17 (isoforms IL-17A and IL-17F), IL-21 and IL-22. Generally, Th1 responses are more effective against intracellular pathogens (viruses and bacteria that are inside the host cells), while Th2 responses are more

effective against extracellular pathogens (bacteria, parasites and toxins). Th17 cells play a role in play a key role in autoimmunity and cell-mediated tissue injury (2).

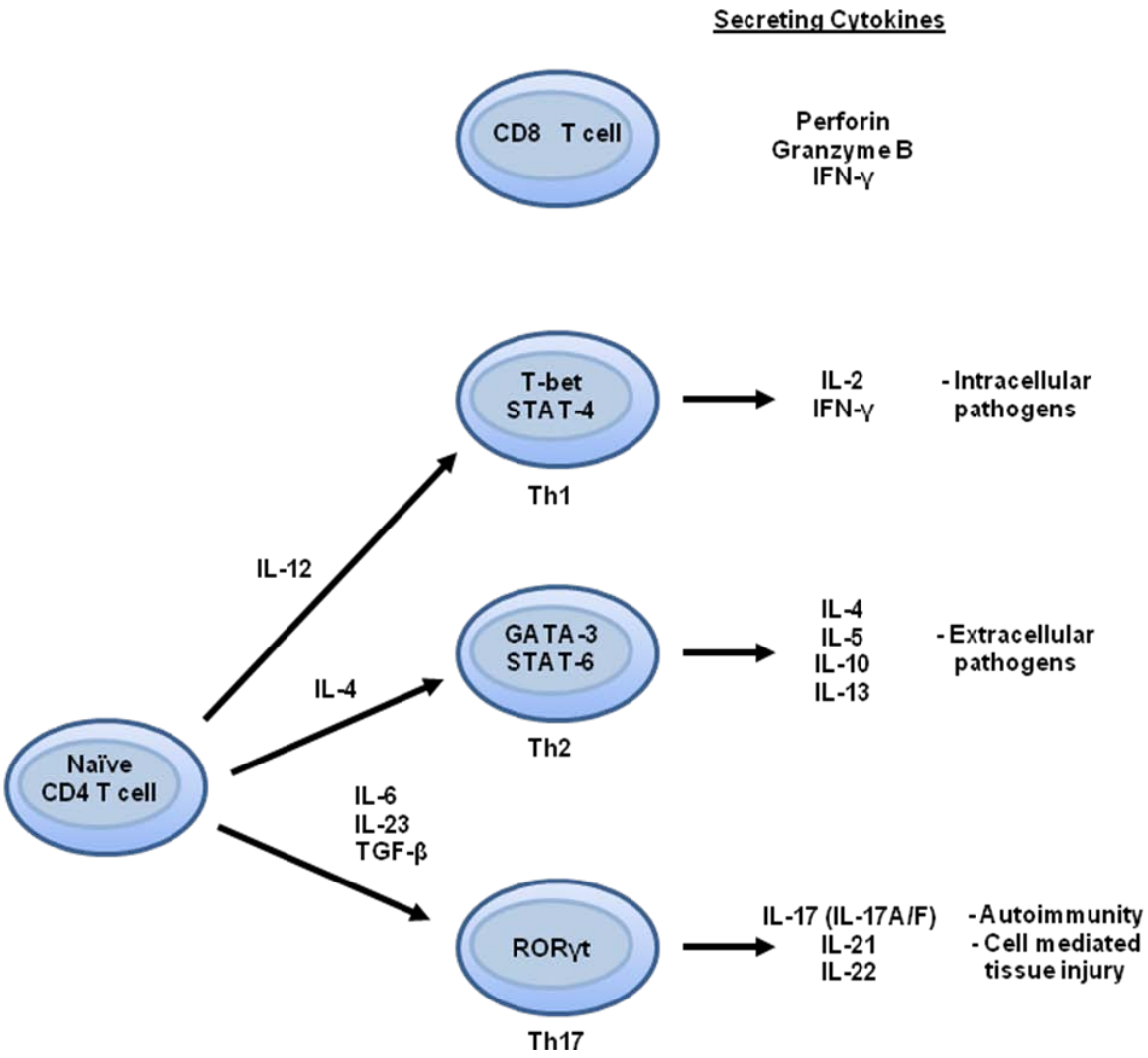

Figure 1. T cell subsets
General diagram of T cells involved in the adaptive immune response. Naïve T cells can differentiate into T cell subsets in response to the cytokine signals received.

B. T cell activation

Ligation of the T-cell antigen receptor (TCR) initiates a complex signaling cascade that involves three signals: 1) Recognition of the alloantigen peptide:MHC complex by the TCR on the T cell surface; 2) Interaction of co-stimulatory molecules (CD28 on T cells interacting with its ligands, CD80 and CD86, expressed on APCs (DCs); 3) Cytokine/chemokine production, leading to clonal expansion and differentiation. Activation of essential downstream signaling pathways, including the phosphatidylinositol-4,5-bisphosphate (PIP2), Ras-mitogen-activated protein kinase (MAPK), and phosphatidylinositol-3-kinase (PI3K) pathways, is dependent upon the activity of protein tyrosine kinases (3, 4).

The T cell receptor exists as a complex of several proteins. Structurally, the T cell receptor is composed of two separate peptide chains, the alpha and beta (TCRα and TCRβ) chains [figure 2]. The other proteins in the complex are the CD3 proteins, which consist of the CD3εγ and CD3εδ heterodimers and a CD3ζ homodimer, which has a total of six ITAM motifs (5). The earliest step in intracellular signaling following TCR ligation is the activation of Src family ($p56^{Lck}$ (Lck) and $p59^{Fyn}$ (Fyn) protein tyrosine kinases (PTKs), leading to phosphorylation of the CD3ζ ITAMs. Recruitment of zeta-chain-associated protein kinase 70 (ZAP-70) follows, leading to a cascade of phosphorylation events. To demonstrate the importance of Src PTKs, a study by Rapecki et al. reported that Src kinase inhibitors, which inhibit Lck and Fyn, attenuated anti-CD3 Ab-induced T cell proliferation and block interleukin (IL)-2, IL-4, and interferon-γ production, and IL-2Rα (CD25) expression in anti-CD3 Ab-activated T cells (6).

Among the most important of the ZAP-70 targets are the transmembrane adapterprotein linker for the activation of T cells (7) and the cytosolic adapter protein Src homology 2 (SH2) domain-containing leukocyte phosphoprotein of 76 kDa (SLP-76) (7, 8). These two adapters form the backbone of a complex that organizes effector molecules in the correct spatiotemporal manner to allow for the activation of multiple signaling pathways. The importance of these adapters is highlighted by studies showing that the loss of either LAT or SLP-76 results in a near complete loss of TCR signal transduction. Similar results were seen in Syk/ZAP-70 or Lck/Fyn double-deficient T cells (7, 9, 10).

LAT, which localizes to lipid rafts, contains nine tyrosines that are phosphorylated following TCR engagement, which bind the C-terminal SH2 domain of phospholipase C γ (PLCγ1), the p85 subunit of phosphoinositide 3-kinase (PI3K), and the adapters growth factor receptor-bound protein 2 (GRB2) and GRB2-related adapter downstream of Shc (Gads) (9). SLP-76 is then recruited to phosphorylated LAT via their mutual binding partner Gads (11). SLP-76 itself contains three modular domains: 1) an N-terminal acidic domain with three phosphorylatable tyrosines that interact with the SH2 domains of the adaptor proteins Vav1, Nck, and IL-2-induced tyrosine kinase (Itk); 2) a proline-rich region that binds constitutively Gads and PLCγ1; and 3) a C-terminal SH2 region that can bind adhesion and degranulation-promoting adapter protein (ADAP) and hematopoietic progenitor kinase 1 (HPK1) (7). Activated PLCγ1 and PI3K then hydrolyze the membrane lipid phosphatidylinositol 4,5-bisphosphate ($PI(4,5)P_2$) on the inner leaflet of the membrane producing the second messengers inositol-1,4,5 triphosphate (IP_3) and diacylglycerol (DAG). These two messengers are essential for T cell function.

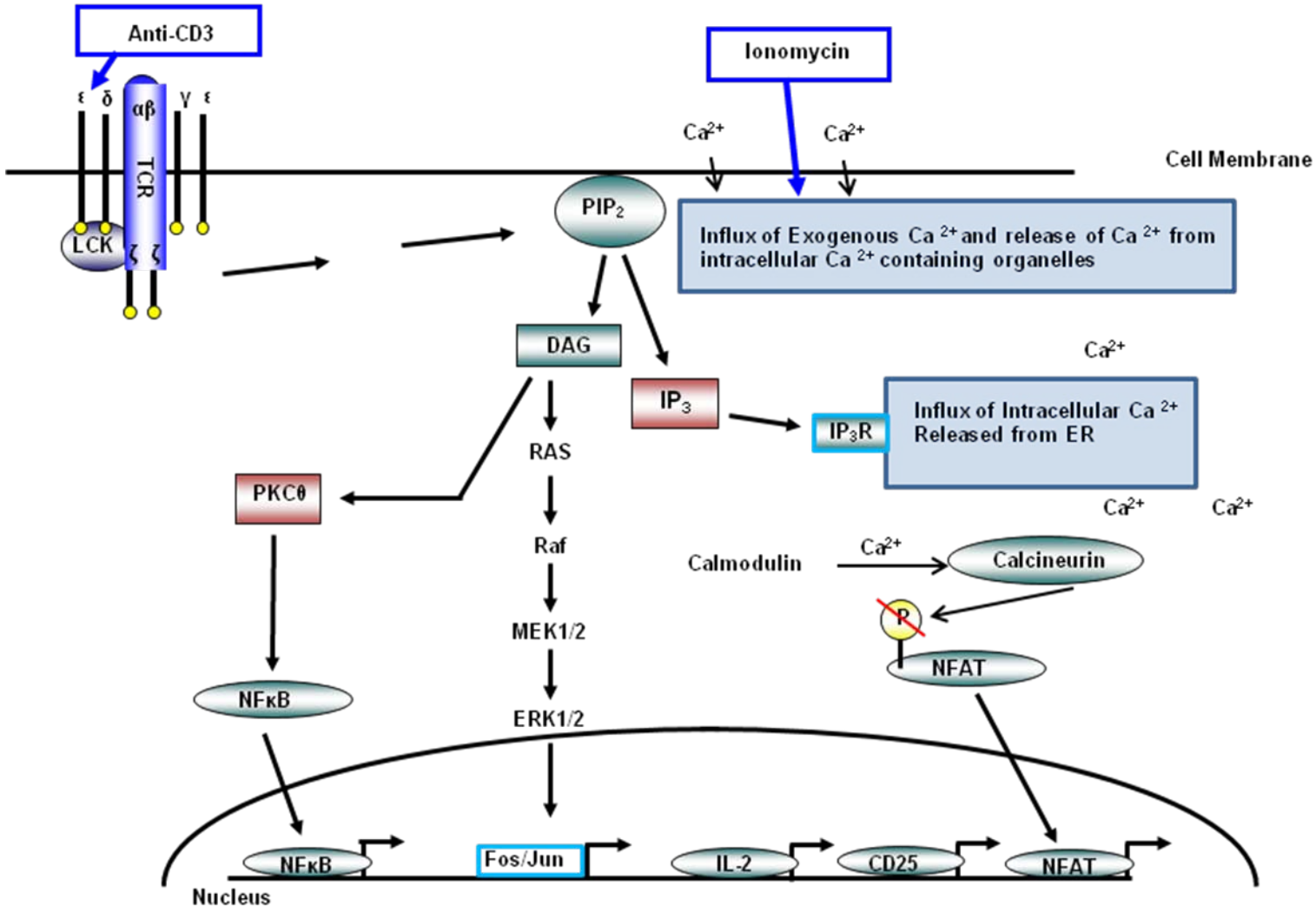

Figure 2. T cell signaling pathway Adapted from www.cellsignal.com

DAG results in the activation of two major pathways involving Ras and protein kinase C (PKCθ). Ras is a GTPase, or a guanine-nucleotide-hydrolase required for the activation of the serine-threonine kinase Raf-1. Raf-1 initiates mitogen-associated protein kinase (MAPK) phosphorylation and an activation cascade. Raf-1 is a MAPK kinase kinase (MAPKKK) that phosphorylates and activates MAPK kinases (MEK1/2), which in turn phosphorylate and activate the MAPK's extracellular signal-regulated kinase 1 (Erk1) and Erk2. Erk kinase activity results in the activation of the transcription factor Elk1, which contributes to the activation of the activator protein-1 (AP-1) (Jun/Fos) transcription complex (12). PKCθ, a member of the PKC family, contains a lipid-binding domain specific for DAG, which is important for recruiting PKCθ to the plasma membrane. PKCθ is involved in the activation of the transcription factor nuclear factor kappa-light-chain-enhancer of activated B cells (NF-κB).

In conjunction with DAG, IP3 is released from the membrane by PLCγ1 and diffuses rapidly to activate calcium permeable ion channel receptors (IP3Rs) on the endoplasmic reticulum (ER) membrane leading to the release of ER calcium (Ca2+) stores into the cytoplasm. Depletion of ER calcium triggers a sustained influx of exogenous calcium through the activation of plasma membrane calcium release-activated calcium (CRAC) channels in a process known as store-operated calcium entry (SOCE). This calcium influx activates the phosphatase, calcineurin (13). Activated calcineurin dephosphorylates members of the nuclear factor of activated T cells (NFAT) family, leading to their translocation to the nucleus. In the nucleus, NFAT isoforms (NFAT1-4) can form cooperative complexes with a variety of other transcription factors, thereby

integrating signaling pathways, resulting in differential gene expression patterns and functional outcomes, depending on the context of the TCR signal.

One of the most-well-studied interaction is, NFAT/AP-1, which integrates Ca^{2+} and Ras signals and results in the expression of genes important for T cell activation including the production of IL-2. In contrast, NFAT activity in the absence of AP-1 activation induces a pattern of gene expression that ultimately results in T cell anergy and a characteristic lack of IL-2 production (14). The regulatory T cell lineage–specific transcription factor forkhead box protein 3 (FOXP3) also cooperates with NFAT and antagonizes NFAT/AP-1 gene transcription, resulting in regulatory T cell (Treg) functional gene expression and a lack of IL-2 production (15). Finally, NFAT family members can also cooperate with signal transducers and activator of transcription (STAT) proteins to induce either Th1 or Th2 differentiation through expression of T box expressed in T cells (T-bet) or GATA binding protein 3 (GATA3), respectively (13) or Th17 differentiation through RORγt (16, 17).

It is important to note that although T cell activation is often discussed and diagramed as a linear pathway starting at the receptor and ending in the nucleus, there appears to be complex feedback and feed-forward regulation at each step. Many of the proteins interact closely and function as docking sites and adaptor proteins which exert their actions in sync. Following TCR ligation, there are many events that occur within the cell that are necessary for proper T cell function.

C. Matrix metalloproteinases

Matrix Metalloproteinases (MMPs) were first described by Jerome Gross and

Charles Lapiere in 1962, who observed enzymatic cleavage of collagen triple helix during tadpole tail metamorphosis. Since then the MMP family has grown to consist of over 25 secreted and cell surface zinc-dependent endopeptidases. The members within this family share structural similarities but differ in their substrate specificity and expression profiles. MMPs are responsible for the turnover of the extracellular matrix (ECM) and basement membranes (BMs). The ECM is a complex network composed of protein constituents including collagens and elastin, glycoproteins such as laminin, fibronectin, as well as various proteoglycans and glycosaminoglycans. Because they are tightly apposed and highly cross-linked triple helical fibrils, collagens I, II, and III are known to be extremely resistant to cleavage by most proteinases. Collagenases (MMP-1, -8, -13) cleave fibrillar collagens at unique sites in the triple helix near the N-terminal end, generating collagen fragments. Due to thermal degradation and loss of stability, these collagen fragments unfold their triple helix and fall apart into fragmented single α-chains, the so-called gelatins (MMP2 and MMP9 substrates) (18). They all initially cleave at a specific Gly-Leu/Ile bond to generate characteristic 1/4 and 3/4 fragments that are then degraded further by the collagenase itself as well as by gelatinolytic enzymes, such as gelatinases A and B (MMP2 and MMP9, respectively), neutrophil elastase (NE) and plasmin.

The ECM is not only a mechanical support for cells, but also acts as a reservoir for cytokines and growth factors. The integrity of the ECM is controlled by a dynamic equilibrium between synthesis and local degradation of its different components. MMPs are the main physiological mediators of ECM degradation. MMPs have a broad range of substrate specificity and participate in a plethora of biological processes, such as cellular

proliferation, embryonic development, morphogenesis, bone remodeling, angiogenesis, wound healing and inflammation.

D. Matrix metalloproteinase structure

MMPs are classified by their conserved protein domains: a pro-domain, and a catalytic domain, which contains a Zn^{2+} binding domain [figure 3]. All MMPs, with the exception of MMP-7 and -26, contain an additional carboxyterminal hemopexin domain. Due to differences in substrate specificity and structural characteristics, the MMPs are divided into several subclasses: collagenases (MMP-1, -8, -13), gelatinases (MMP-2, -9), stromelysins (MMP-3, -10, -11), matrylysin (MMP-7), elastase (MMP-12), enamelysin (MMP-20) and membrane type-MMPs (MMP-14, -15, -16, -17) (19). In general, the pro-domain is ~80 amino acids with a hydrophobic residue at the N-terminus, and contains a cysteine residue in the conserved sequence PRCXXPD. The cysteine within this conserved sequence is termed the "cysteine switch" due to its interaction with a Zn^{2+} ion in the catalytic site. The catalytic domain contains the active site, is ~160 residues and contains a Zn^{2+} binding motif of the conserved sequence HEXXHXXGXXH. The three conserved histidine residues within the catalytic site are responsible for the coordination of the catalytic Zn^{2+} ion. The catalytic domain also includes a conserved methionine, which forms a unique "met-turn" structure, structural binding sites for 2-3 Ca^{2+} ions, which are important for stability. The C-terminal hemopexin-like domain is ~ 200 residues and is thought to modulate substrate specificity and the binding of Tissue Inhibitors of MMPs (TIMPs).

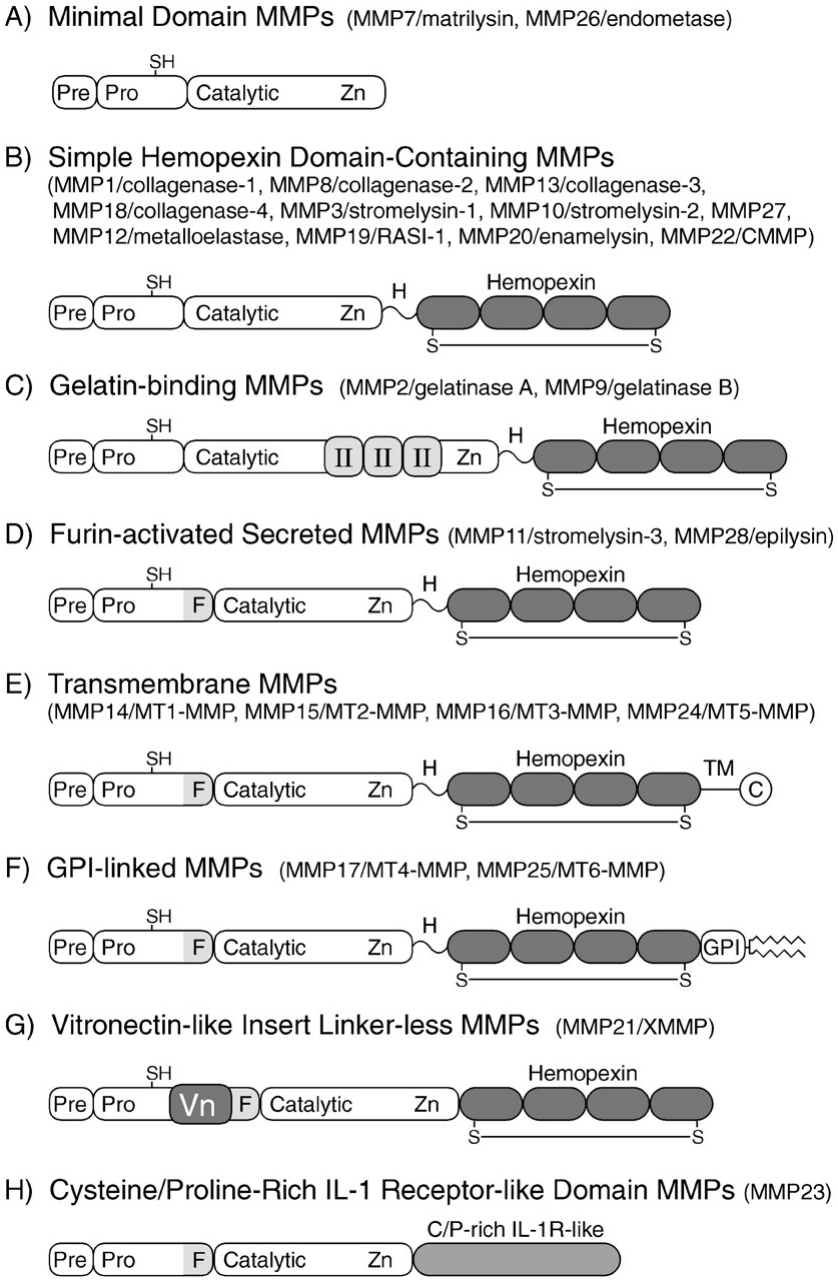

Figure 3. General structure and classification of matrix metalloproteinases
Diagram showing the structural domains of matrix metalloproteinases. Adapted from (20).

Within the context of this dissertation, the gelatinases MMP-2 (Gelatinase A) and MMP-9 (Gelatinase B), are of particular interest because they have been clinically shown to be key enzymes in several pulmonary diseases including emphysema, pulmonary fibrosis, bronchial asthma and pulmonary infection (21, 22). These two MMPs have an additional gelatin binding fibronectin domain composed of 3 fibronectin type II repeats. These repeats are within the catalytic domain, and are responsible for binding gelatin, laminin and collagens type I and IV. MMP-9 also contains an additional Ser/Thr/Pro-rich collagen type V domain situated in the hinge region which is ~75 amino acid residues in length (23-26). It is of interest to point out that in the gelatinases, collagen binding is conferred by the fibronectin type II-repeats and the Ser/Thr/Pro-rich collagen type V domain, whereas in collagenases, collagen binding is conferred by the hemopexin domain (27, 28). The hemopexin-like domain of MMP-2 is also required for the cell surface activation of pro-MMP-2 by MT-MMP1 (29).

E. Matrix metalloproteinases and cytokine modulation

Apart from digesting the ECM, the gelatinases modulate the activity of other proteases and cytokines and chemokines that are important in lung diseases. MMP-2 and MMP-9 have certain chemokines and cytokines as their substrates. As such, the gelatinases have the ability to have varying affects on the biological properties of cytokines and chemokines, ranging from potentiation to inactivation to antagonistic formation. Both MMP-2 and MMP-9 can release TGF-β from an inactive extracellular complex that consists of TGF-β latent-associated protein, and latent TGF-β-binding protein (30). MMP-2 cleaves the proinflammatory molecule monocyte chemoattractant

protein (MCP-3) into a truncated anti-inflammatory molecule which helps in the dampening of the inflammatory processes. MMP-9 cleaves IL-8 at its N-terminal increasing its chemotactic activity for neutrophils 10-fold. But it also inactivates other neutrophil chemokines (31). IL-1β and TNF-α have been reported to be increased in lung allograft BAL fluid. MMP-9 is also able to cleave the membrane-bound forms of tumor necrosis factor-alpha (TNF-α) and transforming growth factor-beta (TGF-β) into their active forms. Both gelatinases are able to generate the active form of interleukin-1 beta (IL-1β) from its inactive pro-form. MMP-9 degrades α1-antitrypsin, protecting neutrophil elastase activity (32), and potentiates the collagenolytic activity of MMP-13 (33).

Thus, cleavage of cytokines and chemokines by gelatinases can have varying effects on their biological properties, ranging from potentiation to inactivation to antagonist formation thereby affecting different physiological and pathological processes. All of these processes occur by MMPs acting extracellularly. New evidence, however, is suggesting the presence of intracellular MMP substrates that may indirectly regulate cytokine and chemokine activity. The plethora of potential substrates and the diversity of cell types that express these enzymes suggest the possibility of the involvement in multiple events occurring simultaneously in different microenvironments.

F. Matrix metalloproteinase substrates

MMPs function can be regulated at many levels. In addition to transcriptional and translational regulation, MMPs can be regulated at the levels of secretion, intracellular trafficking, subcellular or extracellular localization, activation of the zymogen form, expression of their endogenous protein inhibitors (TIMPS) and protease degradation.

Also, substrate availability and accessibility determine the degree to which MMP activity is used. Within the lung, multiple factors are involved in MMP regulation including: a large list of growth factors, cytokines, cell adhesion molecules, ECM proteins and their bioactive fragments, intracellular signaling factors, and agents that cause actin cytoskeletal reorganization, all of which can directly or indirectly regulate the expression of MMPs (34). Interestingly, most of the same factors that regulate the expression of MMPs in the lung can also act as their substrates, providing a built-in and, most likely, essential component of the regulatory cascades. This coordination between MMP and substrate ensures efficient activation and control of MMPs (35).

Recently, using a proteomics approach analyzing bronchoalveolar lavage fluid (BALF) from the lungs of wild-type and MMP2/9 double deficient mice following allergen-challenge, Kheradmand et al. reported three new in vivo substrates for MMP2 and MMP9; Ym1, S100A8 and S100A9, all of which are involved in chemotaxis (36). Ym1 is synthesized and secreted as an enzymatically inactive member of the chitinase family of proteins and has been identified in macrophages and airway epithelium of airway challenged mice (36). Intracellular and extracellular crystalline material corresponding to Ym1 has been identified in macrophages of NADPH deficient mice, which leads to the development of progressive crystalline macrophage pneumonia (37). S100A8 and S100A9 are small calcium-binding proteins of the S100 protein family that are highly expressed in neutrophil and monocyte cytosol and are found at high levels in the extracellular milieu during inflammatory conditions (38). Intracellular S100A8/A9 complexes play an important role in cell trafficking (39). To identify these proteins in vivo, BALF from wild-type and MMP2/9 double deficient (MMP2/9-/-) mice were

analyzed using two-dimensional differential in gel electrophoresis (2D-DIGE) followed by mass spectrometry. Western blot analysis revealed an increase in Ym1 protein fragments in the BALF of wild-type allergen-challenged mice as compared to MMP2/9-/- allergen-challenged mice, in which the Ym1 protein fragments were absent.

Furthermore, probing with a polyclonal Ym1 Ab that only detects the full-length Ym1 protein revealed increased levels of Ym1 in the BALF of MMP2/9-/- mice and not in wild-type allergen-challenged mice. These results demonstrate that MMP2 and or MMP9 are needed to process Ym1. To verify that Ym1 is cleaved by MMP2 or MMP9, silver staining studies were performed on purified Ym1 after incubation with recombinant MMP2 and MMP9. The results demonstrated that Ym1 is in fact a substrate of MMP2 and MMP9. Due to the size of the S100 proteins, in vitro cleavage assays were performed which revealed that S100A8 and S100A9 are substrates of MMP2. In an in vivo model of asthma, it was found that inhibition of S100 proteins by function-blocking Abs to S100A8 and S100A9, altered migration of allergic inflammatory cells in the alveolar space (36). These proteins have been identified in adult and juvenile rheumatoid arthritis, chronic bronchitis, cystic fibrosis, systemic lupus erythematosus, langerhans cell histiocytosis (40) and granulomatous conditions, such as tuberculosis and sarcoidosis (38). The identification of these new in vivo intracellular substrates, suggest a potential intracellular role for MMP2 and MMP9.

G. Matrix metalloproteinase activation

MMPs are present on the cell surface or secreted as latent, stable, pro-peptides known as zymogens. MMP2 is secreted as a 72kDa pro-form and MMP9 as a 92kDa pro-

form. These enzymes are in an inactive state due to the thiol (SH-) group of the cysteine residue within the pro-domain interacting with the Zn^{2+} ion in the catalytic domain. Disruption of this cysteine-zinc interaction, by proteolysis for example, causes a conformational change thereby allowing the zinc to interact with the hydroxyl group (OH-) of a hydrolytic water molecule resulting in the activation of the enzyme. This mechanism is termed the cysteine-switch mechanism (41, 42). In most cases, the pro-domain is cleaved to yield the truncated active forms of MMP-2 and -9, 64kDa and 83kDa, respectively. MMPs may also be activated by other MMPs.

H. Tissue inhibitors of matrix metalloproteinases (TIMPs)

The major physiologic inhibitors of the MMPs in vivo, are a group of specific tissue inhibitors of MMPs (TIMPS). These naturally occurring inhibitors are comprised of a family of four structurally related members, TIMP-1, -2, -3, and -4. TIMPs have an N- and C- terminal domain, each of which contains three conserved disulfide bonds. TIMPs bind to MMPs in a 1:1 stoichiometry. TIMP expression is regulated during development and tissue remodeling. These secreted proteins bind to the catalytic site of active MMPs resulting in their loss of proteolytic activity. Of the four TIMPs, TIMP-1 and -2 have been shown to have key roles in the pathogenesis of lung disease. The balance between TIMPs and MMPs is believed to be important in regulating protease activity, suggesting that disruption of this balance can lead to serious pathological conditions (43, 44). Although TIMPs play an important role in MMP regulation, they are beyond the scope of this report, and therefore will not be discussed.

I. Matrix metalloproteinase inhibitors

Thus far, the known pharmacological inhibitors of MMPs are broad-spectrum molecules, which are designed to chelate the active-site zinc ions. Two broad spectrum inhibitors were tested, COL-3, a chemically modified tetracycline and 1,10 Phenanthroline, a heterocyclic broad spectrum inhibitor of MMP activity. COL-3 is a synthetic inhibitor that lacks antibiotic activity but retain anti-MMP activity. 1,10 Phenanthroline, is commonly used as a chelating agent for divalent metals such as Zinc and Ca^{2+} thereby inhibiting MMPs stability and potential activation (45). These two inhibitors were shown to be challenging due to their lack of specificity and their effects on other non-related signaling events. CMT-3 has been shown to interact with PKC which can effect cell growth and differentiation. 1,10 Phenanthroline chelates Zn^{2+} and Ca^{2+} ions which can lead to cell dysfunction.

Although there is a plethora of evidence confirming MMP involvement in lung injury, it is difficult to selectively pinpoint which of the up-regulated MMP activities are responsible for the tissue injury seen in various pulmonary diseases. This has largely been due to the lack of selective inhibitors. Mobeshery et al. has synthesized a selective gelatinase inhibitor (SB-3CT) [figure 4] to selectively inhibit MMP-2 and MMP-9 (46, 47). This inhibitor is unique in that it works through a mechanism-based approach with the presence of a thiirane-containing inhibitor. The thiirane sulfur first coordinates with the active-site zinc ion. The coordinated thiirane predisposes it to nucleophilic attack by the active site glutamate, which leads to covalent modification of the MMP and attendant loss of activity. Through a series of reactions, the MMP2 and MMP9 are irreversibly inhibited by permanently blocking the cysteine switch interaction.

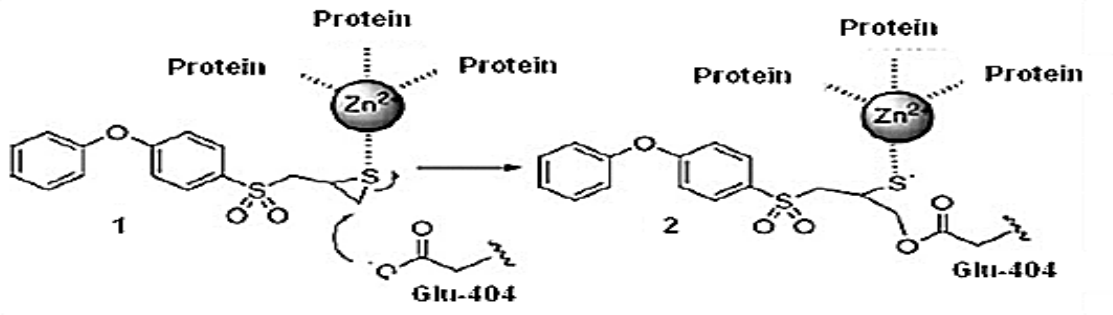

Figure 4. Schematic diagram of MMP activation and inhibition by SB3CT
Diagram showing the mechanism based inhibitor SB3CT binding to the catalytic site of a matrix metalloproteinase (MMP2 or MMP9). Adapted from (48).

J. Matrix metalloproteinases in the normal lung

Under normal physiological conditions, cells in the lung do not normally express MMP2 and MMP9, with the exception of the constitutive expression of MMP2 in the endothelium. During infection and inflammatory disease, bronchial epithelial cells, Clara cells, alveolar type II cells, smooth muscle cells and fibroblasts are all capable of producing MMP9. Infiltrating leukocytes are another major source of MMP2 and MMP9, as neutrophils and eosinophils constitutively produce MMP9, whereas macrophages, mast cells and lymphocytes release MMP9 under inflammatory conditions (49). The gelatinases are able to modulate the process of tissue remodeling and therefore abnormal activation or inhibition of these enzymes is associated with many pulmonary pathologies. In the lung, MMP-2 and MMP-9 are implicated in the migration of epithelial cells following injury, by degrading components of the basement membrane allowing migration (50). In MMP-9 knock-out mice, there are reduced numbers of T lymphocytes and dendritic cells in the BAL fluid following antigen challenge (51). Infiltration of neutrophils, lymphocytes and dendritic cells into the lung further confirms a role for the gelatinases under normal and pathological conditions.

K. Matrix metalloproteinases in cancer

MMPs, specifically the gelatinases, have been linked to a myriad of disease states. From a cancer perspective, MMP2 and MMP9 have been shown to be required for tumor cell invasion and angiogenesis (52). For example, in an experimental model for spontaneous metastasis of rat mammary carcinoma, increased serum and plasma levels of MMP-9 were associated with the development and extent of metastases in the lung and

lymph nodes (53). MMP2 and MMP9 have been reported in human prostate cancer tissue, with the increase in MMP2 correlating to the degree of disease progression (54). Additionally, studies have reported an increase in MMP2 and MMP9 in expression and activity in the parenchyma of lung cancer patients (55). Thus, MMP2 and MMP9 participate in migration, tumor cell invasion, angiogenesis and inflammation-induced tissue remodeling, and have been clinically shown to be key enzymes in the regulation of lung immunobiology.

L. Matrix metalloproteinases in pulmonary disease

The mechanisms that initiate lung inflammation are important to understanding the immunobiology of pulmonary diseases such as asthma, chronic obstructive pulmonary disease (COPD), cystic fibrosis and idiopathic pulmonary fibrosis (IPF) (56). It is also important to understand the factors that are involved in resolution of the inflammation. This is a poorly understood topic that is of great importance because failure to resolve the inflammation results in irreversible airway remodeling and obstruction. We briefly discuss these diseases below and what is known of MMP2 and MMP9s involvement in each, and suggest a potential role for T cell-derived MMPs in these diseases.

1. *Asthma*

In the case of asthma, this disease is one that occurs when exposure to respiratory allergens triggers a systemic response, characterized by activation of the adaptive immune cells that are drive by Th2 cell-mediated airway inflammation (57). IL-4 and IL-13 induce up-regulation of chemokines and cytokines that allow for homing of activated

Th2 cells to the site of inflammation (58). MMP2 and MMP9 have been shown to act downstream of Th2 cytokine signaling, but their presence is not required for the development of allergic and obstructive lung phenotype (59, 60). Interestingly, there has been a correlation between asthma severity and the expression of MMP9. MMP9 levels in the sputum, BAL and serum are higher in patients with severe asthma, as compared with milder asthmatics (61).

In murine models of allergen-induced asthma, the absence of MMP9 is responsible for a decrease of infiltration of airways and BAL by inflammatory cells. MMP9 deficient mice failed to develop allergen-induced airway hyperresponsiveness, suggesting a role for MMP9 in facilitating the egression of inflammatory cells into the airway lumen (62). With regard to allergen-induced asthma in MMP2 deficient mice, the absence of MMP2 causes inflammatory cell infiltration of alveolae and a decrease of inflammatory cells recovered in the BAL despite a strong peribronchovascular cell accumulation (63). These results suggest that MMP2 may play a role in the luminal clearance of inflammatory cells. MMP9 gene deletion reduces allergen-induced inflammatory process by decreasing dendritic cell (DC) trafficking, one of the key events during initiation of allergic immune responses, including asthma (51). Although asthma is known to be a Th2 driven disease and MMP2 and MMP9 are up-regulated, the potential connection between $CD4^+$ T cells and MMPs in the regulation of this disease has not been studied.

2. Chronic obstructive pulmonary disease (COPD)

Asthma and chronic obstructive pulmonary disease (COPD) are both obstructive airway disorders, but differing types of inflammation are involved in the pathogenesis of

these distinct lung diseases. COPD is a disease that encompasses chronic bronchitis, small airway disease, and emphysema (64). It is characterized by a progressive chronic obstruction to airflow with a persistent inflammatory process. Among the cells involved in the inflammation reaction, alveolar macrophages are the predominant cell population identified by BAL with the addition of increased numbers neutrophils, and T lymphocytes (65). The development of COPD is characterized by an excess of extracellular matrix deposition in bronchial walls, sputum production and destruction of alveolar septa, resulting in reduced functional lung parenchyma and reduced elasticity due to elastolytic enzymes, such as neutrophil elastase and MMP9 (66). Within this disease, there are excess numbers of CD8+ T cytotoxic cells in the airways (67). This increase in CD8+ T cells may be due to the fact that these cells are known for their potential to eradicate infected cells. It is well known that COPD patients suffer from frequent exacerbations triggered by virus or bacteria, leading to an accelerated decline in lung function. It has been reported that $CD4^+$ and $CD8^+$ T cells are increased with the increasing number of CD8+ cells in both lung parenchyma and pulmonary arteries of COPD patients significantly correlates with the degree of airflow limitation, therefore suggesting an important role for T cells in COPD (68).

Elastin is important to lung integrity, and in emphysema elastin degradation occurs, leading to airway obstruction and disease severity. A study by Lee et al., highlighted the importance of T cells in mediating emphysema (69). They reported that activated T cells in emphysematous lungs exhibit a predominantly Th1 effector phenotype. They found a significant correlation between peripheral blood Th1 responses to elastin peptides, and severity of lung disease and airway obstruction, with an increase

in Th1 infiltration leading to severity of lung disease. They went on to propose that exposure to cigarette smoke (as is seen in emphysema patients) induces secretion of proteolytic enzymes (likely MMPs) from cells of the innate immune system that liberate lung elastin fragments, which in susceptible individuals could initiate T- and B- cell-mediated immunity against elastin, leading to exacerbation of the disease (69). This study again links the potential relationship between MMPs and T cells.

MMPs have been suggested as the major proteolytic enzymes involved in the pathogenesis of this disease. Patients with COPD exhibit significantly elevated levels of MMP2 and MMP9 expression and activity in their lung parenchyma, as well as increased gelatinolytic activity in their sputum (21, 70). A report by Segura-Valdez et al. found increased MMP-2 and MMP-9 in the airway and lung parenchyma of COPD patients (71). Patients with stable chronic asthma or emphysema also showed increased levels of MMP-2 and MMP-9 in the sputum and BAL fluid (72, 73). The study of MMPs involvement in these diseases has largely focused on matrix degradation and remodeling, causing immunological changes and progression of the disease. However, there may be another important idea that has been overlooked. COPD and asthma are both diseases that involve T cell infiltration and have elevated levels of MMPs. These characteristics suggest that T cells could be involved in the elevated MMP expression within these diseases, since T cells are capable of expressing MMPs. These data suggest a potential link between T cells and MMP2 and MMP9 in COPD and asthma.

3. Cystic fibrosis

Cystic fibrosis (CF) is a genetic disorder in which abnormal ion transport predisposes patients to infection and neutrophilic inflammation (74). A predominant

feature of CF is the dynamic structural changes in the airway, such as the widening of airways and loss of normal mucociliary clearance mechanisms. These structural changes can lead to bronchiectasis and pulmonary hypertension and are a direct cause of the pulmonary morbidity and mortality seen in the majority of CF patients, due to the insistent airway inflammation in the disease (75).

A few studies have examined MMP9 in CF and have reported an increase in MMP-9 activity in CF sputum (76). A report from Ratjen et al. examined bronchoalveolar lavage fluid from CF patients and found increased MMP-9 in children with CF compared with healthy controls (77). It has been reported by Sagel et al. that MMP-9 expression is dramatically increased in the lower airway secretions of CF patients, and a negative correlation exists between MMP-9 levels and lung function [forced expiratory volume in 1s (FEV_1)] (77).

4. Pulmonary fibrosis

Pulmonary fibrosis is a severe chronic disease characterized by a loss of lung epithelial cells, replaced by interstitial myofibroblasts and deposition of extracellular matrix proteins in the lung interstitium leading to pulmonary structural remodeling (78). Idiopathic pulmonary fibrosis is a chronic disorder characterized by excessive matrix degradation and interstitial and intraalveolar fibrosis, which leads to dyspnea, impaired oxygen transfer and alveolar collapse (79). The defects in the alveolar epithelium and basement membrane allow the migration of mesenchymal cells from the interstitium into the intraluminal compartment. This is a major characteristic of IPF and is associated with the recruitment of inflammatory cells, including lymphocytes into the airways leading to an imbalance between synthesis and degradation of extracellular matrix molecules in the

local environment (80). The pathogenesis of idiopathic pulmonary fibrosis, however, is not completely understood. Its main features include epithelial injury, fibroblastic proliferation, inflammation, and increased matrix production (78). The ultimate feature is the progressive fibrosis, resulting from expansion of the extracellular matrix (ECM), and extensive remodeling of the lung parenchyma, where matrix metalloproteinases (MMPs) are believed to play important roles.

In lung fibrosis, studies have reported a temporal difference observed in expression and localization of MMPs (81, 82). In the earlier stages of the disease, MMP9 seems to be predominant, likely contributing to disruption of alveolar epithelial basement membrane, and enhances fibroblast invasion to alveolar spaces. In the later stages of the disease, MMP2 seems to become predominant and is localized in structural cells like regenerated alveolar epithelial cells (83, 84). The expression of MMP2 and MMP9 at different stages of pulmonary fibrosis suggest, MMP9s involvement in inflammation-induced tissue remodeling, while MMP2 may be associated with an impairment of tissue remodeling, leading to the exacerbation of fibrosis by increased collagen deposition and interstitial fibrosis.

In many cases, these chronic and often end-stage pulmonary diseases have limited therapeutic options. For many of these patients, lung transplantation is the only therapeutic option. Despite significant medical improvements, patient survival rates 5-years after transplantation is estimated to be 50 percent (85). The major cause of mortality and morbidity among these patients following transplantation is chronic rejection (86), clinically manifested as obliterans bronchiolitis (OB) (87, 88). OB is characterized by accumulation of granulation tissue in the lumen of the bronchioles

which may be accompanied by the accumulation of monocytes, neutrophils, eosinophils and lymphocytes (89, 90). The mechanism by which chronic lung rejection leads to OB is poorly understood. It is thought however, that airway inflammation and aberrant tissue remodeling play a major role in the pathogenesis (91). Rejection is mediated by host T cells that have been activated by host or donor-derived dendritic cells (DCs), antigen presenting cells. Alloreactive T cells infiltrate the graft resulting in varying degrees of perivascular and peribronchiolar infiltrates characteristic of the rejection response. DC-induced T cell activation is a complex process involving bidirectional signaling between these cells mediated by cell surface molecules, soluble extracellular mediators and intracellular pathways.

M. Matrix metalloproteinases in transplant biology

Recent studies have revealed interesting roles for MMPs in transplant biology. There have been reports suggesting a link between MMP activity, specifically MMP-9 and the onset of OB (43, 44). Other studies show that ischemia-reperfusion injury associated with lung transplantation, is sufficient to cause a significant up-regulation of MMP-9 and/or MMP-2 in lung grafts, and that MMP inhibition attenuates this process (92, 93). A report by Trello et al. demonstrated that MMP-2 and MMP-9 are increased in BAL fluid in stable lung transplant recipients, indicating that up-regulated proteolytic activity in clinically stable lung transplant recipients may have a role in chronic rejection after transplantation (94). Data from our laboratory showed that acute lung allograft rejection in rat transplant recipients was associated with up-regulated MMP-2 expression. Additionally, we reported that MMP inhibition by a broad spectrum MMP inhibitor

(COL-3), inhibited MMP activity, decreased TNF-α and IL-1β and abrogated T cell proliferation (93).

Another study by Campbell et al. showed that MMP-2 and MMP-9 play different roles in the process of mononuclear cellular influx into the allograft, as well as in the process of activation and expansion of alloreactive T cells during cardiac allograft rejection (95). BALB/c cardiac allografts were transplanted into MMP2 deficient and MMP9 deficient mice. MMP2 deficiency significantly prolonged allograft survival time and functioning allografts harvested from MMP2 deficient mice showed lower cellular infiltration than rejected allografts harvested from wild-type mice. In contrast, MMP9 deficiency significantly decreased allograft survival time and functioning allografts harvested from MMP9 deficient mice showed higher cellular infiltration than rejected allografts harvested from wild-type mice. Additionally, MMP2 deficient recipients showed a decrease in T cell alloreactivity, whereas, MMP9 deficient recipients showed an increase in T cell alloreactivity (95).

Ischemia-reperfusion injury associated with lung transplantation can cause a significant up-regulation of MMP-2 and MMP-9 in lung allografts, which is attenuated by non-selective MMP inhibition (92, 96). In a report by Hubner et al. it was shown that the MMP-9 to TIMP-1 ratio is significantly increased in patients with BOS (bronchiolitis obliterans syndrome), known as chronic rejection, following lung transplantation (44). Data from our laboratory confirm that MMP-9 is strongly up-regulated in transplanted lungs (96). Taken together these data suggest that MMP-2 and MMP-9 play an important role in transplant rejection. Further investigation is required to delineate the functional roles of these MMPs in the process of T cell mediated pulmonary disease and transplant

rejection. Reports from other investigators show that bulk splenocytes isolated from mice genetically deficient in either MMP-2 or MMP-9 have diminished ability to stimulate proliferation in allogeneic T cells (95, 97), suggesting a role of MMPs in T cell proliferation.

These data support the notion that MMPs have some regulatory role in T cells and pose a question as to whether they function extracellularly or intracellularly. Recent publications have identified the presence of MMPs in the nucleus. A report by Luo and colleagues found a variant of MMP-11 that is expressed as an intracellular active form (98). Another group identified the nuclear localization of MMP2 in cardiac myocytes and rat liver (99). An intriguing study by Si-Tayeb et al. elucidated a mechanism for nuclear localization of an MMP by identifying a nuclear localization signal and showed that nuclear MMP3 can induce apoptosis via its catalytic activity (100). Since MMPs are generally thought to be secreted or transmembrane proteins, studies showing their intracellular presence or regulation are of great importance and suggest a potentially new path of MMP regulation and activity.

With much of the focus of MMPs being on their extracellular regulation and with studies highlighting the role of MMPs, specifically MMP2 and MMP9, in the pathogenesis of many T cell mediated lung diseases, it is of interest to understand the interconnection between MMPs and T cells. The new identification of intracellular MMP activity, offers a new potential mechanism of action for MMPs. Although studies have demonstrated the presence of MMPs within T cells, the role that MMPs may play in regulating T cell activation remains unknown. More importantly, no reports have identified potential intracellular MMP substrates that may be involved in regulating T cell

signaling events. This understanding would shed light on the potential mechanism of action that MMPs may be exerting in T cells to regulate their activation. The objective of the studies in this dissertation is to provide experimental evidence evaluating the regulatory role of matrix metalloproteinases, MMP2 and MMP9 in T cell activation at the functional level, intracellularly and in the context of T cell mediated lung injury in vivo.

The initial studies examined the expression levels of MMP9 in T cells, followed by the T cell functional response, as measured by T cell activation, in the presence of broad spectrum MMP inhibitors (1,10 phenanthroline and COL-3). Further studies more closely examined T cell in the presence of an MMP2 and MMP9 specific inhibitor (SB3CT) or in T cells that were deficient in MMP2 or MMP9, to determine if MMPs are important in T cell activation. Next, the intracellular signaling pathways in T cells were evaluated to determine if MMPs regulate intracellular signaling events important for T cell activation, such as the calcium and NFAT signaling pathways. Cell phenotypic studies were performed to analyze the expression of T cell surface activation markers following MMP inhibition or absence. Finally, MMP inhibition is evaluated in vivo to determine MMPs involvement in antigen-specific $CD8^+$ T cell mediated lung injury.

N. Hypothesis

Matrix Metalloproteinases, specifically MMP2 and MMP9 regulate T cell activation.

II. MATERIALS AND METHODS

A. Animals

Female Balb/c and C57BL/6 mice 6-10 weeks old, were purchased from Harlan (Indianapolis, IN) or bred in the Laboratory Animal Resource Center at Indiana University School of Medicine (Indianapolis, IN). MMP2 null, MMP9 null and MMP2/MMP9 double null mice (C57BL/6 background) were a generous gift from Dr. Farrah Kheradmand (Baylor College of Medicine, Houston, TX) (59). CC10-OVA mice (C57BL/6 background) and OT-1 TCR transgenic mice (C57BL/6-Thy1.1 background) were a generous gift from Dr. Rebecca Shilling (University of Chicago Medical Center, Chicago, IL) (101). All mouse studies were conducted in accordance with institutional animal care and usage guidelines.

B. Formulation of buffers and media

MACS buffer

In a 2L beaker, 50ml of 10X PBS is added to 448ml of ddH_20. To that 2ml of 0.5M EDTA is added followed by 2.5g of BSA (Fisher Scientific, Pittsburgh, PA). Buffer is then filter sterilized and degassed.

Cell lysis buffer

In a 2L beaker, 8.29g of NH_4Cl, 1g of $KHCO_3$, 0.372g of Na EDTA ($C_{10}H_{12}N_2Na_4O_8$) are added to approximately 1L of ddH_20 adjusted to a final volume of 1L and then the buffer is then filter sterilized.

Complete RPMI (cRPMI)

RPMI, 400 mM l-glutamine, 100 U penicillin streptomycin (Gibco, Carlsbad, CA), 10% FCS (Hyclone, Logan, UT), and 5 x10^5 M 2-mercaptoethanol (Sigma, St. Louis, MO).

C. Isolation of murine T cells from the spleen

Single cell suspensions were prepared from the spleens of five to seven mice. Red blood cells were lysed with an NH_4Cl lysis buffer. Cell suspensions were then centrifuged at 300 x g for 10 minutes. Supernates were aspirated and cells were resuspended in 900µl of MACS buffer per 10^8 total cells. 100µl of either CD4 (L3T4) or CD8 (CD8a-Ly2) Microbeads (Miltenyi Biotech, Auburn CA) were then added per 10^8 total cells. Cells containing the CD4 Microbeads or CD8 Microbeads were mixed well and incubated at 4 degrees C for 15 minutes. 5-10ml of MACs buffer was added to the cell suspension followed by centrifugation at 300 x g for 10 minutes. Supernates were aspirated and cell pellets were resuspended in 500µl MACs buffer per 10^8 total cells. $CD4^+$ or $CD8^+$ T cells were then isolated from the splenocytes through positive magnetic selection steps using the autoMACS Seperator run on the "posseld" program. The purity of $CD4^+$ and $CD8^+$ T cells determined by staining cells with anti-CD4 FITC labeled Ab and anti-CD8 PE labeled Ab, respectively. Stained cells were then analyzed by flow cytometry and purity ranged from 97 to 99%. This isolation protocol was used to isolate T cells from C57BL/6 wild-type mice, MMP2 deficient, MMP9 deficient, MMP2/9 deficient, OT-I transgenic and OT-II transgenic mice.

D. Isolation of murine dendritic cells from the spleen

Single cell suspensions were prepared from the spleens of five to seven mice. Red blood cells were lysed with an NH_4Cl lysis buffer. Cells were collected by centrifugation (200 x g, 10 minutes). Supernates were aspirated and cell pellets were resuspended in 400µl of MACS buffer per 10^8 total cells. 100µl of cD11c Microbeads (Miltenyi Biotech, Auburn CA) were then added per 10^8 total cells. Cells were mixed well and incubated at 4 degrees C for 15 minutes. 5-10ml of MACs buffer was added to the cell suspension, and suspensions were centrifuged at 200 x g for 10 minutes. Supernates were aspirated and cell pellets were resuspended in 500µl MACs buffer per 10^8 total cells. $CD11c^+$ dendritic cells were then isolated from the splenocytes through positive magnetic selection steps using the autoMACS Seperator run on the "posseld" program. The purity of $cD11c^+$ dendritic cells determined by staining cells with anti-CD11c FITC labeled Ab. Stained cells were then analyzed by flow cytometry flow cytometry, ranged >90%.

E. Isolation of murine regulatory T cells from the spleen

Tregs were isolated from splenocytes through a series of magnetic selection steps using the mouse $CD4^+CD25^+$ Isolation Kit (Miltenyi Biotech, Auburn, CA). Single cell suspensions were prepared from the spleens of ten to twenty mice. Red blood cells were lysed with an NH_4Cl lysis buffer. Cells were collected by centrifugation (300 x g, 10 minutes). Supernates were aspirated and cell pellets were resuspended in 400µl of MACS buffer per 10^8 total cells. 100µl of Biotin-Antibody Cocktail, which consists of biotin-conjugated monoclonal anti-mouse antibodies against: CD8a (Ly-2; isotype: rat IgG2a), CD11b (Mac-1; isotype: rat IgG2b), CD45R (B220; isotype: rat IgG2a), CD49b (DX5;

isotype: rat IgM) and Ter-119 (isotype: rat IgG2b (Miltenyi Biotech, Auburn CA) was then added per 10^8 total cells. Cells were mixed well and incubated at 4 degrees C for 10 minutes. 300µl of MACS buffer, 200µl of Anti-Biotin MicroBeads and 100µl of CD25-PE antibody were added per 10^8 total cells. Cells were mixed well and incubated at 4 degrees C for 15 minutes in the dark. 5-10ml of MACs buffer was added to the cell suspension, and suspensions were centrifuged at 300 x g for 10 minutes. Supernates were aspirated and cell pellets were resuspended in 500µl MACs buffer per 10^8 total cells. The $CD4^+$ cell fraction was then isolated from the splenocytes through negative magnetic selection steps using the autoMACS Seperator run on the "Depl025" program. The negative fraction consisted of the $CD4^+$ cell population. The $CD4^+$ cells were centrifuged at 300 x g for 10 minutes, supernatant was completely aspirated and cells were resuspended in 900µl of MACS buffer and 100µl of Anti-PE MicroBeads. Cells were mixed well and incubated at 4 degrees C for 10 minutes. Cells were mixed well and incubated at 4 degrees C for 15 minutes in the dark. Cells were then washed by addition of 5-10ml of MACs buffer and centrifuged at 300 x g for 10 minutes. Supernatant was completely aspirated and cells were resuspended in 500µl MACs buffer per 10^8 total cells. The $CD4^+25^+$ cell fraction was then isolated from the splenocytes through double positive magnetic selection steps using the autoMACS Seperator run on the "Posseld2" program. Treg cell purity determined by flow cytometry, ranged from >93%. Where indicated, the CD4- fraction was γ-irradiated (2000 rads) and used as APCs. The $CD4^+CD25^-$ cell fraction was also retained and used as fresh T cells. The purity of Tregs and Th cells, determined by flow cytometry, ranged from 93-97% and 93-99%, respectively.

F. Preparation of matrix metalloproteinase inhibitors (MMPIs)

Broad spectrum MMPIs, 1,10 Phenanthroline and COL-3, or MMP2/9 specific MMPI, SB3CT,were used in the following experiments. 1,10 Phenanthroline (Sigma, St. Louis, MO) was reconstituted in tissue culture grade dimethyl sulfoxide (DMSO) to a 1M solution then diluted to concentrations ranging from 0.001-0.1uM in cRPMI. CMT-3, a chemically modified tetracycline, and generous gift from Dr. Brad Zerler (CollaGenex Pharmaceuticals, Inc., Newtown, PA) was reconstituted in carboxy-methylcellulose to a 1M solution then diluted to concentrations ranging from 1-100uM in cRPMI. SB3CT, a specific mechanism-based MMP2/9 inhibitor, and generous gift from Dr. Shriar Mobashery (University of Notre Dame, Notre Dame, IN) was reconstituted in DMSO and polyethylene glycol (PEG) to a 1M solution then diluted to concentrations ranging from 0.0001-1mM in cRPMI.

G. Mixed leukocyte reactions

Purified $CD4^+$ T cells from Balb/c mice ($1x10^6$/ml) were treated with the indicated concentrations of MMPIs. Cells were then co-culture with γ-irradiated $CD11c^+$ dendritic cells (DC), purified based on CD11c expression from C57BL/6 mice. DCs and T cells were co-cultured at DC: T cell ratios of 0.01, 0.075 and 0.1, in the presence of anti-mouse CD3 (0.5μg/ml, BD Biosciences, San Jose, CA) in 200μl of cRPMI at 37°C for 72h. 18h prior to harvest, cultures were pulsed with ^{3}[H]-thymidine (0.5 μCi/well). Plates were harvested using a Skatron Basic 96 Harvestor (Molecular Devices, Sunnyvale, CA). ^{3}[H]-thymidine incorporation was measured using a liquid scintillation counter (Beckman, Fullerton, CA).

H. T cell proliferation assays

Purified $CD4^+$ or $CD8^+$ T cells from Balb/c or C57BL/6 mice ($1x10^6$/ml) were incubated with the indicated concentrations of MMPIs. Cells were then washed in RPMI and plated in the presence of anti-CD3 Ab (0.5μg/ml, BD Biosciences, San Jose, CA) in 200μl of cRPMI at 37°C for 72h. 18h prior to harvest, cultures were pulsed with ^{3}[H]-thymidine (0.5 μCi/well). Plates were harvested using a Skatron Basic 96 Harvestor (Molecular Devices, Sunnyvale, CA). ^{3}[H]-thymidine incorporation was measured using a liquid scintillation counter (Beckman, Fullerton, CA).

Purified $CD4^+$ and $CD8^+$ T cells from MMP2, MMP9 or MMP2/9 double knock out C57BL/6 mice ($1x10^6$/ml) were cultured in the presence of anti-CD3 Ab (0.5μg/ml) in 200μl of cRPMI at 37°C for 72h. $CD4^+$ and $CD8^+$ T cells were also incubated with the indicated concentrations of SB3CT for 6h and then washed three times with RPMI 1640. Drug or vehicle-treated T cells were cultured ($1x10^6$/ml) with anti-CD3 Ab (0.5μg/ml) in 200μl of cRPMI at 37°C for 72h. Cells were harvested as indicated above.

I. OT-I and OT-II Ag-specific T cell proliferation

Pure splenic $CD4^+$ and $CD8^+$ T cells from OT-II transgenic or OT-I transgenic C57BL/6 mice were incubated with the indicated concentrations of MMPIs. Cells were then washed in RPMI and plated at $1x10^5$/well in a 96 well plate in the presence of OVA-pulsed (OT-II:ova peptide and OT-I: SIINFEKL peptide) antigen presenting cells (APCs) for 72 hours. 18 hours prior to harvest, 3H thymidine (0.5μCi/well) was added to the culture. T cell proliferation was measured by the amount of 3H thymidine incorporation.

J. $CD4^+25^-$ T cell suppressor assay

Purified $CD4^+25^-$ T cells from C57BL/6 mice were incubated with the indicated concentrations of SB3CT or vehicle control for 6 hours. Cells were then washed in RPMI and added at varying ratios (1:1, 2:1, 4:1, 6:1 treated: untreated) in co-culture with untreated $CD4^+25^-$ T cells in the presence of irradiated antigen presenting cells (APCs) in 200µl of cRPMI at 37°C for 72h. 18h prior to harvest, cultures were pulsed with ^{3}[H]-thymidine (0.5 µCi/well). Plates were harvested using a Skatron Basic 96 Harvestor (Molecular Devices, Sunnyvale, CA). ^{3}[H]-thymidine incorporation was measured using a liquid scintillation counter (Beckman, Fullerton, CA).

K. Regulatory T cell (Treg) suppressor assay

Purified $CD4^+25^+$ T cells from C57BL/6 mice were incubated with the indicated concentrations of SB3CT or vehicle control for 6 hours. Cells were then washed in RPMI and added at varying ratios (0.5:1 and 1:1 treated: untreated) in co-culture with untreated $CD4^+25^-$ T cells in the presence of irradiated antigen presenting cells (APCs) in 200µl of cRPMI at 37°C for 72h. 18h prior to harvest, cultures were pulsed with 3[H]-thymidine (0.5 µCi/well). Plates were harvested using a Skatron Basic 96 Harvestor (Molecular Devices, Sunnyvale, CA). 3[H]-thymidine incorporation was measured using a liquid scintillation counter (Beckman, Fullerton, CA).

L. Gelatin zymography

Cell lysates and conditioned media supernatant were collected, concentrated to 16X and centrifuged to remove any cell debris, and stored at -80°C prior to assay. The

concentrated samples were suspended in sodium dodecyl sulfate (SDS) electrophoresis sample buffer but not heated, and subjected to SDS-page under non-reducing conditions on 10% acrylamide gels containing 2 mg/ml gelatin. The gels were soaked in two 25-min changes of 0.05 M Tris-HCl, 5 mM CaCl2, 1 µM ZnSO4, 2.5% Triton X-100 to remove SDS, then washed for 5 min in the same buffer without Triton X-100. Then the gels were incubated overnight at 37°C in 0.05 M Tris-HCl, 5 mM CaCl2, 1 µM ZnSO4, 1% Triton X-100, pH 7.6, containing 1 mM aminophenylmercuric acetate (APMA) to activate the MMP within the gel. After incubation, the gels were stained with 1% Coomassie Blue. Gelatinolytic activity was identified as clear bands of lysis on a uniform blue background. To confirm that the observed gelatinolysis was due to MMP activity, gels were incubated in assay buffer containing 1mM 1,10 phenanthroline, a matrix metalloproteinase inhibitor.

M. Cytokine profiling by quantitative real-time PCR

Purified $CD4^+$ T cells were incubated with the indicated concentrations of SB3CT for 6h and then washed three times with RPMI 1640. Drug or vehicle-treated T cells were cultured ($1x10^6$/ml) with anti-CD3 Ab (0.5µg/ml) in cRPMI for 1-12h. Supernatants were collected and stored at -80°C. Cells were collected and total RNA was isolated using an RNeasy RNA extraction kit (Qiagen, Inc., Valencia, CA). Total RNA quantity and purity was assessed using a NanoDrop ND-1000 (Thermo Scientific, Wilmington, DE). cDNA was synthesized using 1µg of RNA with qScript™ cDNA SuperMix (Quanta Biosciences, Gaithersburg, MD) according to the manufacturer's instructions. mRNA expression levels were measured by real-time quantitative PCR and detected with

PerfeCTa™ SYBR Green FastMix, Low ROX (Quanta Biosciences, Gaithersburg, MD) on a Applied Biosystems 7500 according to the manufacturer's instructions. Briefly, 2μL of cDNA was amplified for 40 cycles at 95°C for 15 sec, 60°C for 1 min, and 72°C for 30sec. Each sample was run in triplicate and normalized with murine β-actin.

Primer	Sequence
β-actin	F: CAATAGTGATGACCTGGCCGT R: AGAGGGAAATCGTGCGTGAC
IL-2	F: TCCAGAACATGCCGCAGAG R: CCTGAGCAGGATGGAGAATTACA
TNF-α	F: TGGGAGTAGACAAGGTACAACCC R:CATCTTCTCAAAATTCGAGTGACAA
IFN-γ	F: TGGCTCTGCAGGATTTTCATG R: TCAAGTGGCATAGATGTGGAAGAA
NFATc1	F: TGGAAGCAAAGACTGACCGG R: CTGGTTGCGGAAAGGTGGTAT
Foxp3	F: CTTACAGCTGAGAGGGGTGC R: CCAGATGTTGTGGGTGAGTG
CD25	F: TACAAGAACGGCACCATCCTAA R: TTGCTGCTCCAGGAGTTTCC
IL-10	F: GGTTGCCAAGCCTTATCGGA R: ACCTGCTCCACTGCCTTGCT

Table 1. Primer pairs used for qRT-PCR analysis.

N. Cytokine profiling by cytometric bead array (CBA)

Purified MMP9 deficient or SB3CT treated (10μM) $CD4^+$ T cells were incubated with 10μM of SB3CT for 6h and then washed three times with RPMI 1640. Drug or vehicle-treated T cells were cultured ($1x10^6$/ml) with anti-CD3 Ab (0.5μg/ml) in cRPMI for 1-12h. Supernatants were collected and cytokine protein levels were measured using the Mouse Inflammatory Cytokine Bead Array Kit (BD Biosciences, San Jose, CA) according to the manufacturer's instructions. Briefly, Mouse Inflammation Capture Bead suspensions for each cytokine to be assayed were mixed together and 50μl aliquots were

added into FACS tubes (Falcon 12x75mm 5ml round-bottom polystyrene tubes) (BD Biosciences, San Jose, CA) containing PE detection reagent and sample supernatant. Samples were washed and analyzed on a Beckman Coulter Flow Cytometer using BD CBA Software.

O. Intracellular calcium flux

Calcium flux was measured in $CD4^+$ and $CD8^+$ wild-type or MMP9 deficient or SB3CT treated (10μM) T cells using the Fluo-4 NW Calcium Assay kit (Molecular Probes, Carlsbad, CA) in accord with the provided instructions. In brief, 2.5 x 10^6 T cells were resuspended in 1.0 ml Assay Buffer (1x HBSS, 20mM HEPES), which contains calcium or calcium-free media (Invitrogen) then aliquoted in 50μl (1.25 x 10^5 cells) in a 96-well plate and incubated for 1h at 37^0C. The cells were then loaded with the 50μl of Fluo-4 dye diluted in Assay Buffer with 2.5mM probenecid acid for 30 minutes at 37°C, followed by a 30 minute incubation at room temperature. Cells were then stimulated and read in real time (0-300sec) on a Molecular Devices FlexStation I (Sunnyvale, CA) for 300 seconds.

P. Total and phosphorylated MEK1/2 colorimetric assay

$CD8^+$ T cells were isolated from wild-type C57BL/6 mice. Cells were then treated with vehicle or SB3CT for 6 hours. A 96-well culture plate was treated with 10μg/ml poly-L-lysine for 30 minutes at 37°C. The plate was then washed twice for 5 minutes with PBS. Following the incubation with SB3CT, cells were then washed and plated in a 96-well culture plate that had been treated with 10μg/ml poly-L-lysine. Cells were then

plated at $3x10^5$ cells/well. Cells were then stimulated for varying times (0-60 minutes) with soluble anti-CD3 Ab (0.5µg/ml). Cells were then fixed by replacing the growth medium with 100µl of 8% formaldehyde in PBS. Cells were then incubated for 20 minutes at room temperature, then washed 5 times. 100µl of quenching buffer was added to the cells and incubated for 20 minutes at room temperature. Cells were again washed 2 times. 100µl of blocking buffer was added to the plate and incubate 1 hour at room temperature. The primary antibody (anti-MEK1/2 Ab) was then added and the cells were again incubated for 1 hour. Plates were again washed 3 times. 100µl diluted secondary antibody was added to the plate and the plate was covered and incubated at room temperature for 1 hour. The plate was then washed 2 times with 1X PBS. 100µl of developing solution was added to each well and incubated for 20 minutes at room temperature protected from direct light. 100µl of stop solution was added to each well and absorbance was read on a spectrophotometer at 450nm.

Q. Activation of $CD8^+$ $Thy1.1^+$ T cells for adoptive transfer into CC10-OVA mice

Lymph node and spleen were isolated from OT-I transgenic mice and $CD8^+$ T cells were isolated as stated above. OT-I cells were then treated with 10µM of SB3CT or the corresponding vehicle control (DMSO + PEG) for 6 hours, followed by three washes in culture media. Splenocytes were isolated from wild-type C57BL/6 mice and irradiated (2500 rad) to serve as the antigen presenting cells (APCs)/feeder cells in the activation co-culture. $5x10^7$ irradiated splenocytes were cultured in 30ml of 10% DMEM supplemented with 0.7µg/ml of OVA peptide (SIINFEKL) for 5 min, followed by the addition of OT-1 T cells ($5x10^6$), anti-CD28 Ab (2µg/ml), IL-2 (132.02 U/ml) and IL-12

(10 ng/ml). On day 3, cells the cells were split and supplemented with more IL-2 (25U/ml) in a final volume of 30mls. On day 5, cells were harvested and prepared for adoptive transfer into CC10-OVA mice. Cells were resuspended in PBS, and 7.5x105 cells were then intratracheally instilled into the lungs of CC10-OVA mice.

R. Isolation of lymphocytes from the lung of CC10-OVA mice in preparation for flow cytometry

The lungs of CC10-OVA mice were perfused and excised 10 days after adoptive transfer of SB3CT or vehicle treated OT-I Tg T cells. The lung was finely minced on ice, followed by a 60-90 minute digestion at 37°C with collagenase/dispase (0.2mg/ml of each) in RPMI medium with 5% fetal calf serum (FCS), in the presence of 25µg/ml DNase. To improve tissue disintegration, lungs were pipetted every 5 minutes using a pasteur pipet. Ethylenediaminetetraacetic acid was added to a final concentration of 5 mM, followed by an additional 5 minute incubation at 37°C. Cells were passed through a 70 µm cell strainer, washed, and lung lymphocytes were isolated by density centrifugation. Briefly, lung samples were resuspended in 5mL of a solution of 44% percoll in 1X PBS. Five mililiters of 66% percoll in 1X sterile PBS was gently added under the lung sample in 44% percoll. The samples were then centrifuged at 2000 rpm for 20 min, no break, at room temperature. The top layer was carefully aspirated to the interface. The interface was transferred into a new tube and washed. The cells were then resuspended in 2ml of lysis buffer for 1 minute, then washed in cRPMI. Following isolation, cells were analyzed by flow cytometry for the presence of $CD8^+$ $Thy1.1^+$ T

cells, corresponding to OT-I Tg T cell migration into the lung. The percentage of macrophage and eosinophil populations present in the lung were also measured by flow cytometry.

S. Flow Cytometry

1. Cell phenotyping in MMP9 deficient mice

$CD4^+$ and $CD8^+$ T cells were isolated from wild-type and MMP9 deficient mice. In some studies, the wild-type mice were treated with SB3CT or the corresponding vehicle control, as stated above. Following the various treatment conditions, the cells were collected and washed in FACs buffer (10% BSA in PBS). Non-specific binding was blocked with FACs buffer supplemented with anti-CD16/anti-CD3 Ab2 Ab (0.5μg/well, eBioscience, San Diego, CA). Cells were then stained with anti-mouse CD4-FITC, CD8-PE, CD25-PE, CD40L-PE, CD44-PE, CD45RO-FITC, CD62L-APC, CD69-FITC, and CTLA-4-PE Abs along with the corresponding isotype controls (all from eBioscience). After staining, cells were fixed in a 3% paraformaldehyde solution and read immediately on the flow cytometer. The data from 10,000 cells in the live gate were analyzed with a FACScan flow cytometer (Beckton Dickinson). FCS Express (DeNovo Software, Los Angeles, CA) was used for further analysis.

2. Cell phenotyping of SB3CT treated T cells

$CD4^+$ T cells were isolated from C57BL/6 wild-type mice and treated with SB3CT or the corresponding vehicle control. Following the various treatment conditions, the cells were collected and washed in FACs buffer (10% BSA in PBS). Non-specific

binding was blocked with FACs buffer supplemented with anti-CD16/anti-CD3 Ab2 Abs (0.5µg/well, eBioscience, San Diego, CA). Cells were then stained with anti-mouse CD25-PE and CD69-FITC Ab along with the corresponding isotype controls (all from eBioscience). After staining, cells were fixed in a 3% paraformaldehyde solution and read immediately on the flow cytometer. The data from 10,000 cells in the live gate were analyzed as stated above.

3. Cell phenotyping of $CD8^+$ $Thy1.1^+$ T cells in the lung of CC10-OVA mice following adoptive transfer of SB3CT treated OT-I Tg T cells.

Total lung cells were isolated as stated above. Cells were then collected and washed in FACs buffer (10% BSA in PBS). Cells were then analyzed immediately on the flow cytometer. The data from 10,000 cells in the live gate were analyzed as stated above.

4. Cell subset identification in BAL

Assessment of neutrophilic alveolitis in the animal model was determined by neutrophil accumulation in the BAL. BAL was collected from the lungs of wild-type and CC10 mice following adoptive transfer of vehicle or SB3CT treated OT-1 Tg T cells, by washing the mouse lung with 1.0ml of sterile 1X PBS. Collected fluid was then centrifuged for 10 minutes at 2000 rpm. Cell supernatant was then removed, and cell pellets were resuspended in 200µl of sterile 1XPBS. Cells were then stained with anti-GR1 Ab, which was used as a marker of neutrophils, and analyzed immediately on the flow cytometer. To measure the percentages of other cell populations present within the

BAL, cells were collected and washed in FACs buffer (10% BSA in PBS). Non-specific binding was blocked with FACs buffer supplemented with anti-CD16/anti-CD3 Abs (0.5μg/well, eBioscience, San Diego, CA). Cells were then stained with anti-mouse CD9 Ab, a surface marker for eosinophils and anti-CD11b Ab, a surface marker for macrophages. After staining, cells were fixed in a 3% paraformaldehyde solution and read immediately on the flow cytometer. The data from 10,000 cells in the live gate were analyzed with a FACScan flow cytometer (Beckton Dickinson). FCS Express (DeNovo Software, Los Angeles, CA) was used for further analysis.

T. Total BAL cell counts

BAL was collected by washing the mouse lung with 1.0ml of sterile 1X PBS. Collected fluid was then centrifuged for 10 minutes at 2000 rpm. Cell supernatant was then removed. Cell pellets were resuspended in 200μl of sterile 1XPBS. Cells were then diluted 1:10 or 1:20 in trypan blue and counted at 20X using an Olympus microscope

U. Histology

Lungs were perfused, inflated and fixed with neutral buffered formalin. The sections were then embedded in paraffin, sectioned, and stained with hematoxylin and eosin (performed at University of Chicago Medical Center). Images were acquired at 20X using an Olympus microscope and DP12 digital camera (Olympus, Center Valley, PA).

V. Statistical analysis

Data were analyzed by either 2-way Analysis of Variance (ANOVA) with paired t-test or non-parametric t-test using Prism 4 (GraphPad Software for Windows, San Diego, CA) or Microsoft Office Excel 2007 (Microsoft, Seattle, WA)

III. RESULTS

Chapter 1. The effects of matrix metalloproteinase inhibition on $CD4^+$ and $CD8^+$ T cell proliferative responses

A. MMP9 expression in primary murine $CD4^+$ and $CD8^+$ T cells

Among the members of the MMP family, MMP2 and MMP9 have been shown to be important in inflammation due to their critical role in the process of cell infiltration into tissues and matrix remodeling (24, 102). As such, many reports have highlighted a role for MMP9 in a variety of pulmonary diseases such as bronchiolitis obliterans syndrome (103), which results from alloimmune-mediated injury following lung allograft rejection and in asthma, which is thought to be a T cell-mediated disease. Abnormalities in MMP9 production have been observed in bronchoalveolar lavage fluid, bronchial tissue and serum of BOS and asthmatic patients (44, 51). Additionally, previous studies have demonstrated that MMP9 is inducible in both $CD4^+$ and $CD8^+$ T cells, in response to various stimuli (104, 105). However, the role of MMP9 in regulating T cell activation remains unknown.

To begin to address the role of MMP9 in T cell activation, we first wanted to determine whether T cell derived MMP-9 is present in the primary murine splenic $CD4^+$ and $CD8^+$ T cells of the C57BL/6 mouse strain. T cells were isolated from C57BL/6 mice and cultured in the presence or absence of soluble anti-CD3 Ab (0.5μg/ml) for 24 hours. Anti-CD3 is polyclonal agonistic antibody that binds the epsilon chain of the T cell

receptor to mimic antigen-MHC complex ligation, thereby inducing T cell activation and proliferation. MMP-9 mRNA and protein expression was measured in the cell lysates and conditioned media of activated $CD4^+$ and $CD8^+$ T cells by means of real-time PCR and substrate zymography, respectively.

As shown in [figure 5], there were detectable levels of MMP9 mRNA expression in unstimulated $CD4^+$ [figure 5A] and $CD8^+$ [figure 5B] T cells. Interestingly, following anti-CD3 Ab stimulation, an increase in MMP9 mRNA expression was detected in $CD8^+$ T cells [figure 5B] but not in $CD4^+$ T cells [figure 5A]. To determine if there was a correlation with MMP9 expression at the protein level, MMP9 expression was measured in the cell lysates and conditioned media of activated $CD4^+$ and $CD8^+$ T cells. As shown in [figure 5C], lysate from unstimulated $CD4^+$ T cells display a prominent band which corresponds to pro-MMP9 (105kDa). T cell lysates from activated (anti-CD3 Ab stimulated) $CD4^+$ T cells reveal a faint band again corresponding to pro-MMP9. Conditioned media from the activated cell culture supernatant revealed two bands, one corresponding to pro-MMP9 and a band below at approximately 95kDa, corresponding to the conversion of pro MMP9 to the active form [figure 5C].

Observation of unstimulated $CD8^+$ T cell lysate also reveals a prominent band representing pro-MMP9 [figure 5C]. Cell lysate from activated $CD8^+$ T cells reveal a faint band representing pro-MMP9, whereas conditioned media from the activated cell culture supernatant revealed two bands, again corresponding to the pro- and active form of MMP9 [figure 5C]. As expected, media from unstimulated cells displays no MMP-9 expression. All the gelatinolytic activities were blocked by the addition of 1,10 phenanthroline, which inhibits MMP activity, to ensure that the activity seen is

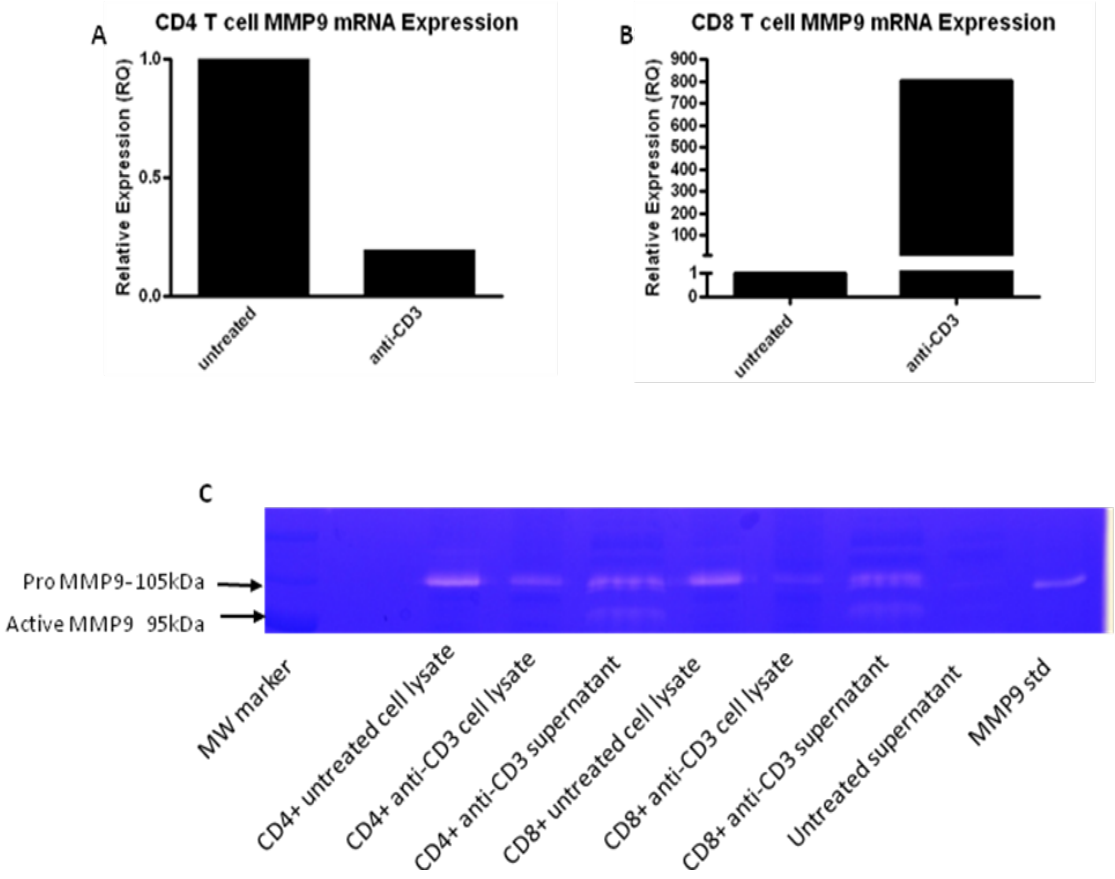

Figure 5. Differential MMP9 mRNA and protein expression in $CD4^+$ and $CD8^+$ T cells

Pure splenic A) $CD4^+$ and B) $CD8^+$ T cells were isolated from C57BL/6 mice. T cells were plated at $2x10^6$/well in a 24 well plate in the presence of anti-CD3 Ab (1μg/ml) for 24 hours. RNA was isolated, cDNA synthesizes and mRNA expression levels were measured by real-time quantitative PCR. Data were normalized to β-actin. A and B are data are representative of two separate experiments performed in triplicate. C) Gelatin zymogram analysis of $CD4^+$ and $CD8^+$ T cell lysates and supernatant. Data representative of four separate experiments.

gelatinolytic (data not shown). These data confirm that T cell derived pro- and active MMP-9 is expressed in murine $CD4^+$ and $CD8^+$ T cells.

B. Broad-spectrum MMP inhibition abrogates alloantigen- and anti-CD3 Ab induced T cell proliferation

Our laboratory recently reported that blocking MMPs in vivo using a broad-spectrum MMP inhibitor, COL-3, a chemically modified tetracycline, abrogated alloantigen-induced T cell proliferation in a rat model of lung transplantation, suggesting a role for MMPs in T cell activation (106). To address this question, we utilized mixed leukocyte reactions to determine if murine splenic T cells treated with broad-spectrum MMP inhibitors (1,10 phenanthroline or COL-3) were able to respond to alloantigen stimulation. Dendritic cells (antigen presenting cells) isolated from C57BL/6 mice were co-cultured at varying ratios (0.01 and 0.075) in the presence of allogeneic T cells from Balb/c mice with the addition of varying concentrations of 1,10 phenanthroline (0.001-0.1μM). As anticipated, untreated T cells proliferated in response to alloantigen stimulus at both ratios [figure 6A]. As shown in figure 6A, treatment with a very low concentration (0.001μM) of 1.10 phenanthroline showed proliferative responses similar to those seen in untreated cells (white bar). In contrast, compared to untreated cells, treatment with 0.01μM (striped bar) and 0.1μM (shaded bar) of 1,10 phenanthroline completely abrogated the alloantigen-induced proliferative responses.

To further examine the effects of MMP inhibition on T cells specifically, T cell proliferation assays were utilized, in which, T cells were treated for 6 hours with 1,10 phenanthroline followed by stimulation with soluble anti-CD3 Ab.

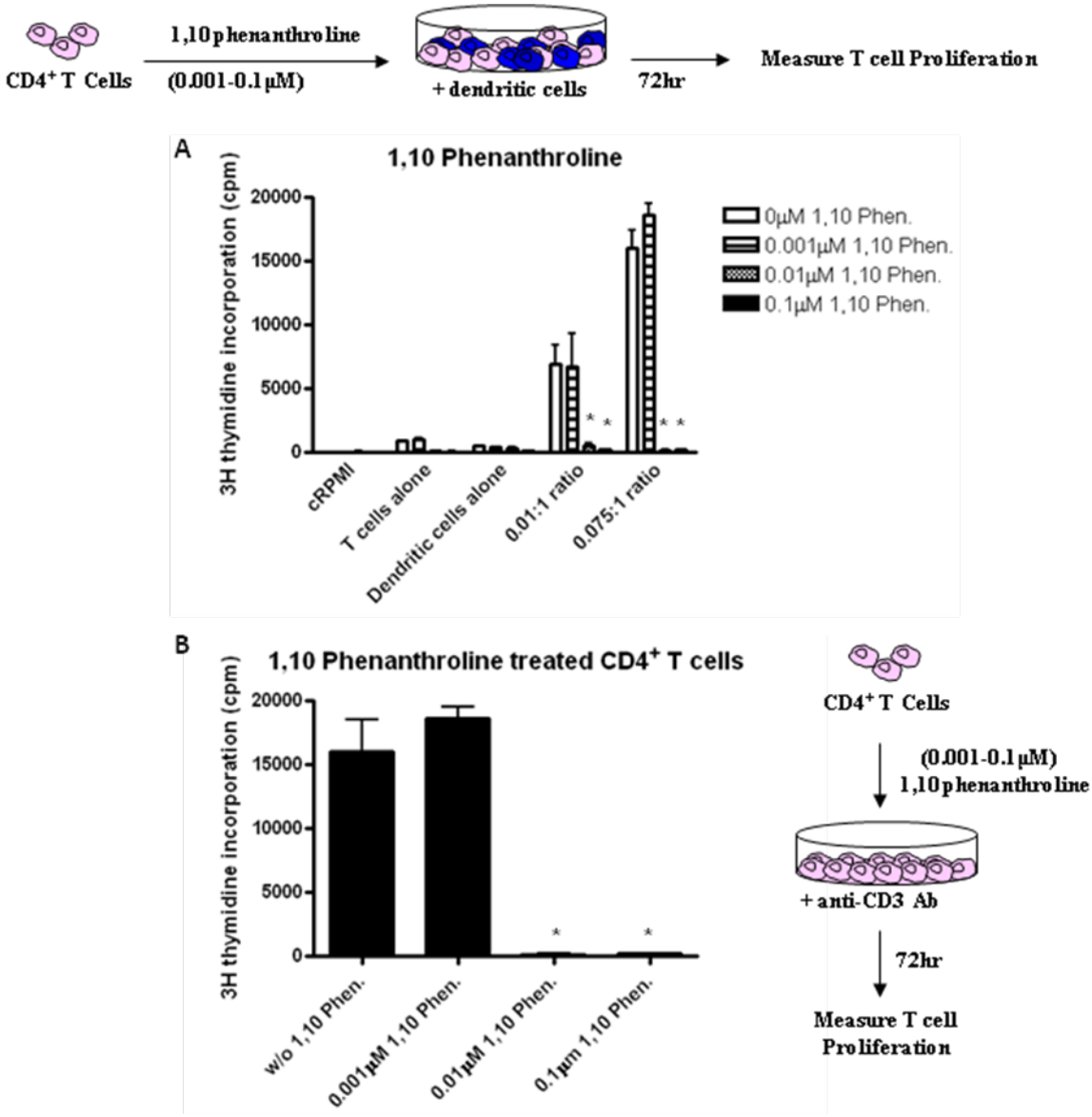

Figure 6. Broad spectrum MMP inhibition by 1,10 phenanthroline (0.001-0.1µM) reduced alloantigen and anti-CD3 induced T cell proliferation

Pure splenic $CD4^+$ T cells were isolated from Balb/c or C57BL/6 mice. A) $CD4^+$ Balb/c T cells were treated with varying concentrations of 1,10 phenanthroline (0.001-0.1µM) and cocultured with allogeneic (C57BL/6) dendritic cells at various ratios (0.01-0.15:1 DC:T cell). B) $CD4^+$ T cells isolated from C57BL/6 mice were treated with varying concentrations of 1,10 phenanthroline (0.001-0.1µM). Cells were then washed in RPMI and plated at $3x10^5$/well in a 96 well plate in the presence of anti-CD3 Ab (0.5µg/ml). 18 hours prior to harvest, 3H thymidine (0.5µCi/well) was added to the culture. T cell proliferation was measured by the amount of 3H thymidine incorporation. These data are representative of the mean ± SD of one of three separate experiments performed in triplicate. *p<0.001 compared to anti-CD3 Ab stimulated untreated T cells. (n=3)

As shown in [figure 6B], untreated anti-CD3 Ab stimulated cells exhibited a normal proliferative response. Similar to the results shown in the mixed leukocyte reaction above, T cells treated with1,10 phenanthroline [figure 6B] exhibited a significant decrease in proliferation at 0.01μM and 0.1μM ($p<0.001$). It is worth nothing that testing a concentration between 0.001 and 0.01 such as 0.005 may provide more accurate dose-dependent examination of 1,10 phenanthroline. To examine the effects of COL-3 on alloantigen stimulation, mixed leukocyte reactions were performed as above. Dendritic cells (antigen presenting cells) were isolated from C57BL/6 mice and co-cultured at varying ratios (0.01 and 0.075) in the presence of allogeneic T cells from Balb/c mice with the addition of varying concentrations of COL-3 (1-100μM).

Observation of COL-3 treatment revealed a significant decrease in alloantigen-induced proliferation in response to 100μM treatment of COL-3 ($p<0.001$), as compared to untreated cells, [figure 7A]. Likewise, examination of COL-3 treated T cells [figure 7B] in T cell proliferation assays reveals a dose-dependent decrease in proliferative ability as the concentration of COL-3 increases from 1μM to 100μM ($p<0.001$). Collectively, these data demonstrate that broad-spectrum MMP inhibition abrogates alloantigen-induced and anti-CD3 Ab-induced T cell proliferation, thereby confirming the in vivo data from the rat lung transplant model (106), suggesting an important role for MMPs in T cell activation.

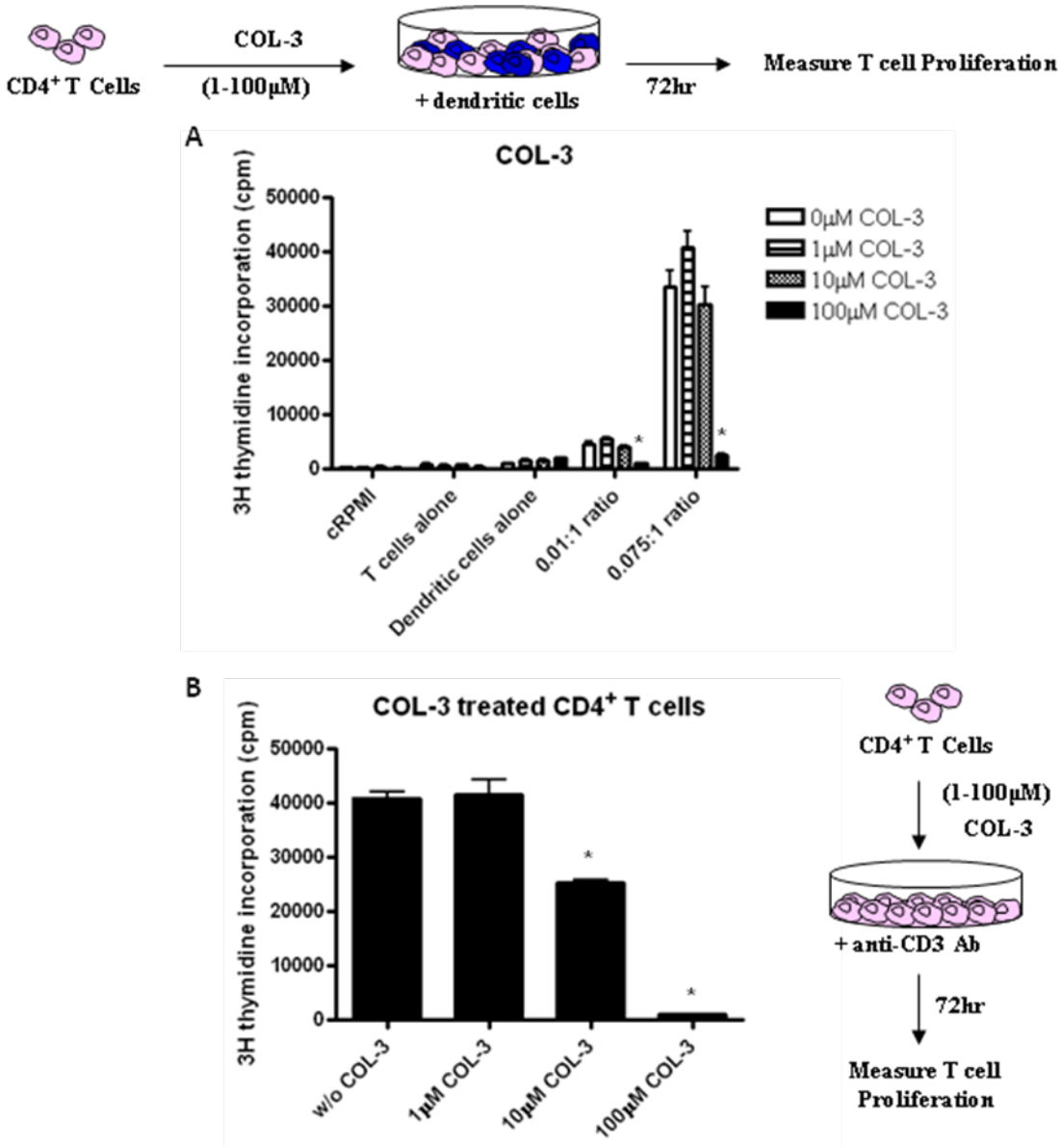

Figure 7. Broad spectrum MMP inhibition by COL-3 (1-100µM) reduced alloantigen and anti-CD3 induced T cell proliferation

Pure splenic $CD4^+$ T cells were isolated from Balb/c or C57BL/6 mice. A) $CD4^+$ Balb/c T cells were treated with varying concentrations of 1,10 phenanthroline (1-100µM) and cocultured with allogeneic (C57BL/6) dendritic cells at various ratios (0.01-0.15:1 DC:T cell). B) $CD4^+$ T cells isolated from C57BL/6 mice were treated with varying concentrations of COL-3 (1-100µM). Cells were then washed in RPMI and plated at $3x10^5$/well in a 96 well plate in the presence of anti-CD3 Ab (0.5µg/ml). 18 hours prior to harvest, 3H thymidine (0.5µCi/well) was added to the culture. T cell proliferation was measured by the amount of 3H thymidine incorporation. These data are representative of the mean ± SD of one of three separate experiments performed in triplicate. *$p<0.001$ compared to anti-CD3 Ab stimulated untreated T cells. (n=3)

C. Anti-CD3 Ab- induced T cell proliferation is abrogated following specific MMP9 inhibition

Many studies have used broad-spectrum MMP inhibitors (MMPIs) to prevent MMP activity. Many of the earlier reports studying the role of MMPs in various disease states have used broad-spectrum MMP inhibitors (MMPIs), such as COL-3. These inhibitors are designed to chelate the active-site zinc ions. However, they have also been shown to be problematic due to their lack of specificity and their effects on other non-related signaling events. One such study reported that COL-3 inhibits the activity of protein kinase C (PKC) in mast cells, suggesting that COL-3 functions as more than just an MMPI and can negatively affect cell growth and differentiation (107). To circumvent these limitations, a MMP2 and MMP9 (gelatinase) specific mechanism-based inhibitor, SB3CT, was utilized, which irreversibly inhibits MMP9 by permanently blocking the cysteine switch interaction (47). That is, the inhibitor prevents activation by blocking the disruption of the cysteine residue (thiol group) interaction with the Zn^{2+} ion. As shown in figure 4, the thiirane sulfur group of the inhibitor first coordinates with the zinc in the active site of the MMP. The coordinated thiirane is then predisposes the inhibitor to nucleophilic attack by the glutamate located in the active site of the MMP. This mechanistic series of events leads to covalent modification and the loss of activity.

With the previous data implicating the importance of MMP inhibition in T cell activation, it was first important to determine if SB3CT inhibited MMP9 expression in $CD4^+$ and $CD8^+$ T cells. To accomplish this, $CD4^+$ and $CD8^+$ T cells were isolated from wild-type C57BL/6 mice were treated with 10μM of SB3CT for 6 hour, washed and then cultured in the presence of soluble anti-CD3 Ab for 72 hours. Cells were then collected

and processed for gene analysis by means of real-time PCR. SB3CT treated $CD4^+$ T cells [figure 8A] and $CD8^+$ T cells [figure 8B] exhibited fewer MMP9 gene transcripts as compared to vehicle treated cells. To assess enzymatic activity, $CD8^+$ T cells were treated with 10μM of SB3CT for 6 hours, washed and then cultured in the presence of soluble anti-CD3 Ab for 24 hours. Cell lysates and conditioned media were collected and analyzed by substrate zymography. As shown in figure 8C, pro and active MMP9 is expressed in untreated CD8+ T cell lysate. Six hour treatment of SB3CT decreases the expression of active MMP9, while not decreasing pro-MMP9 expression. Following stimulation with anti-CD3 Ab, pro- and active MMP9 expression is diminished. Supernatant from SB3CT treated CD8+ T cells displayed a decrease in pro-MMP9 expression, although some active MMP9 is still present. These data demonstrate that SB3CT inhibits MMP9 mRNA expression, as well as, pro- and active MMP9 protein expression.

Next, we wanted to determine whether specific MMP inhibition by means of SB3CT, would affect T cell activation in a similar manner as was shown following broad spectrum treatment with COL-3. To explore this, mixed leukocyte reactions were utilized. Dendritic cells (antigen presenting cells) isolated from C57BL/6 mice were co-cultured at varying ratios (0.01, 0.075 and 0.15) in the presence of allogeneic T cells from Balb/c mice with the addition of varying concentrations of SB3CT (1-10μM) for 72 hours. As expected, untreated T cells proliferated in response to alloantigen stimulus at all three ratios [figure 9A]. As shown in figure 9A, 0.01μM (striped bar) and 1 μM (shaded bar) of SB3CT showed proliferative responses similar to those seen in untreated

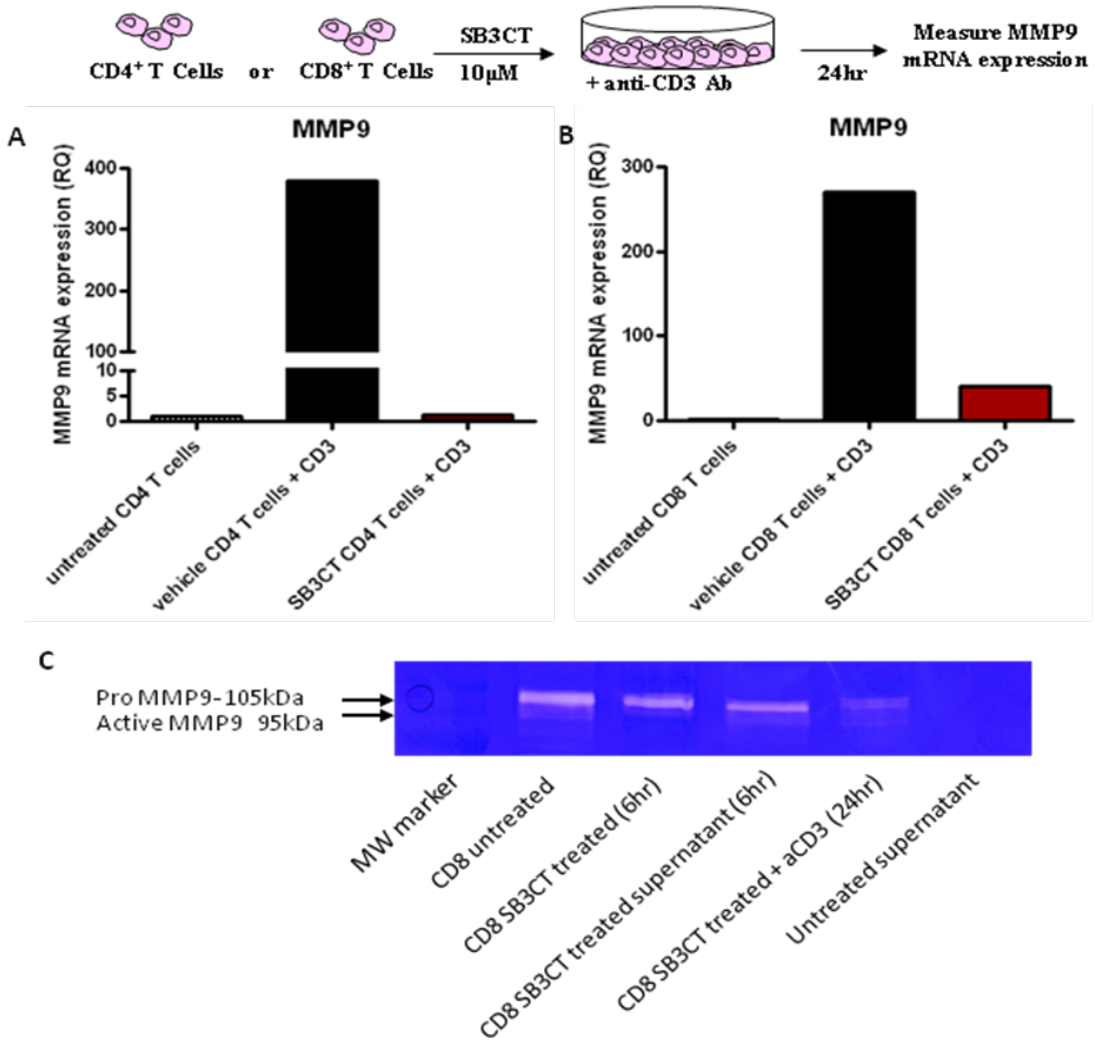

Figure 8. MMP9 specific inhibition by SB3CT treatment abrogates MMP9 expression in $CD4^+$ and $CD8^+$ T cells

A) Pure splenic $CD4^+$ and B) $CD8^+$ T cells were isolated from wild-type C57BL/6 mice. Cells were treated with 10µM of SB3CT or VCtl for 6 hours, then plated at $2x10^6$/tube in 3ml tissue culture tubes in the presence of anti-CD3 Ab (0.5µg/ml) for 24 hours. MMP9 mRNA expression levels were measured by real-time quantitative PCR. These data are representative of two separate experiments performed in triplicate (n=2) C) Gelatin zymogram analysis of CD8 T cell lysates and supernatant. n=1

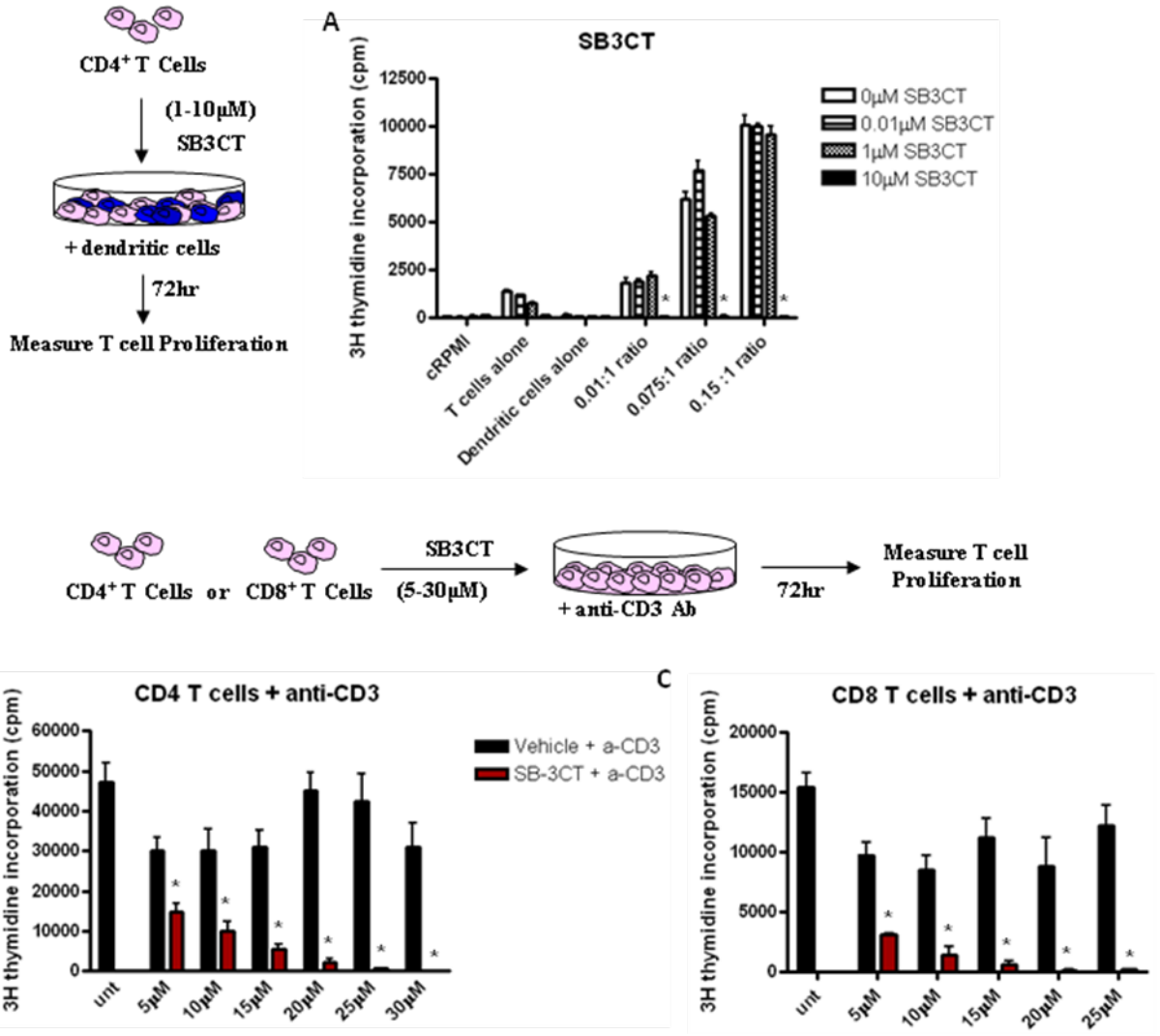

Figure 9. MMP9 specific inhibition by SB-3CT (1-30μM) reduced alloantigen and anti-CD3 induced T cell proliferation

Pure splenic $CD4^+$ and $CD8^+$ T cells were isolated from Balb/c or C57BL/6 mice. A) $CD4^+$ Balb/c T cells were treated with varying concentrations of SB3CT (0.01-10μM) or vehicle (VCtl) and cocultured with allogeneic (C57BL/6) dendritic cells at various ratios (0.01-0.15:1 DC:T cell). B) C57BL/6 $CD4^+$ T cells or C) $CD8^+$ T cells were treated with varying concentrations of SB3CT (5-30μM) or VCtl for 6 hours. Cells were then washed in RPMI and plated at $3x10^5$/well in a 96 well plate in the presence of anti-CD3 Ab (0.5μg/ml) for 72 hours. 18 hours prior to harvest, 3H thymidine (0.5μCi/well) was added to the culture. T cell proliferation was measured by the amount of 3H thymidine incorporation. These data are representative of the mean ± SD of one of three separate experiments performed in triplicate. *p<0.001 compared to anti-CD3 Ab stimulated untreated T cells. (n=3)

cells (white bar). Strikingly, treatment of cells with 10μM of SB3CT (black bar) completely abrogated T cell proliferation.

To next investigate T cells specifically, $CD4^+$ and $CD8^+$ T cells were isolated from wild-type C57BL/6 mice and treated with varying concentrations of SB3CT (5-20μM) for 6 hour, washed and then cultured in the presence of soluble anti-CD3 Ab for 72 hours. Notably, SB3CT treated $CD4^+$ [figure 9B] and $CD8^+$ [figure 9C] T cells exhibited a dose-dependent decrease in proliferative ability in response to anti-CD3 Ab stimulation, as compared to vehicle treated cells. These data corroborate the previous data shown with broad-spectrum MMPIs and further suggest that specific gelatinolytic MMP inhibition significantly abrogates T cell activation.

D. SB3CT does not induce cell death or anergy in $CD4^+$ or $CD8^+$ T cells

It is well known that the activation of T cells via ligation of the T cell receptor (TCR) induces a myriad of signaling events, including an increase in intracellular calcium that leads to the nuclear translocation of NFAT (nuclear factor of activated T cells) which activates the transcription of many pleiotropic genes, such as IL-2 and the IL-2 receptor (CD25). The data raise thus far the possibility that the decrease in T cell activation may be due to cell death or anergy. Trypan blue exclusion along with annexin V and propidium iodide (PI) staining, used to detect early cell death revealed that cell viability was greater than 90 percent following treatment with SB3CT, suggesting that the decrease in proliferative ability is not due to cells death [figure 10]. To assess whether or not SB3CT treatment induces T cell anergy, T cell proliferation assays were utilized, in which exogenous IL-2 was added to vehicle or SB3CT treated T cells cultured in the

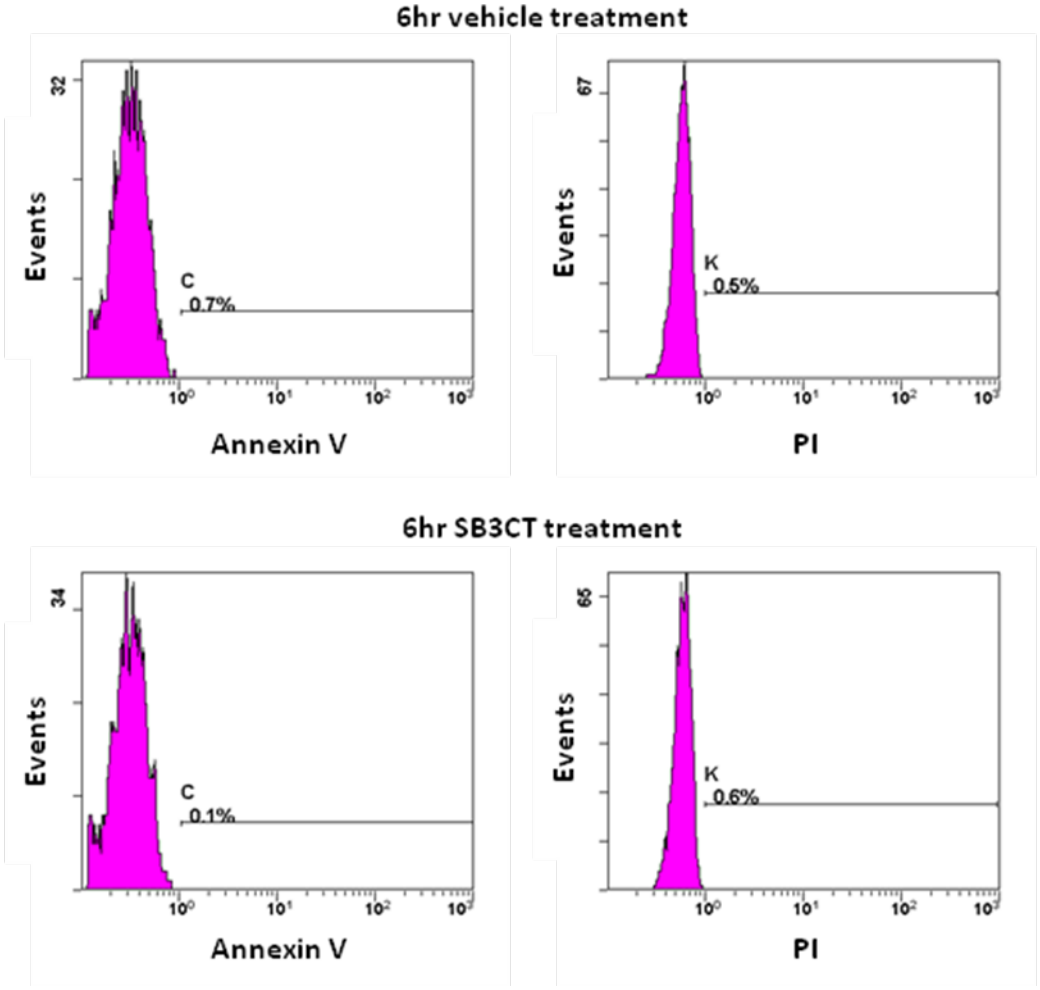

Figure 10. Cell viability of SB3CT treated CD4$^+$ T cells
Pure splenic CD4$^+$ T cells were isolated from wild-type C57BL/6 mice. Cells were treated with 10μM of vehicle or SB3CT for 6 hours. Cells were collected and stained with annexin V and propidium iodide (PI). Cells were analyzed by flow cytometry. These data are representative of the mean ± SD of one of two separate experiments (n=2).

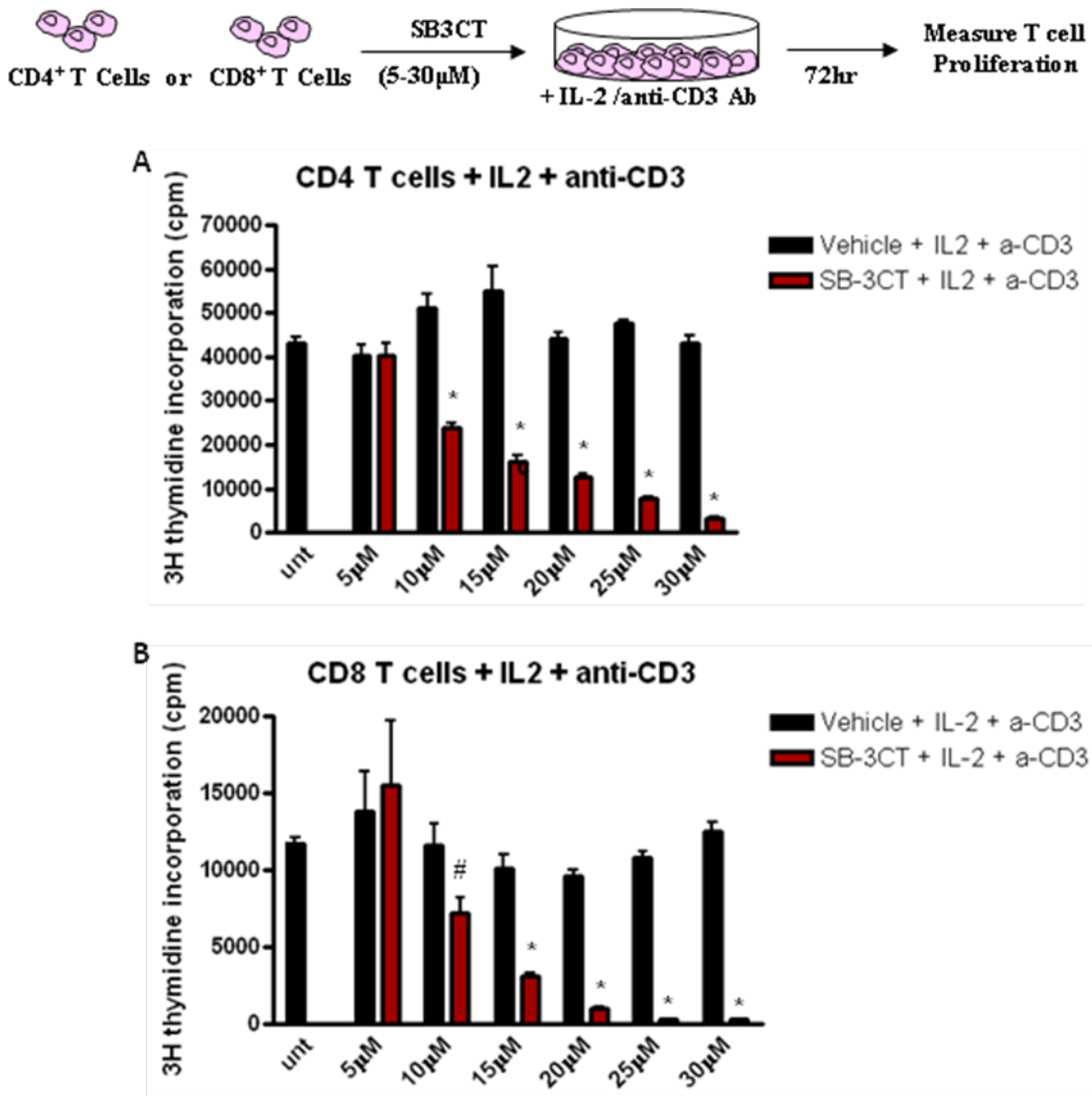

Figure 11. Exogenous IL-2 partially rescues anti-CD3 induced T cell proliferation in response to SB3CT treatment

Pure splenic $CD4^+$ and $CD8^+$ T cells were isolated from C57BL/6 mice. A) $CD4^+$ T cells or B) $CD8^+$ T cells were treated with varying concentrations of SB3CT (5-30µM) or VCtl for 6 hours. Cells were then washed in RPMI and plated at $3x10^5$/well in a 96 well plate in the presence of anti-CD3 Ab (0.5µg/ml) with 20U of IL-2 for 72 hours. 18 hours prior to harvest, 3H thymidine (0.5µCi/well) was added to the culture. T cell proliferation was measured by the amount of 3H thymidine incorporation. These data are representative of the mean ± SD of one of three separate experiments performed in triplicate. #$p<0.05$, *$p<0.001$ compared to anti-CD3 Ab stimulated untreated T cells. (n=3)

presence of soluble anti-CD3 Ab. As shown in [figure 11A] ($CD4^+$ T cells) and [figure 11B] ($CD8^+$ T cells), the addition of IL-2 induced partial recovery of the proliferative response in $CD4^+$ and $CD8^+$ T cells treated with 5μM of SB3CT, and increased the overall proliferative counts in all treatment groups as compared to the data shown in figure 9 (SB3CT + anti-CD3 Ab in the absence of exogenous IL-2). These data suggest that although partial recovery of T cell proliferation was shown in response to exogenous IL-2, the question of anergy remains unknown. This data does however reinforce that the cells are not undergoing cell death due to their ability to respond to IL-2 treatment.

One other possibility that may be responsible for the lack of a proliferative response may be that the drug (SB3CT) was not fully washed from the cells and therefore was still present in the supernatant. To investigate this possibility, T cell proliferation assays were performed, in which, $CD4^+$ T cells were treated with varying concentrations of SB3CT (10μM-1mM) for 6 hours. The cells were then washed and cultured for 48 hours. Following the 48 hour period, cell supernatants were collected and transferred to freshly plated $CD4^+$ T cells. These cells were cultured for 72 hours in the presence of soluble anti-CD3. As shown in figure 12, fresh T cells that were given cell supernatant from the 10μM SB3CT treatment group display a proliferative trend similar to that seen in untreated cells. 10-fold and 100 fold higher concentrations of supernatant completely abrogated T cell proliferation. These results confirm that at 10μM treatment, SB3CT is effectively washed from the cells and does not remain in the media. This is of importance because 10μM SB3CT is the concentration that was used in the majority of the experiments performed. Additionally, these data ensure that in later experiments in which

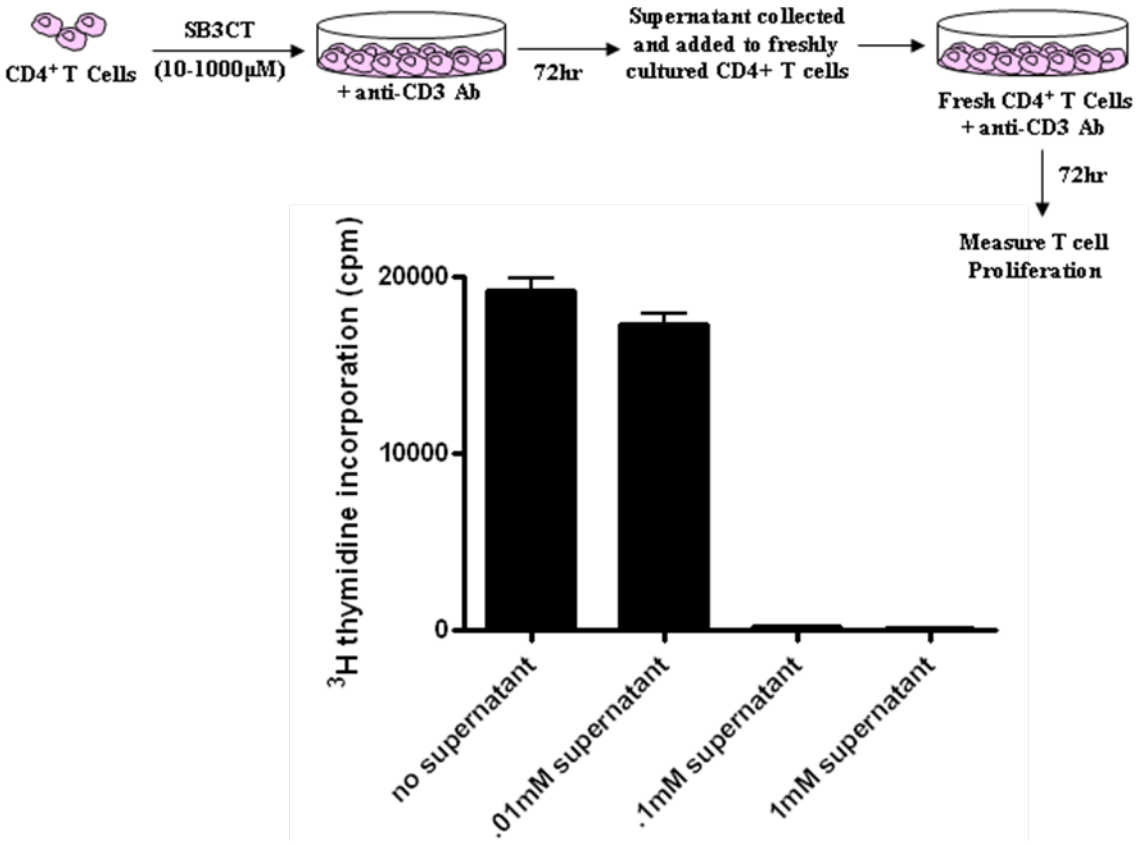

Figure 12. Cell Supernatant from T cells treated with 10µM SB3CT does not alter proliferation when added to fresh untreated T cells

Pure splenic $CD8^+$ T cells were treated with varying concentrations of SB3CT (5-30µM) for 6 hours. Cells were then washed in RPMI and plated at $3x10^5$/well in a 96 well plate in the presence of anti-CD3 Ab (0.5µg/ml) for 72 hours. Cell supernatants were then added to freshly isolated T cells cultured in the presence of anti-CD3 Ab (0.5µg/ml) for 72 hours. 18 hours prior to harvest, 3H thymidine (0.5µCi/well) was added to the culture. T cell proliferation was measured by the amount of 3H thymidine incorporation. These data are representative of the mean ± SD of one experiment performed in quadruplicate. (n=1)

untreated T cells are co-cultured in the presence of SB3CT treated T cells, the effects that are observed will not be due to residual SB3CT in the media.

E. Anti-CD3 Ab- induced proliferation is diminished in MMP9 deficient $CD4^+$ and $CD8^+$ T cells

With the continual advancement of mouse models and the development of MMP genetically deficient mice, we next examined the proliferative capacity of MMP deficient T cells by means of T cell proliferation assays. $CD4^+$ and $CD8^+$ T cells were isolated from MMP2, MMP9 and MMP2/9 deficient C57BL/6 mice and their corresponding wild-type littermates and cultured in the presence of soluble anti-CD3 Ab for 72 hours. As compared to wild-type T cells, MMP2 deficient T cells only exhibited a 20% decrease in proliferation [figure 13A]. Examination of MMP2/9 deficient T cells displayed a 40% decrease in proliferation [figure 13B]. Interestingly, MMP9 deficient cells displayed an 80% decrease in proliferative ability [figure 14A] ($p<0.001$).

Since the most pronounced decrease in T cell proliferation was seen following MMP9 deficiency, we also examined the proliferative ability of MMP9 deficient $CD8^+$ T cells. $CD8^+$ T cells from MMP9 deficient mice and their wild-type littermates were again cultured in the presence of soluble anti-CD3 Ab just as in previous experiments. Surprisingly, the results revealed a significant decrease in T cell proliferation similar to that seen in $CD4^+$ T cells [figure 14B] ($p<0.001$). These results confirm our previous findings and emphasize a key role of MMP9 in the process of T cell activation.

In addition to the anti-CD3-TCR ligation, there is a second co-stimulatory signal that occurs via interaction between the B7 family members, B7.1 or B7.2, on the antigen-

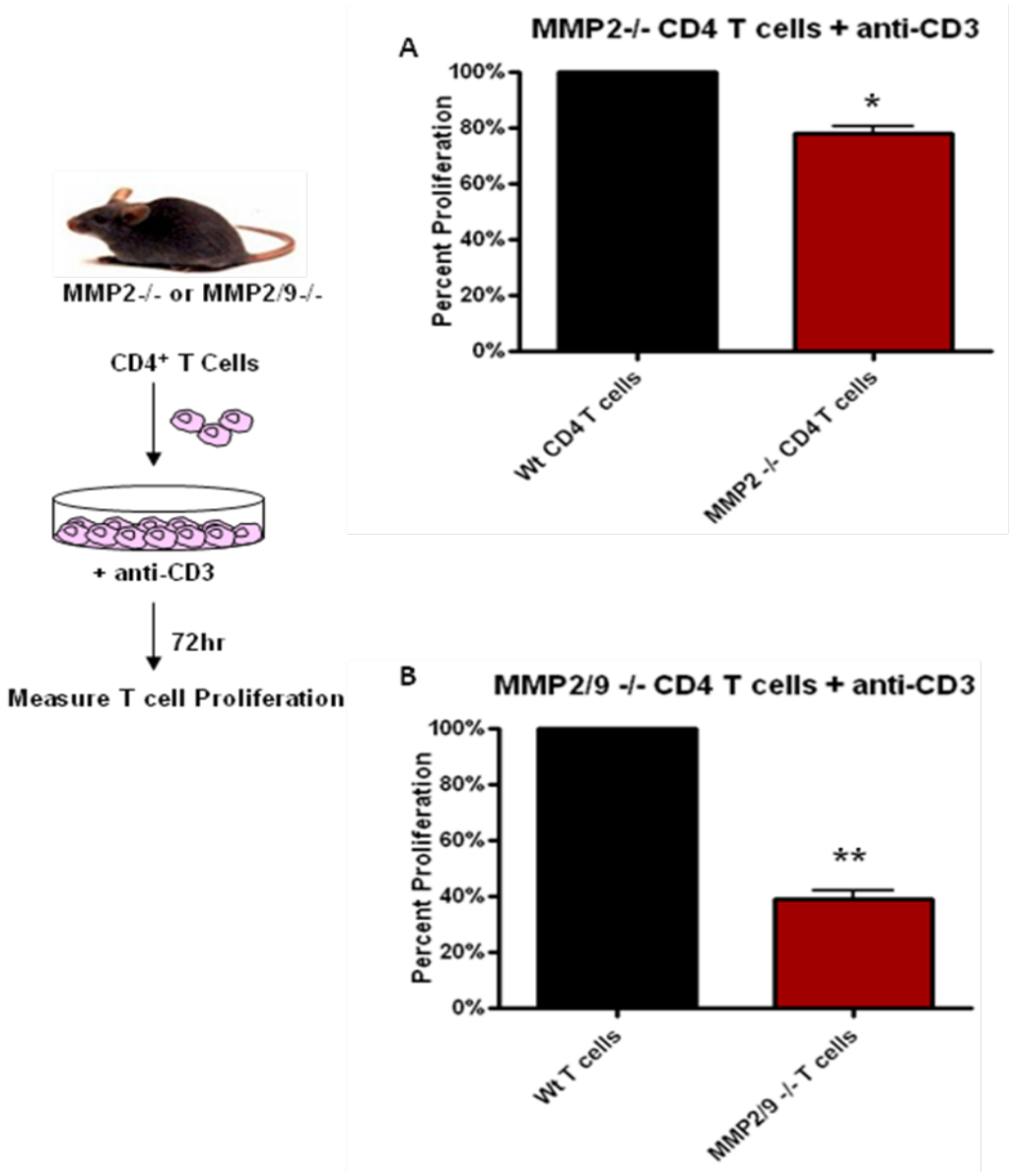

Figure 13. MMP2 and MMP2/9 deficient CD4$^+$ T cells display altered proliferative ability

CD4$^+$ T cells were isolated from wild-type and A) MMP2 or B) MMP2/9 deficient mice. Cells were plated at 3x10^5/well in a 96 well plate in the presence of anti-CD3 Ab (0.5µg/ml) for 72 hours. 18 hours prior to harvest, 3H thymidine (0.5µCi/well) was added to the culture. T cell proliferation was measured by the amount of 3H thymidine incorporation. These data are representative of the mean ± SD of one of three separate experiments performed in triplicate. (n=3) *P=0.02,**p<0.001 compared to wild-type T cells.

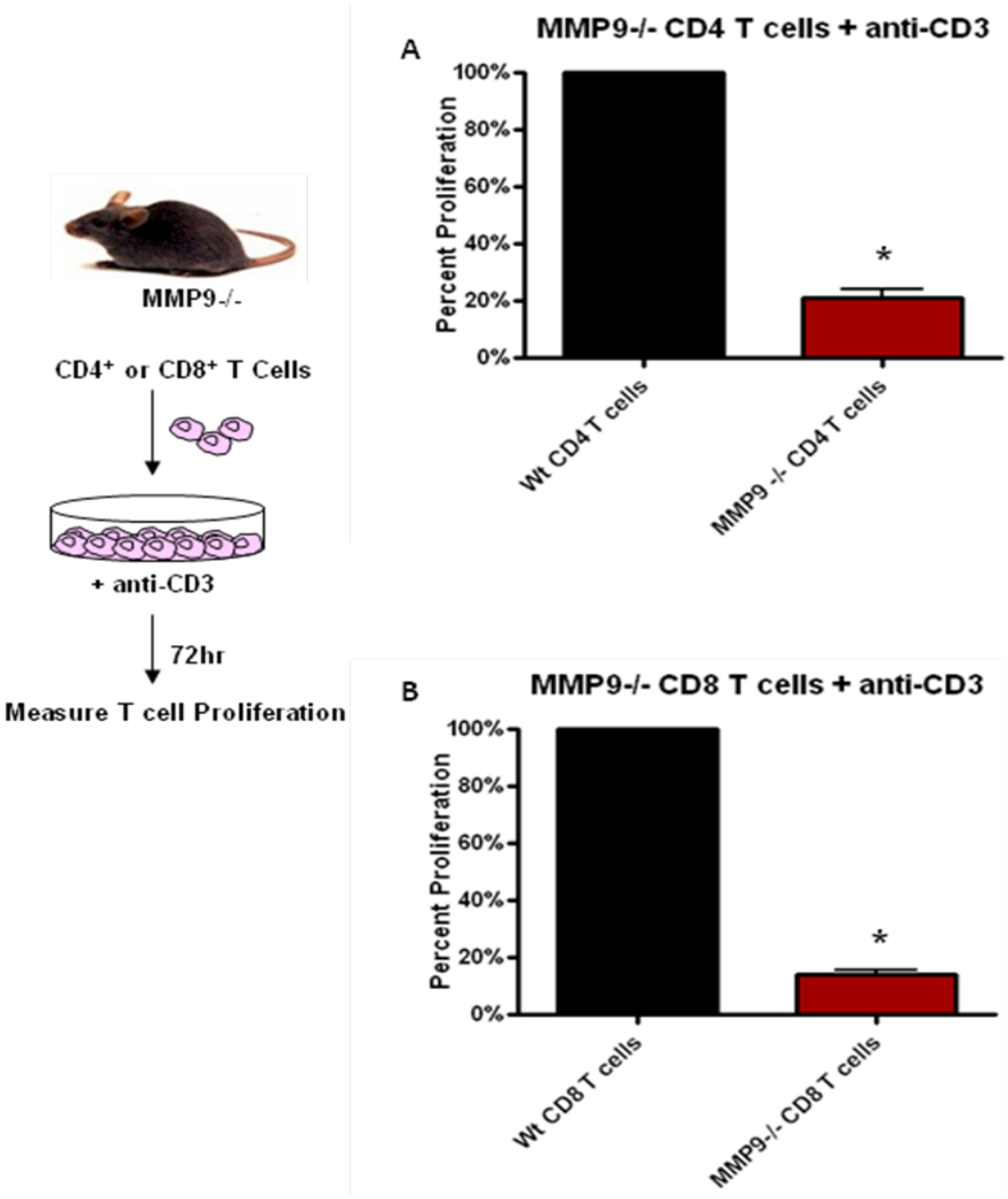

Figure 14. MMP deficient $CD4^+$ and $CD8^+$ T cells display impaired proliferative ability

A) $CD4^+$ and B) $CD8^+$ T cells were isolated from wild-type and MMP9 deficient mice. Cells were plated at $3x10^5$/well in a 96 well plate in the presence of anti-CD3 Ab (0.5μg/ml) for 72 hours. 18 hours prior to harvest, 3H thymidine (0.5μCi/well) was added to the culture. T cell proliferation was measured by the amount of 3H thymidine incorporation. These data are representative of the mean ± SD of one of three separate experiments performed in triplicate. *$p<0.001$ compared to wild-type T cells. (n=3)

presenting cells and CD28 on the T cell. CD28 is a 44-kd subunit found on the surface of most $CD4^+$ cells and 70% of $CD8^+$ cells. Anti-CD28 monoclonal antibodies can substitute for the B7 ligand to stimulate CD28 on the T cell and provide a strong stimulatory signal. With this understanding, we to determine if co-stimulation with anti-CD3/anti-CD28 Abs would alter the proliferation pattern of $CD8^+$ T cells from MMP9 deficient mice or following SB3CT treatment. To address the effects of co-stimulation on MMP9 deficient T cells, $CD8^+$ T cells were isolated from MMP9 deficient C57BL/6 mice and their corresponding wild-type littermates and cultured in the presence of soluble anti-CD3/anti-CD28 Abs for 72 hours. In the presence of co-stimulation T cell proliferation is increased in MMP9 deficient cells, as compared to wild-type co-stimulated cells [figure 15A]. As shown previously, in the presence of anti-CD3 Ab and absence of anti-CD28 Ab stimulation, MMP9 deficient T cells are abrogated, as compared to wild-type cells. These results demonstrate that anti-CD28 Ab co-stimulation is able to rescue the proliferative ability of MMP9 deficient $CD8^+$ T cells.

To examine the effects of co-stimulation on SB3CT treated T cells, $CD8^+$ T cells were isolated from wild-type C57BL/6 mice and treated with varying concentrations of SB3CT (1-25μM) for 6 hour, washed and then cultured in the presence of soluble anti-CD3/anti-CD28 Abs for 72 hours. As displayed in figure 15B, there was a dose-dependent decrease in T cell proliferation even in the presence of anti-CD3/anti-CD28 Abs. These results are similar to those previously shown above in response to stimulation with anti-CD3 alone (figure 11B), demonstrating that anti-CD28 Ab co-stimulation does not rescue T cell proliferation following SB3CT treatment.

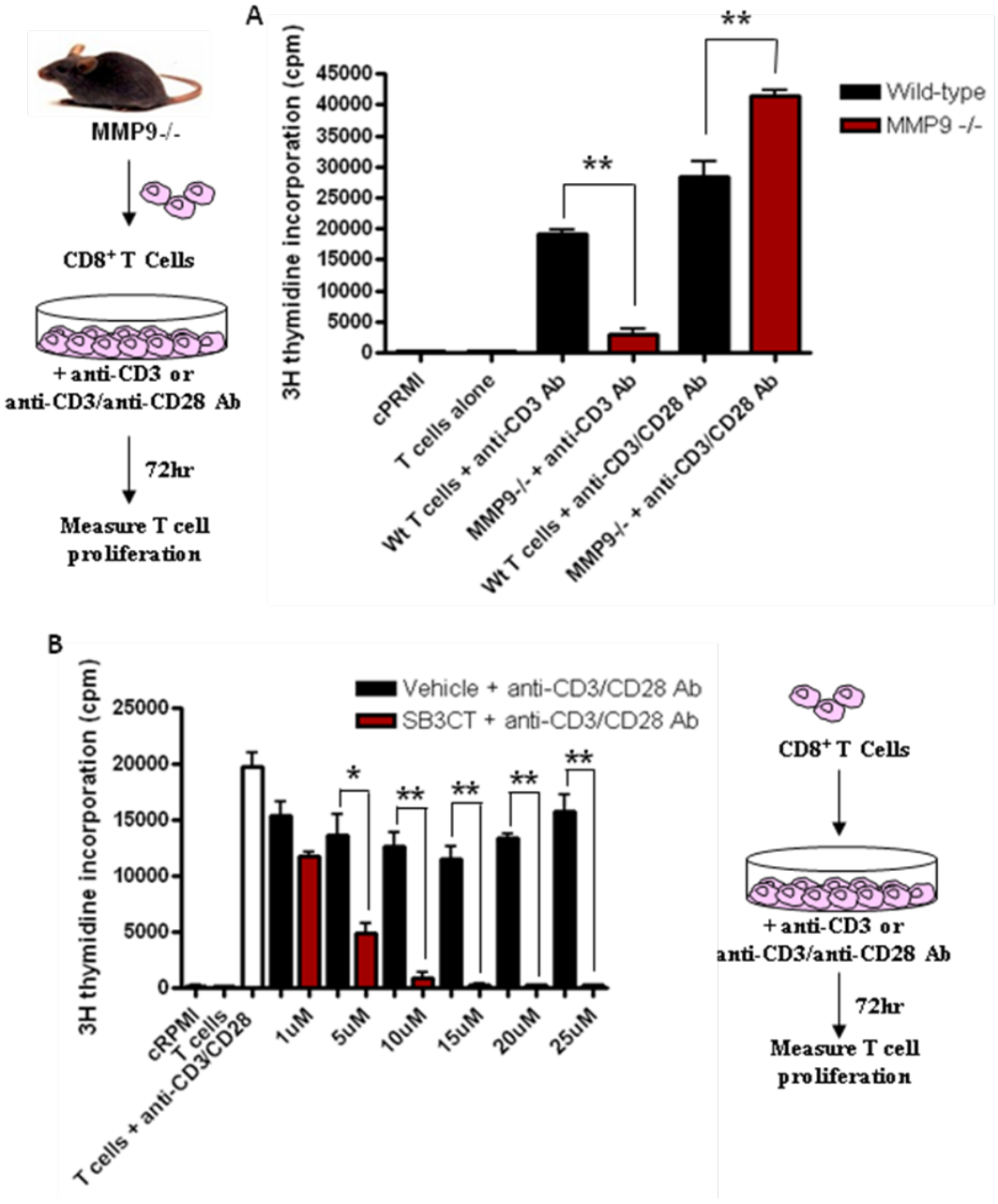

Figure 15. MMP9 deficient or SB3CT treated CD8$^+$ T cell proliferative ability following anti-CD3/CD28 Ab stimulation

A) CD8$^+$ T cells were isolated from wild-type and MMP9 deficient mice. B) Wild-type CD8$^+$ T cells were treated with varying concentrations of SB3CT (1-25μM). A and B) Cells were plated at $3x10^5$/well in a 96 well plate in the presence of anti-CD3 Ab or anti-CD3/anti-CD28 Ab (0.5μg/ml) for 72 hours. 18 hours prior to harvest, 3H thymidine (0.5μCi/well) was added to the culture. T cell proliferation was measured by the amount of 3H thymidine incorporation. These data are representative of the mean ± SD of one of three separate experiments performed in triplicate. *p<0.01, **P<0.001 compared to the corresponding vehicle treatment group. (n=3)

Based in the results above, MMP9 deficient T cells may be anergic, due to the fact that they can be rescued in response to the addition of anti-CD28 Ab, in the presence of anti-CD3 Ab. However, this is not the case in T cells treated with SB3CT. This implies that inhibition of MMP9 by gene deletion may alter T cell activation in a different manner than that observed by pharmacological inhibition. Since MMP9 deficient T cells positively responded to the addition of anti-CD28 Ab, this suggests that CD28 signaling is intact in the T cells in the absence of MMP9. However, in SB3CT treated T cells, the addition of anti-CD28 Ab did not rescue the proliferative response. In addition to the ability of SB3CT to decrease MMP9 gene transcripts, this pharmacological inhibitor may also interfere with the activating action of anti-CD28 Ab by preventing the CD28-anti-CD28 Ab interaction, thereby inhibiting CD28 function and proliferation.

Although the TCR and CD28 are independent signaling components, they share many redundant downstream signaling pathways important in T cell activation. Consequently, it is very difficult to discriminate the effects of the two independent signaling components. Previous studies have identified the PI3K/AKT pathway and NF-κB as the most relevant CD28 biochemical targets. Further investigation is needed to clarify the co-stimulatory differences seen between MMP9 deficient and SB3CT treated T cells. Our data thus far does however, does imply that MMP9 inhibition by means of SB3CT or gene deletion, is likely to affect cell signaling events downstream of TCR ligation. We next investigated how MMP9 may be acting to regulate T cell activation and signaling events.

Chapter 2. T cell signaling events altered in response to matrix metalloproteinase inhibition

A. Anti-CD3 Ab-induced calcium flux is elevated in MMP9 deficient $CD4^+$ and $CD8^+$ T cells in calcium-free media

It is well known that immediately following T cell receptor activation, there is an up-regulation of a multitude of events including the induction of specific protein tyrosine kinases, activation of protein kinase C and an increase in intracellular calcium flux (108, 109) [figure 16]. This calcium flux can occur following the interaction of inositol 1, 4, 5-triphosphate (IP_3) with its receptor, thereby stimulating the release of intracellular calcium from the endoplasmic reticulum (ER) and/or as a result of calcium channels opening, thereby allowing an influx of exogenous calcium into the cell.

With the results thus far suggesting a clear role for MMP9 in T cell activation, and with the understanding of the necessity of calcium in the regulation of T cell signaling, we subsequently examined the effect of MMP9 inhibition on intracellular calcium release from the ER. As diagramed in figure 17, $CD4^+$ and $CD8^+$ T cells from MMP9 deficient C57BL/6 mice and wild-type littermates were plated in calcium-free assay buffer and loaded with fluoro-4 dye. Cells were then stimulated with 10µg of soluble anti-CD3 Ab and calcium flux was measured in real time for 300 seconds. Unexpectedly, $CD4^+$ MMP9 deficient T cells exhibited a greater degree of intracellular calcium influx as compared to wild-type T cells [figure 18A]. $CD8^+$ T cells revealed a similar trend, with MMP deficient T cells also displaying a greater degree of intracellular calcium flux than was seen in the wild-type cells [figure 18B]. Since the experiments were performed in calcium-free media, the increase in intracellular calcium flux

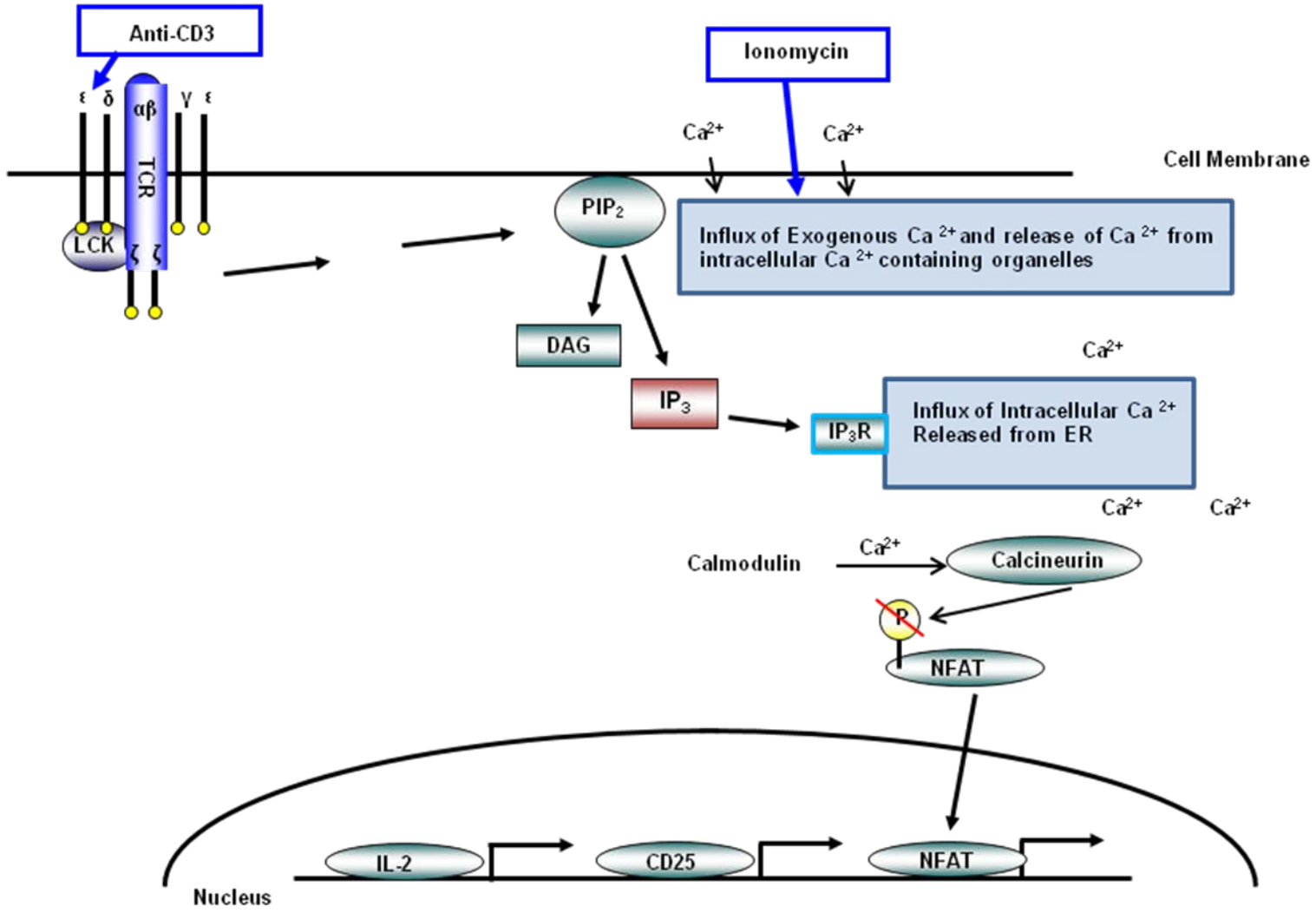

Figure 16. Calcium signaling in T cells Adapted from www.cellsignal.com

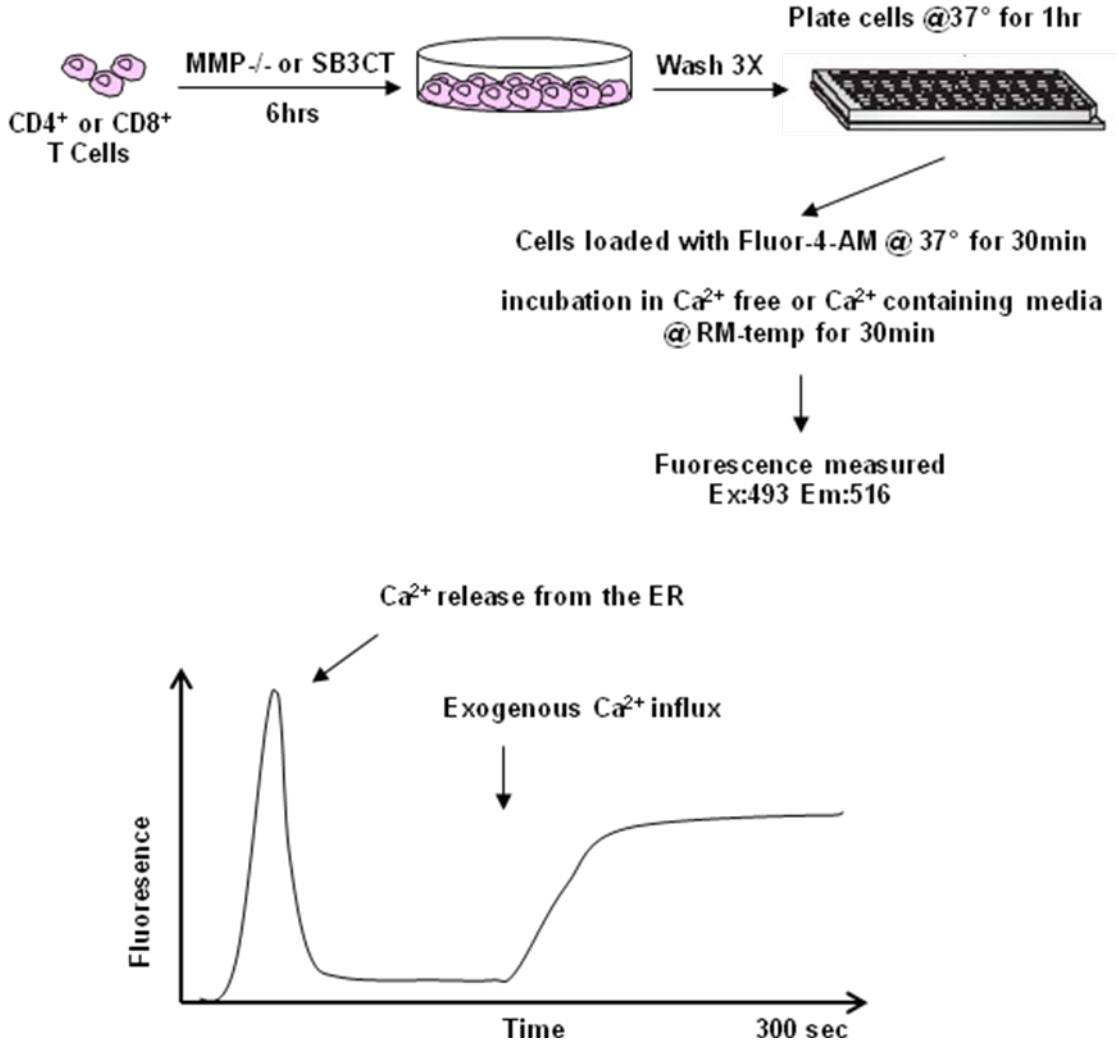

Figure 17. Diagram of calcium flux Assay

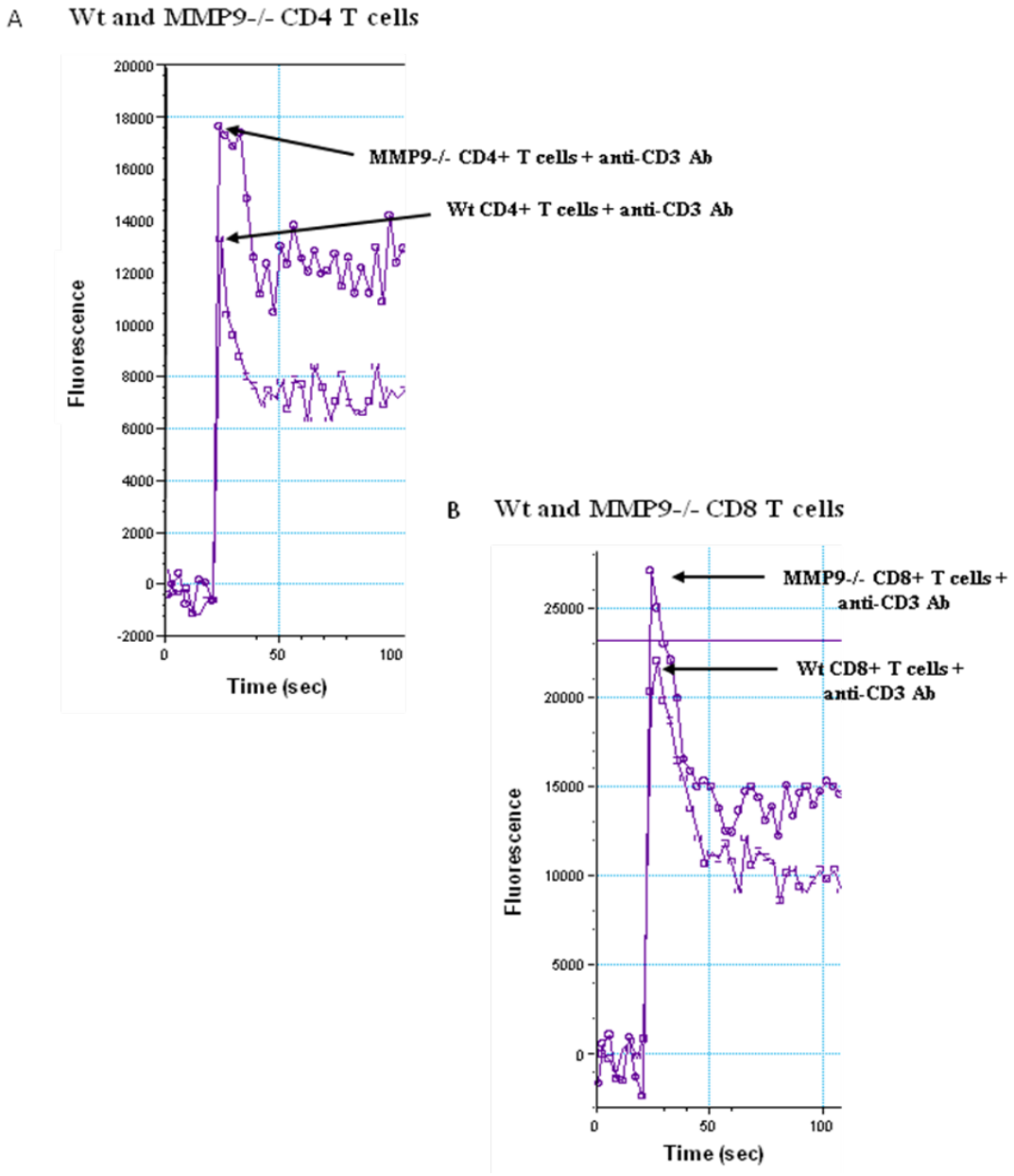

Figure 18. Anti-CD3 induced calcium flux is enhanced in MMP9 deficient T cells in the presence of calcium-free/divalent ion-reduced media

Pure splenic A) $CD4^+$ and B) $CD8^+$ T cells were isolated from wild-type and MMP9 deficient mice. Cells were then plated at 1.25 x 10^5 /well in a 96-well plate in calcium-free/divalent ion-reduced media and loaded with Fluo-4 dye for 30 minutes at 37°C, followed by a 30 minute incubation at room temperature. Cells were then stimulated with 10µg of soluble anti-CD3 Ab and fluorescence read in real time (0-300sec). These data are representative of the mean ± SD of one of three separate experiments performed in triplicate (n=3).

observed, occurred as a result of calcium release from the ER. Taken together, these results may suggest that MMP9 deficient T cells may release more calcium as a compensatory mechanism to overcome their impaired activation. It is worth noting that the calcium-free media contained trace amount of other divalent ions that were capable of reacting with the fluoro-4 dye. This corresponds to the slight increase in calcium flux seen in the corresponding graphs following the initial spike of calcium flux, which corresponds to the release of calcium from the ER.

B. MMP9 specific inhibition by SB3CT enhanced anti-CD3 Ab-induced calcium flux in calcium-free media

Since SB3CT treated $CD8^+$ T cells seem to display the most dramatic changes in calcium influx, we next examined whether SB3CT treatment affected anti-CD3 Ab-induced calcium influx in calcium-free media. $CD8^+$ T cells were again isolated from wild-type C57BL/6 mice and treated with 10μM of SB3CT or the corresponding vehicle control for 6 hours. Cells were then washed and plated in calcium-free media, loaded with fluoro-4 dye and stimulated with 10μg anti-CD3 Ab and measured in real time for 300 seconds. Similar to the results shown in $CD8^+$ MMP9 deficient T cells stimulated with anti-CD3 Ab in calcium-free media, SB3CT treatment increases the amount of free intracellular calcium [figure 19], which is most likely due to the release of calcium from the ER.

C. MMP9 specific inhibition by SB3CT enhanced anti-CD3 Ab-induced calcium influx in calcium containing media

To further examine the significance of MMP inhibition on anti-CD3 Ab-induced calcium flux, we next wanted to determine if the presence of exogenous calcium in the media would alter the influx of calcium following SB3CT treatment. Our hypothesis is that the presence of calcium in the media will cause an increase in calcium influx due to the influx of exogenous calcium from the media. $CD4^+$ and $CD8^+$ T cells were again isolated from wild-type C57BL/6 mice and treated with 10μM of SB3CT or the corresponding vehicle control for 6 hours. Cells were then washed and plated in calcium-free media, loaded with fluoro-4 dye and stimulated with 10μg anti-CD3 Ab and measured in real time for 300 seconds. As predicted, there was a dramatic influx of exogenous calcium in $CD8^+$ SB3CT treated cells following anti-CD3 Ab stimulation [figure 20].

Furthermore, the overall fluorescence was two-fold higher than that seen in calcium-free media. In the presence of calcium, the graph depicts a very pronounced release from the ER (large drop in the graph), followed by the initiation of the store operated calcium entry (SOCE), causing the influx of calcium into the cell. This trend in calcium influx is known based on thapsigargin, which raises the cytosolic calcium concentration by blocking the ability of the cell to pump calcium into the sarcoplasmic and endoplasmic reticula which causes these stores to become depleted. Store-depletion can secondarily activate plasma membrane calcium channels, allowing an influx of calcium into the cytosol. Taken together, these results demonstrate that SB3CT treatment

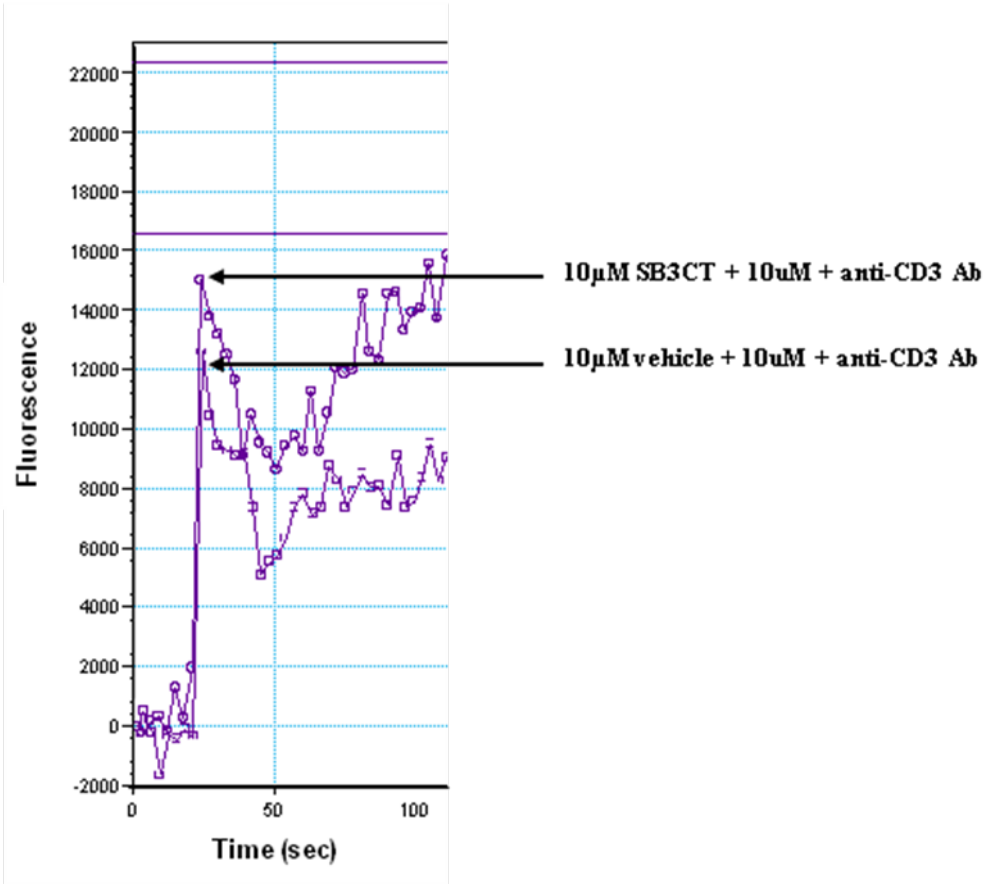

Figure 19. Anti-CD3 Ab-induced calcium flux is up-regulated in SB3CT treated $CD8^+$ T cells in calcium-free/divalent ion-reduced media

Pure splenic $CD8^+$ T cells isolated from wild-type C57BL/6 mice were treated with 10µM of SB3CT or VCtl for 6 hours. Cells were then plated at 1.25 x 10^5 /well in a 96-well plate in calcium-free/divalent ion-reduced media and loaded with Fluo-4 dye for 30 minutes at 37°C, followed by a 30 minute incubation at room temperature. Cells were then stimulated with 10µg of soluble anti-CD3 Ab and fluorescence read in real time (0-300sec). These data are representative of the mean ± SD of one of three separate experiments performed in triplicate (n=3).

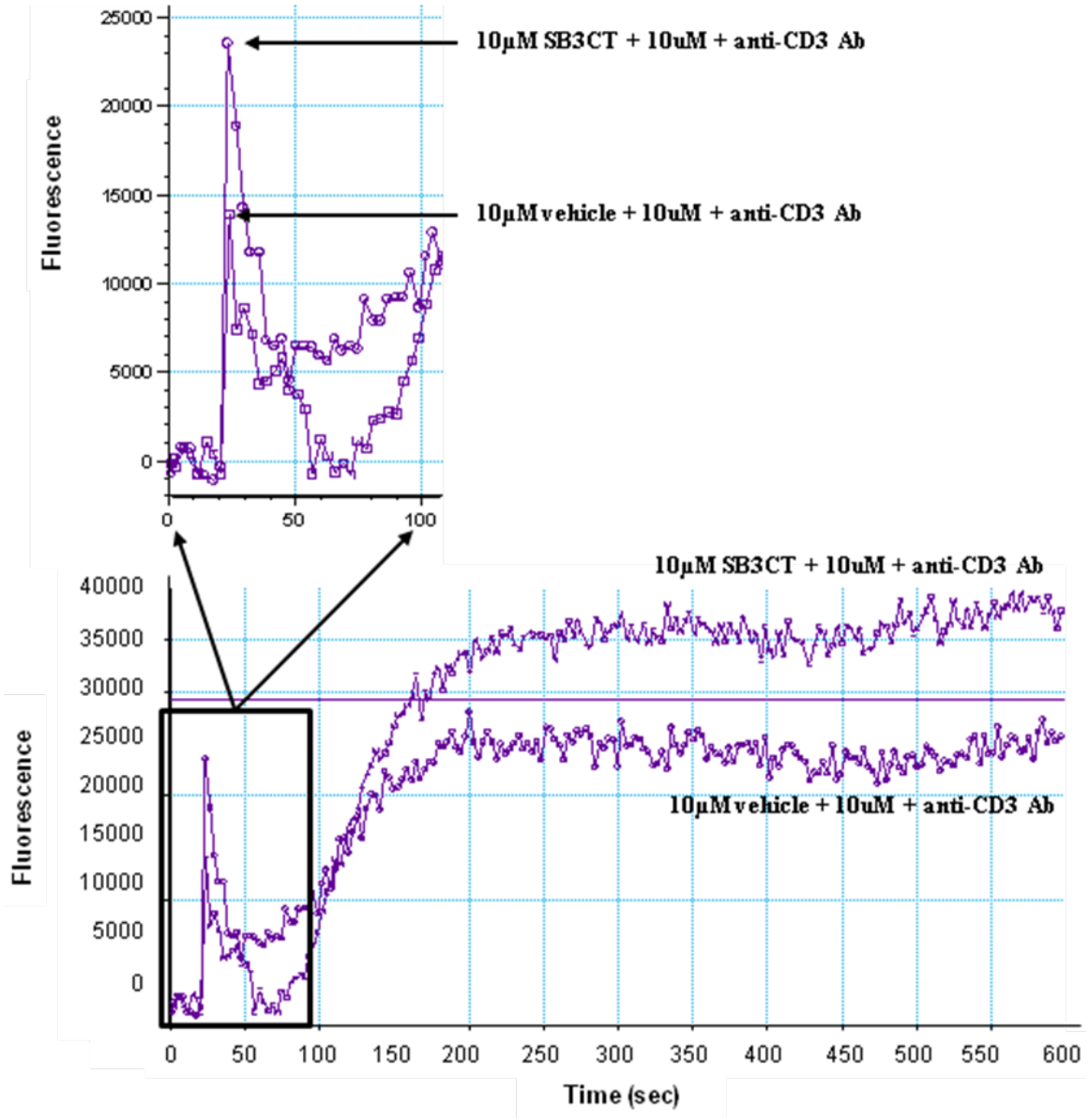

Figure 20. Anti-CD3 Ab-induced calcium flux is up-regulated in SB3CT treated CD8$^+$ T cells in calcium-containing media

Pure splenic CD8$^+$ T cells isolated from wild-type C57BL/6 mice were treated with 10µM of SB3CT or VCtl for 6 hours. Cells were then plated at 1.25 x 10^5 /well in a 96-well plate in calcium-containing media and loaded with Fluo-4 dye for 30 minutes at 37°C, followed by a 30 minute incubation at room temperature. Cells were then stimulated with 10µg of soluble anti-CD3 Ab and fluorescence read in real time (0-300sec). These data are representative of the mean ± SD of one of three separate experiments performed in triplicate (n=3).

or MMP9 deficiency enhanced anti-CD3 Ab- induced calcium flux following T cell activation.

As a result of the calcium data demonstrating that MMP absence or inhibition enhances calcium signaling, it may be beneficial to observe other downstream pathways involved in calcium signaling, such as MEK1/2. Since intracellular calcium flux is elevated, analysis of the MEK1/2 pathway may provide further evidence that other T cell pathways are functional and aid in pinpointing potential intracellular MMP targets. MEK1/2 is activated by a wide variety of growth factors and cytokines and also by membrane depolarization and calcium influx (110). It is also worth noting that another interesting experiment to perform would be to examine MMP9 deficient T cells stimulated with anti-CD3 Ab in the presence of calcium.

D. MMP9 inhibition by SB3CT does not prevent MEK1/2 activity in T cells

MEK1 and MEK2, also called MAPK or Erk kinases, are dual-specificity protein kinases that function in a mitogen activated protein kinase cascade [figure 21] that regulates cell growth and differentiation (110). Activation of MEK1 and MEK2 occurs through phosphorylation by Raf-like molecules of two serine residues at positions 217 and 221, located in the activation loop. MEK1/2 is activated by a wide variety of growth factors and cytokines and also by membrane depolarization and calcium influx (110). Since calcium flux was altered in T cells, we were interested in examining another pathway present in T cell signaling to determine if this pathway is altered in response to MMP inhibition by SB3CT. To explore this, $CD8^+$ T cells were isolated from wild-type

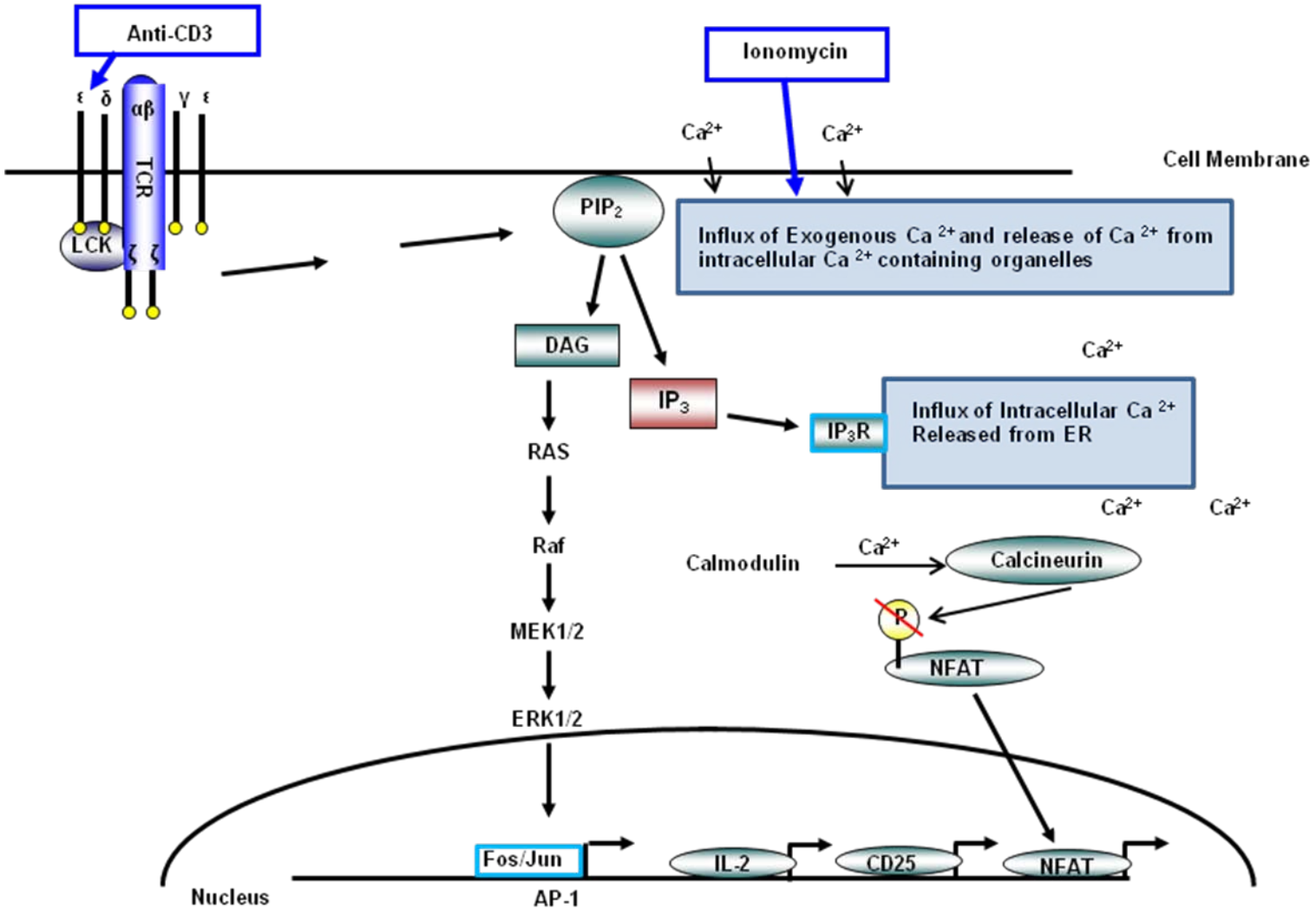

Figure 21. RAS signaling in T cells Adapted from www.cellsignal.com

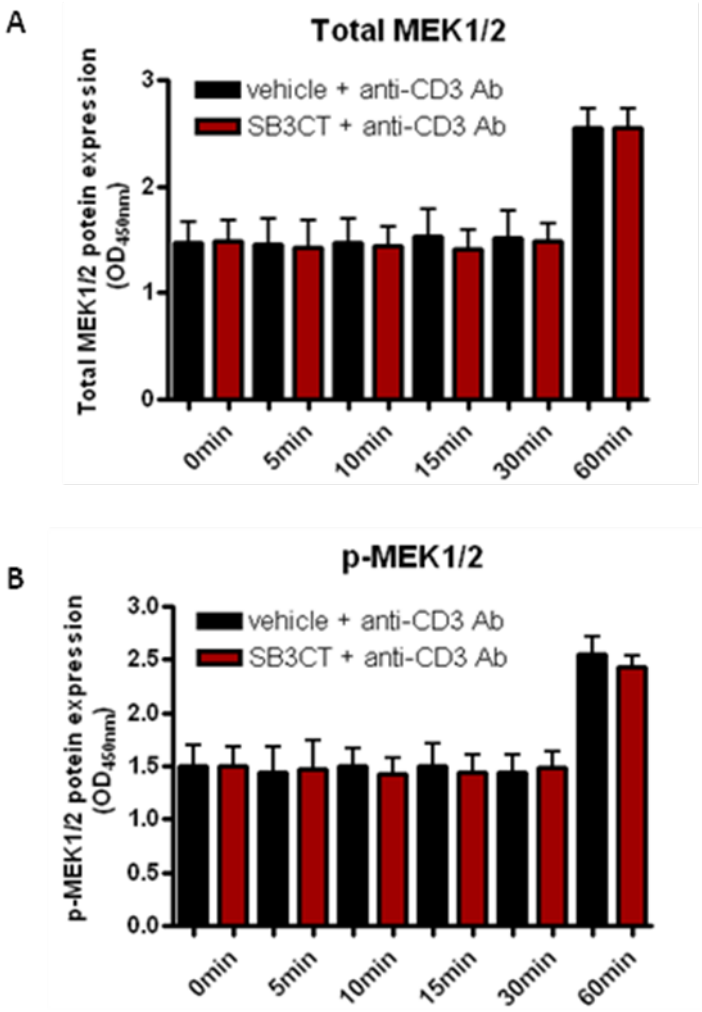

Figure 22. Total and phosphorylated MEK1/2 protein levels are maintained in SB3CT or vehicle treated CD8$^+$ T cells

CD8$^+$ T cells were isolated from wild-type C57BL/6 mice and treated with 10μM of SB3CT or the corresponding vehicle control for 6 hours. Cells were then washed and cultured in the presence of soluble anti-CD3 Ab for varying time-points (5-60 minutes). The cells were then fixed and MEK1/2 total and phosphorylated protein levels were measured. 0 min = non-stimulated group (n=1)

C57BL/6 mice and treated with 10μM of SB3CT or the corresponding vehicle control for 6 hours. Cells were then washed and cultured in the presence of soluble anti-CD3 Ab for varying time-points (5-60 minutes). The cells were then fixed and MEK1/2 total and phosphorylated protein levels were measured. As shown in figure 22A, following treatment with SB3CT or vehicle, total MEK1/2 protein levels remain relatively low and consistent between 5-30 minutes. At 60 minutes however, there was a significant increase in protein expression. It is interesting to note that although there was a dramatic increase in expression, this increase is seen in both the vehicle group as well as in the SB3CT treated group.

These data suggest that MEK1/2 total protein is unaltered following MMP9 inhibition by SB3CT. Analysis of phosphorylated MEK1/2, [figure 22B] revealed a similar trend, showing that the levels of phosphorylated MEK1/2 were unaltered in the presence of SB3CT. Collectively, these data suggest that MEK1/2 protein functions properly in T cell signaling, even following MMP9 inhibition by SB3CT. This data may also imply that MMP9 may be either acting independently or downstream of the MAPK pathway, which may further suggest a potential intracellular target.

E. Ionomycin-induced calcium flux is unaltered between wild-type and MMP9 deficient $CD4^+$ and $CD8^+$ T cells in calcium-free media

T cells may also be activated when the transmembrane signaling process has been bypassed by treatment with pharmacological agents such as ionomycin, which can elevate intracellular calcium levels. To determine whether ionomycin, a calcium ionophore that shuttles calcium across the cell membrane, induces an increase in

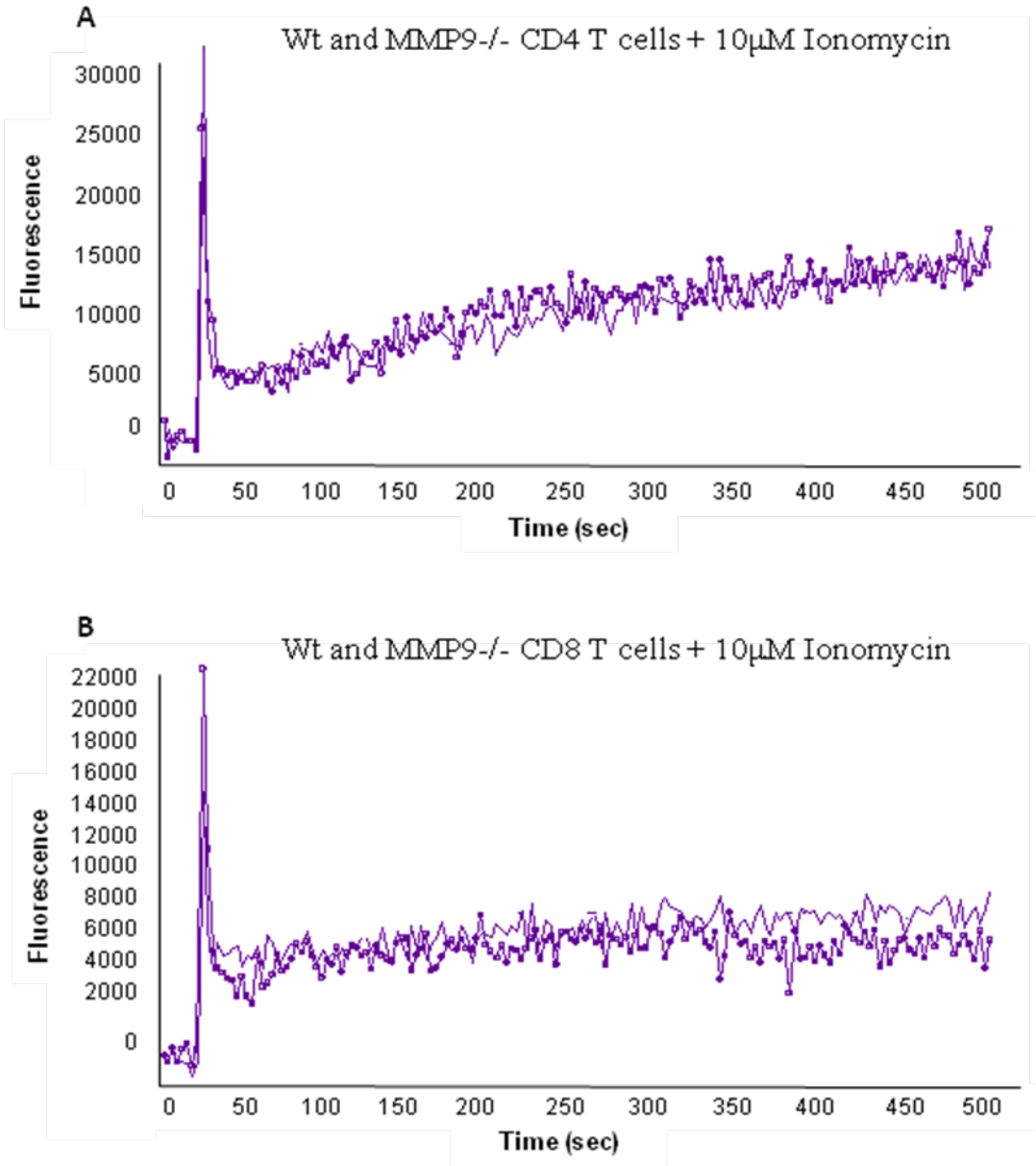

Figure 23. No change in ionomycin-induced calcium flux between wild-type andMMP9 deficient T cells in the presence of calcium-free /divalent ion-reduced media

Pure splenic A) $CD4^+$ and B) $CD8^+$ T cells were isolated from wild-type and MMP9 deficient mice. Cells were then plated at 1.25 x 10^5 /well in a 96-well plate in calcium-free/ divalent ion-reduced media and loaded with Fluo-4 dye for 30 minutes at 37°C, followed by a 30 minute incubation at room temperature. Cells were then stimulated with 10µM ionomycin and read in real time (0-300sec). These data are representative of the mean ± SD of one of three separate experiments performed in triplicate (n=3).

intracellular calcium release from the ER, similar to that seen following anti-CD3 Ab simulation, $CD4^+$ and $CD8^+$ T cells from MMP9 deficient C57BL/6 mice and wild-type littermates were plated in calcium-free assay buffer and loaded with fluoro-4 dye. Cells were then stimulated with 10μM of ionomycin and calcium flux was measured in real time for 300 seconds. Interestingly, there is no difference in ionomycin-induced calcium influx between $CD4^+$ [figure 23A] or $CD8^+$ [figure 23B] MMP9 deficient T cells and their wild-type littermates. Both cell groups equally produce an influx of intracellular calcium. These results suggest that in the absence of exogenous calcium from the media, ionomycin may be able to transverse the cell membrane and nonspecifically stimulate the release of calcium from the inside the cell, either from the ER or other intracellular components that contain calcium, such as the mitochondria. With regard to MMP9, it appears that intracellular calcium release from the ER is not affected by the absence of MMP9 following stimulation with ionomycin.

F. Ionomycin-induced calcium flux is abrogated in MMP9 deficient $CD4^+$ and $CD8^+$ T cells in calcium containing media

Since calcium flux also involves the influx of exogenous calcium via calcium channels, following the release from the ER, we next wanted to determine if calcium channel function was altered in ionomycin-induced calcium influx in MMP9 deficient T cells. To study the influx of exogenous calcium, $CD4^+$ and $CD8^+$ wild-type and MMP9 deficient T cells were plated in calcium containing media and loaded with fluoro-4 dye. As in the previous experiments, cells were again stimulated with 10μM of ionomycin and calcium flux was measured in real time for 300 seconds. As shown in figure 24A,

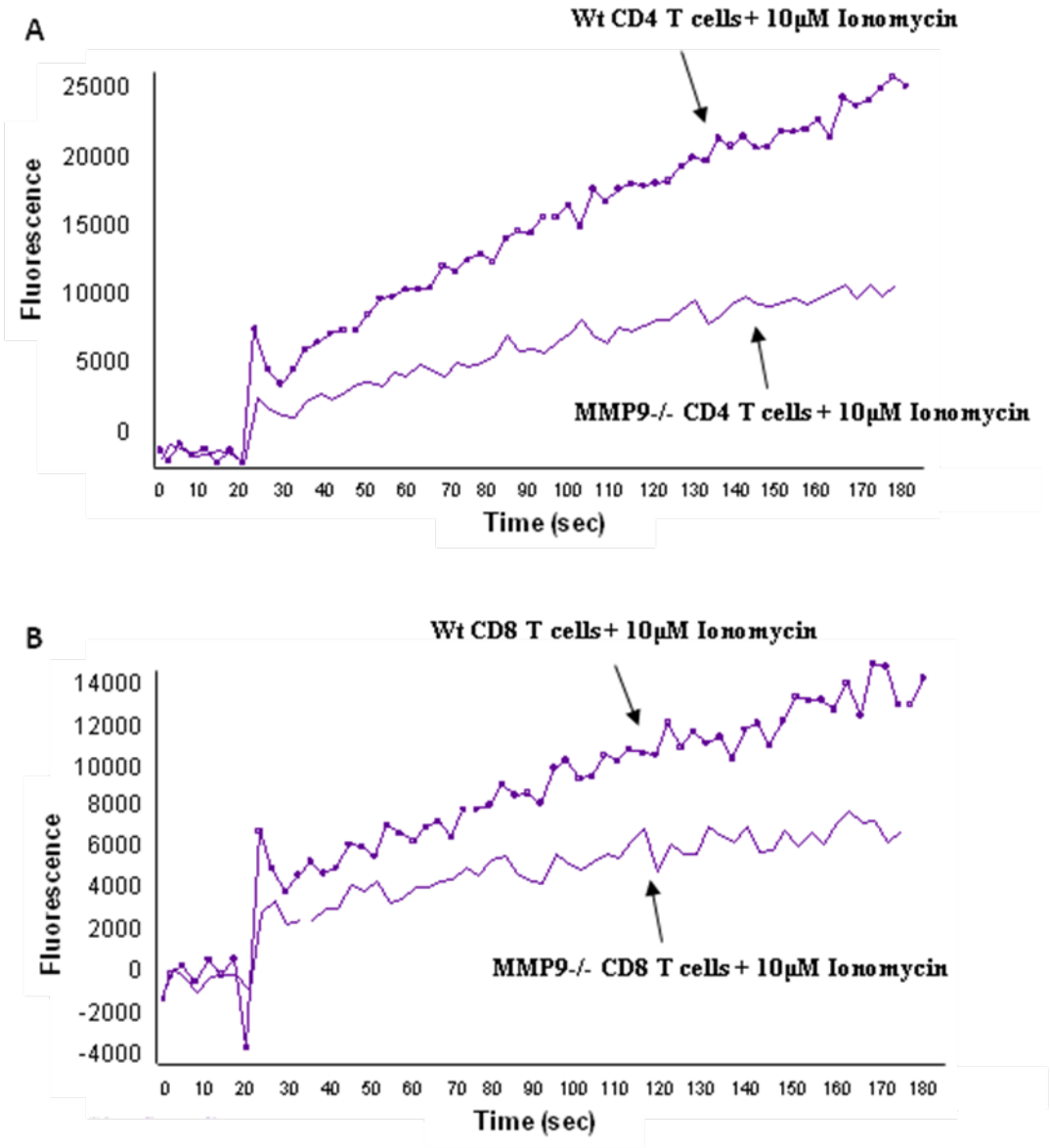

Figure 24. Ionomycin-induced calcium flux is abrogated in MMP9 deficient T cells in the presence of calcium-containing media

Pure splenic A) $CD4^+$ and B) $CD8^+$ T cells were isolated from wild-type and MMP9 deficient mice. Cells were then plated at 1.25 x 10^5 /well in a 96-well plate in calcium containing media and loaded with Fluo-4 dye for 30 minutes at 37°C, followed by a 30 minute incubation at room temperature. Cells were then stimulated with 10µM ionomycin and read in real time (0-300sec). These data are representative of the mean ± SD of one of three separate experiments performed in triplicate (n=3).

exogenous calcium influx in $CD4^+$ MMP9 deficient T cells was significantly impaired, when compared to wild-type cells. Observations of $CD8^+$ MMP9 deficient T cells [figure 24B] also revealed impairment of ionomycin-induced calcium influx, although to a lesser extent than that seen in $CD4^+$ MMP9 deficient T cells. These data displayed differing results than those seen following anti-CD3 Ab TCR stimulation and suggest that MMP9 also plays a role in ionomycin-induced exogenous calcium influx. In the absence of MMP9, ionomycin-induced calcium influx is impaired; suggesting that inhibition of normal MMP9 function within T cells impairs calcium channel function or alters membrane permeability.

G. MMP-9 specific inhibition by SB3CT reduced ionomycin-induced calcium influx in a dose-dependent manner in $CD4^+$ and $CD8^+$ T cells in calcium containing media

Since MMP9 deficient T cells exhibited a defect in ionomycin-induced exogenous calcium signaling, we wanted to determine if inhibition of MMP9 by SB3CT would also affect ionomycin-induced calcium influx in a similar manner. To answer this question, calcium influx assays were performed, in which $CD4^+$ and $CD8^+$ T cells were isolated from wild-type C57BL/6 mice and treated with varying concentrations of SB3CT (5-20μM) or the corresponding vehicle control for 6 hours. Cells were then washed and plated in calcium containing media, loaded with fluoro-4 dye and stimulated with 10μM ionomycin and measured in real time for 300 seconds. As shown in figure 25A, 5μM and 10μM treatment of SB3CT [figure 25B] only slightly reduced calcium influx in $CD4^+$ T

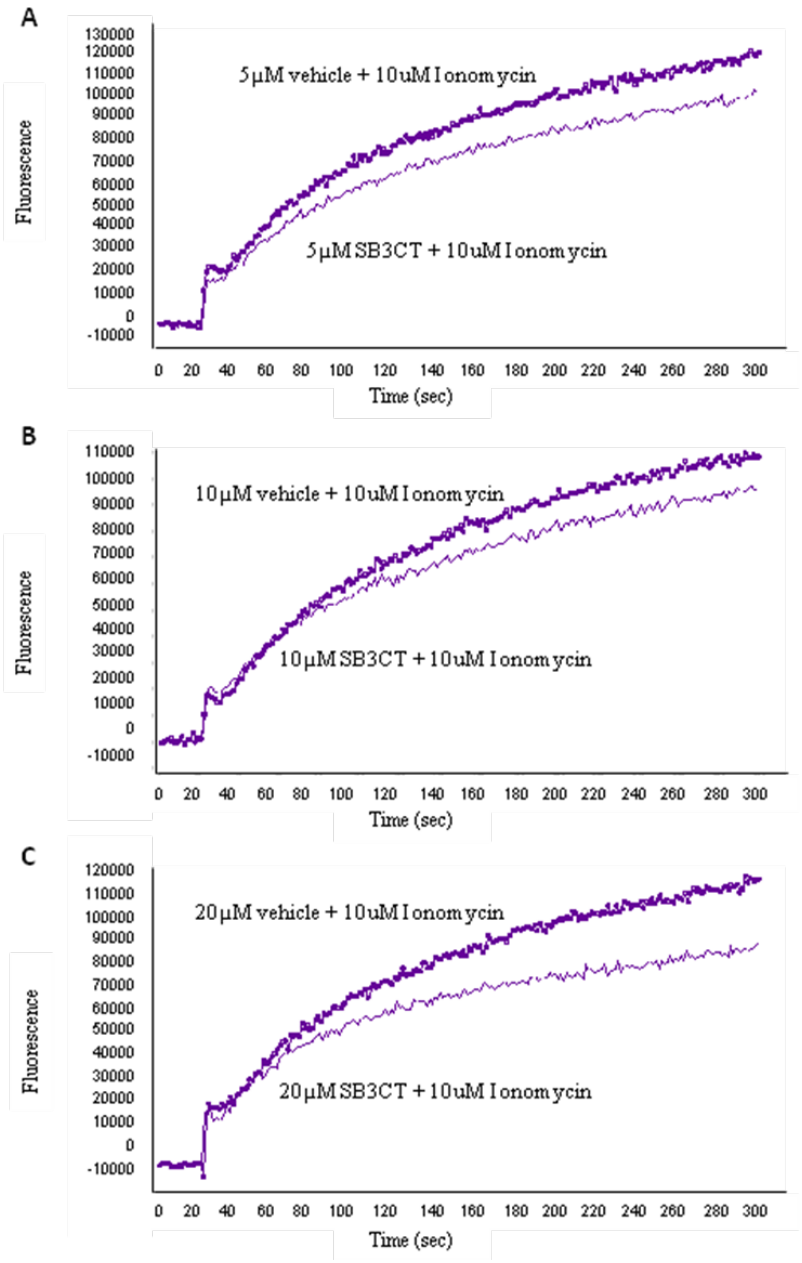

Figure 25. Ionomycin-induced calcium flux is down-regulated in SB3CT treated CD4$^+$ T cells in calcium containing media

Pure splenic CD4$^+$ T cells isolated from wild-type C57BL/6 mice were treated with varying concentrations of SB3CT (5-20µM) or VCtl for 6 hours. Cells were then plated at 1.25 x 10^5 /well in a 96-well plate and loaded with Fluo-4 dye for 30 minutes at 37°C, followed by a 30 minute incubation at room temperature. Cells were then stimulated with 10µM of ionomycin and read in real time (0-300sec). These data are representative of the mean ± SD of one of three separate experiments performed in triplicate (n=3).

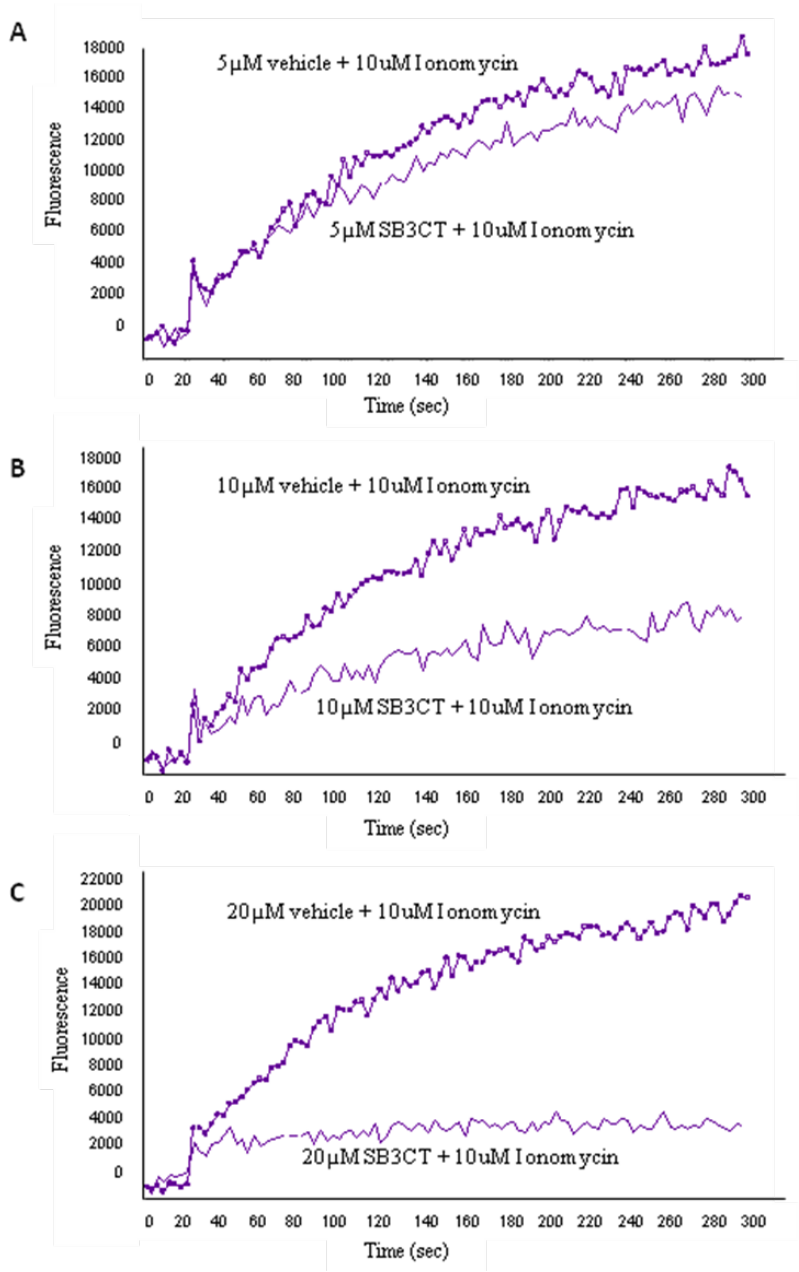

Figure 26. Ionomycin-induced calcium flux is significantly down-regulated in SB3CT treated CD8$^+$ T cells in calcium containing media

Pure splenic CD8$^+$ T cells isolated from wild-type C57BL/6 mice were treated with varying concentrations of SB3CT (5-20µM) or VCtl for 6 hours. Cells were then plated at 1.25 x 10^5 /well in a 96-well plate in calcium containing media and loaded with Fluo-4 dye for 30 minutes at 37°C, followed by a 30 minute incubation at room temperature. Cells were then stimulated with 10µM of ionomycin and read in real time (0-300sec). These data are representative of the mean ± SD of one of three separate experiments performed in triplicate (n=3).

cells. Increasing the concentration of SB3CT to 20μM [figure 25C] yielded a more pronounced reduction in calcium flux.

Interestingly, in examining $CD8^+$ T cells, treatment with SB3CT induced a dose-dependent decrease in exogenous calcium influx [figure 26]. Five micromolar of SB3CT [figure 26A] caused a slight reduction in calcium influx. However, increasing the concentration of SB3CT to 10μM [figure 26B] produced a 50% decrease in calcium influx, whereas 20μM of SB3CT [figure 26C] completely abrogated the influx of exogenous calcium. Collectively, these data not only confirm those shown in the MMP9 deficient T cells, but also imply that in the absence or inhibition of functional MMP9, T cells exhibit significant alterations in calcium signaling. Following anti-CD3 Ab stimulation of the TCR, in the absence of exogenous calcium, intracellular calcium release from the ER was shown to be more pronounced. Additionally, in the presence of exogenous calcium similar results were seen, with the absence or inhibition of MMP9 leading to an increased influx of calcium. On the other hand, following ionomycin stimulation, calcium influx is either unaltered, as was shown in the absence of exogenous calcium, or abrogated, as was seen in the presence of exogenous calcium.

These data highlight the complexity of MMP9s role in T cell signaling events involved in activation and suggest that MMP9 may function differently in calcium signaling depending on the stimulus the T cell receives (TCR = antiCD3 v.s. non-specific = ionomycin). These differences may be due to the nature of the stimulus. Ionomycin is a lipid-soluble ionophore that acts as a mobile carrier of divalent cations across cell membranes. Treatment of cells with 10μM of ionomycin is sufficient to increase the permeability of the plasma membrane. Anti-CD3 Ab, is a polyclonal antibody that ligates

the TCR leading to receptor-mediated signaling events leading to calcium flux. Therefore the differences seen in calcium flux in T cells in response to the absence or inhibition of MMP9 reflect the differences in the T cells ability to response to different stimuli depending on the mode of action.

H. MMP2 and MMP9 deficiency or inhibition by SB3CT alters CD25 and NFATc1 mRNA expression

It has been well established that NFAT is critical for T cell activation (111). NFAT is involved in promoting the transcription of IL-2Rα (CD25) and IL-2 expression following stimulation of the TCR [figure 27]. It has been reported that in T lymphocytes from NF-ATp-deficient mice, the expression of CD25 is severely impaired, causing delayed IL-2 receptor expression after T cell anti-CD3 Ab stimulation (112). These results highlight the importance of the NFAT-CD25 relationship. With this understanding and the results thus far showing a definite defect in T cell activation in response to the absence or inhibition of MMP9, we next examined the effect of SB3CT on NFAT mRNA expression. Since the data thus far show that $CD4^+$ and $CD8^+$ T cells respond similarly to treatment with SB3CT, $CD4^+$ T cells were used in the next set of studies.

$CD4^+$ T cells were isolated and treated with varying concentrations of SB3CT (5-20μM) for 6 hours. Following treatment, $CD4^+$ T cells were washed and cultured in the presence of soluble anti-CD3 Ab for 24 hours. MMP9 deficient $CD4^+$ T cells were cultured in the presence or absence of soluble anti-CD3 Ab for 72 hours. Cells were then collected and analyzed by means of real-time PCR. Strikingly, SB3CT treatment abrogated NFATc1 expression in a dose-dependent manner, as compared to vehicle

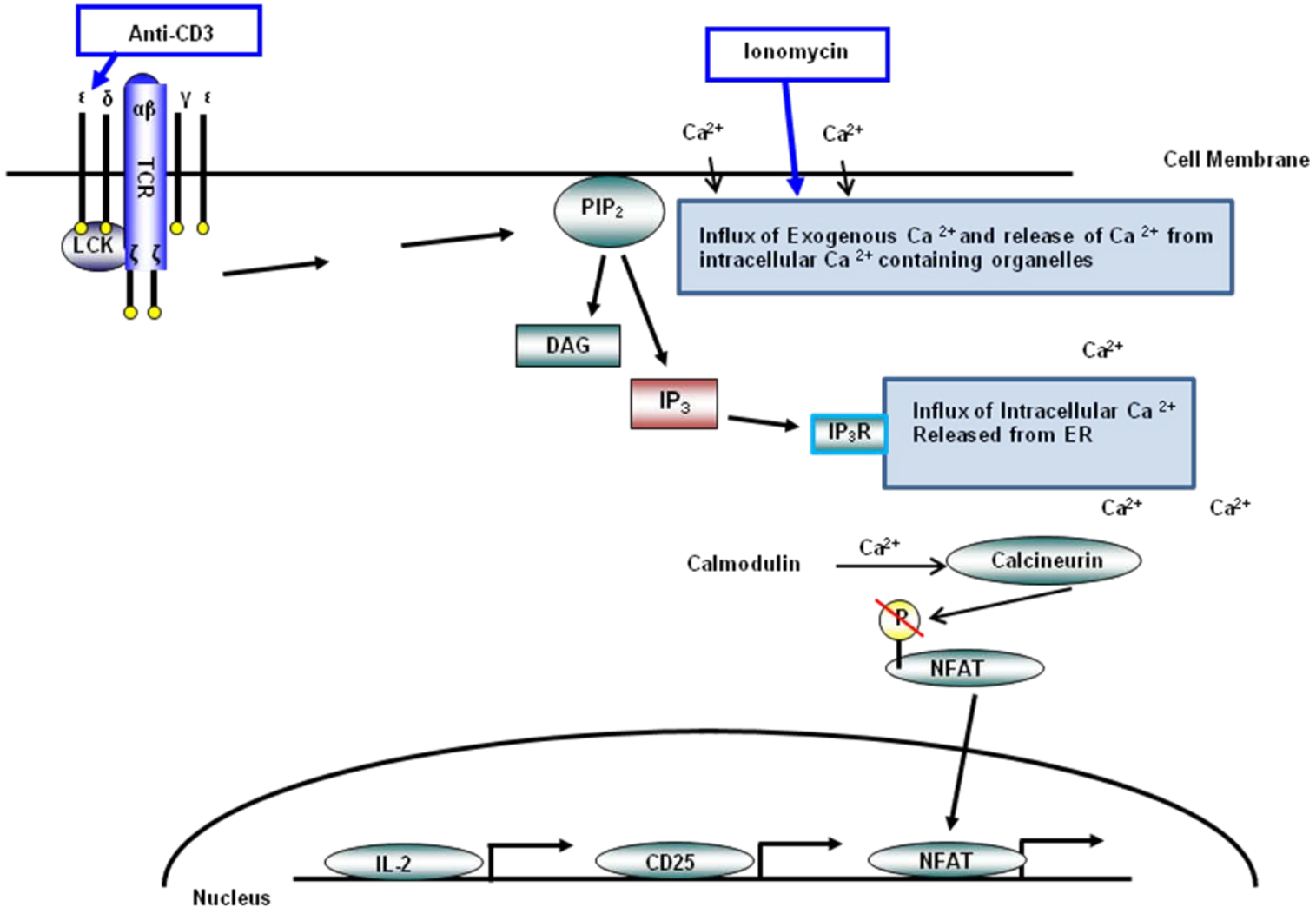

Figure 27. NFAT signaling in T cells Adapted from www.cellsignal.com

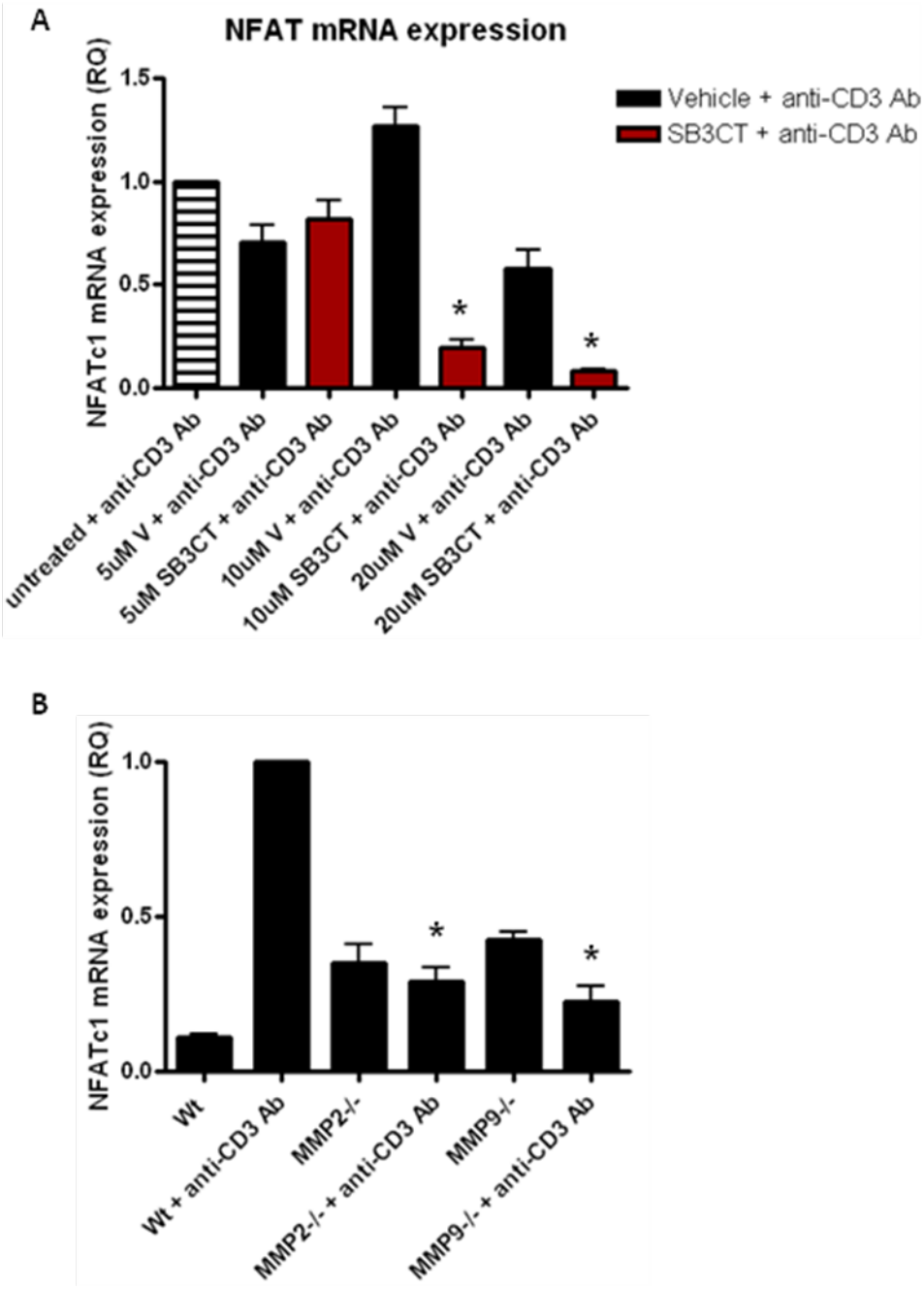

Figure 28. SB3CT treatment and MMP2 and MMP9 deficiency abrogate NFATc1 mRNA expression in CD4$^+$ T cells

Pure splenic CD4 T cells were isolated from wild-type and MMP9 deficient mice. A) CD4$^+$ T cells were treated with varying concentrations of SB3CT (5-20μM) or VCtl for 6 hours. B) MMP2-/- and MMP9-/- CD4$^+$ T cells and A were plated at 2x10^6/tube in 3ml tissue culture tubes in the presence of anti-CD3 Ab (0.5μg/ml) for 24 or 72 hours. Cells were then collected and NFATc1 mRNA expression levels were measured by real-time quantitative PCR. These data are representative of the mean ± SD of three separate experiments performed in triplicate. *p<0.001 compared to corresponding vehicle treatment group (in panel A) or Wt + anti-CD3 treated T cells (in panel B). (n=3)

treatment [figure 28A]. In accordance with this data, examination of MMP9 deficient $CD4^+$ T cells also displayed a significant defect in their ability to express NFATc1 levels following stimulation, as compared to wild-type T cells [figure 28B]. However, examination of MMP2 deficient $CD4^+$ T cells revealed that although NFATc1 levels were significantly less than that seen in wild-type T cells, levels were comparable in the presence or absence of anti-CD3 Ab [figure 28B]. NFAT translocation to the nucleus is required for efficient transcription of many genes, such as IL-2 and IL-2Rα. The interaction of IL-2 with its high affinity membrane receptor IL-2Rα (CD25) plays a key role in T cell activation. This process requires proper synthesis and expression of CD25, to which IL-2 can bind, leading to the cascade of events required for suitable activation.

With the finding that NFAT expression is altered in response to specific MMP9 inhibition or its complete absence, we wanted to determine if this alteration would affect the expression of CD25, which is dependent on NFAT transcriptional expression (113). Based on this fact, we would expect CD25 expression to be decreased in response to the decrease in NFAT gene expression. To address this, wild-type $CD4^+$ T cells were again treated with varying concentrations of SB3CT (5-20μM) or the corresponding vehicle control for 6 hours. Following treatment, $CD4^+$ T cells were washed and cultured in the presence of soluble anti-CD3 Ab for 24 hours. Cells were then collected and analyzed by means of real-time PCR. As shown in figure 29A, the mRNA expression level of CD25 in vehicle-treated cells following anti-CD3 Ab stimulation is similar to that observed in untreated cells stimulated with anti-CD3 Ab. This trend remains even as the concentration of vehicle treatment increases from 5-20μM. Interestingly, increasing the concentration of SB3CT treatment caused a decrease in CD25 mRNA expression in a

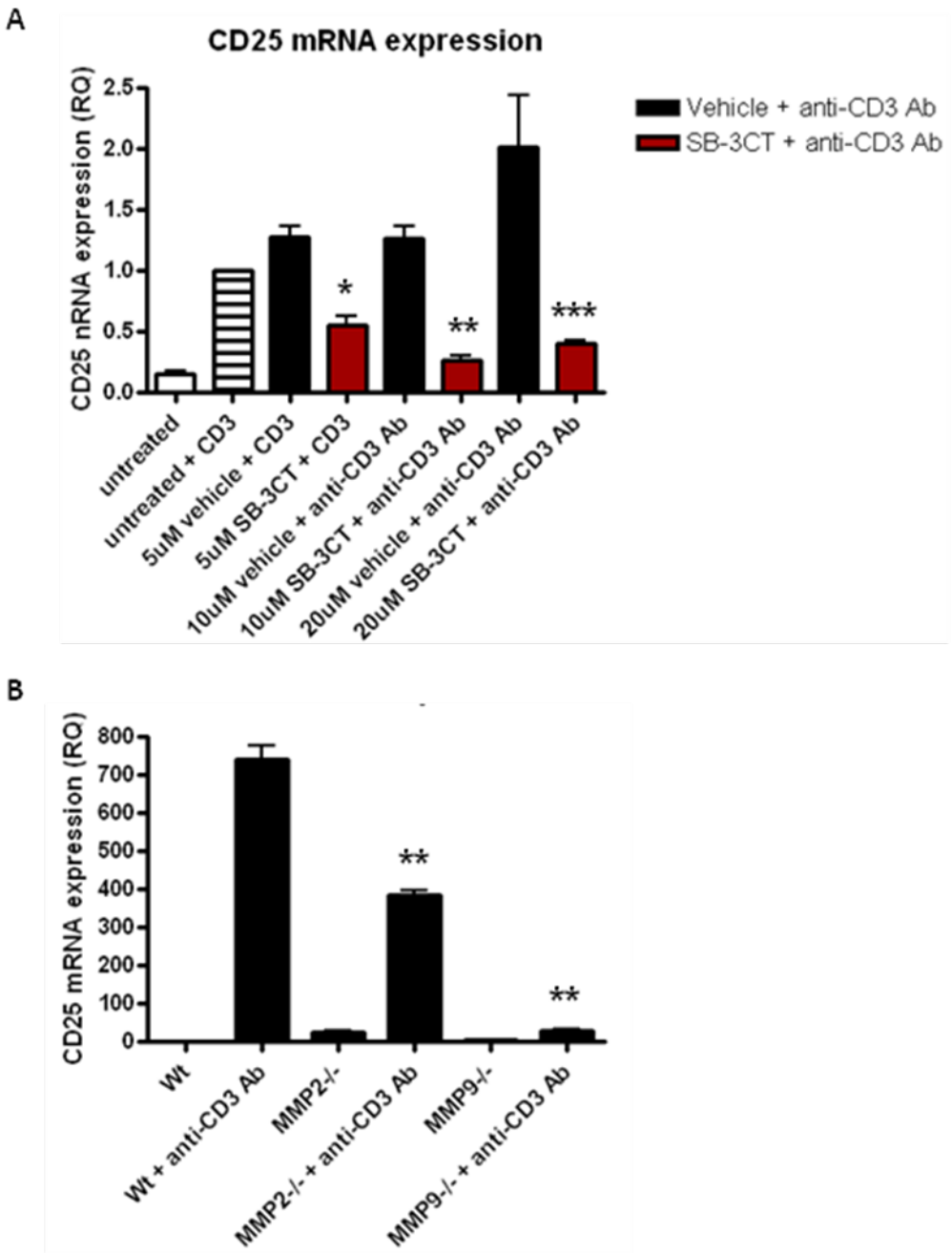

Figure 29. SB3CT treatment and MMP9 deficiency abrogate CD25 mRNA expression in CD4$^+$ T cells

Pure splenic CD4 T cells were isolated from wild-type and MMP9 deficient mice. A) CD4$^+$ T cells were treated with varying concentrations of SB3CT (5-20μM) or VCtl for 6 hours. B) MMP2-/- and MMP9-/- CD4$^+$ T cells and A) were plated at 2x10^6/tube in 3ml tissue culture tubes in the presence of anti-CD3 Ab (0.5μg/ml) for 24 or 72 hours. Cells were then collected and CD25 mRNA expression levels were measured by real-time quantitative PCR. These data are representative of the mean ± SD of three separate experiments performed in triplicate. *p<0.05, **p<0.01, ***p<0.001 compared to corresponding vehicle treatment group (in panel A) or Wild-type + anti-CD3 treated T cells (in panel B). (n=3)

dose-dependent manner [figure 29A]. These results were further confirmed upon examination of MMP9 deficient $CD4^+$ T cells. In figure 29B, as compared to the elevated levels of CD25 seen in stimulated wild-type cells, CD25 expression is impaired in MMP9 deficient T cells.

Additionally, examination of MMP2 deficient T cells also revealed diminished CD25 expression levels, although not as dramatic. These data point to the importance of MMP9 in regulating NFAT and CD25 expression, thereby affecting proper T cell activation. Taken together, these results further highlight the role of MMP9 in T cell activation. The decrease seen in NFAT and CD25 expression, both of which are regulated intracellularly, in response to MMP9 inhibition or absence suggests that MMPs may regulate T cell activation by targeting an intracellular substrate that affects NFAT and CD25 expression, thereby preventing proper T cell activation.

I. MMP9 inhibition does not induce regulatory T cell function

Studies have shown that regulatory T cells (Tregs) are unable to proliferate or produce IL-2 following anti-CD3 Ab stimulation. However, Tregs are capable of suppressing proliferative responses and cytokine production by effector T cells (114). It has been reported that following TCR stimulation, nuclear NFAT expression in Tregs remains low, whereas in T helper cells nuclear NFAT levels increase. Inhibition of NFAT induction has been described as a hallmark of Tregs. Analysis of forkhead transcription factor (Foxp3), a specific molecular marker of Tregs, revealed high mRNA and protein expression in Treg cells and low expression in naive T cells (115). Studies have shown that Foxp3 antagonizes NFAT function by competition for DNA binding sites and acting

as a transcriptional repressor. It has also been proposed that Foxp3 is induced in a variety of cell types as a general mechanism of negative immune regulation by repressing production of inflammatory cytokines (115).

To determine if MMP9 deficient or SB3CT treated T cells exhibited other Treg characteristics, we examined Foxp3 expression. $CD4^+$ T cells were isolated from wild-type and MMP9 deficient mice and cells were cultured in the presence or absence of soluble anti-CD3 Ab for 72 hours. Cells were then analyzed by means of real-time PCR. Surprisingly, as shown in figure 30A, foxp3 transcript levels were significantly increased in MMP9 deficient $CD4^+$ T cells, as compared to MMP2 deficient and wild-type T cells.

We also examined SB3CT treatment on foxp3 expression in $CD4^+$ T cells to determine if MMP9 inhibition by SB3CT would yield results similar to those seen in MMP9 deficient T cells. $CD4^+$ T cells were isolated and treated with varying concentrations of SB3CT (5-20μM) for 6 hours. Following treatment, $CD4^+$ T cells were washed and cultured in the presence of soluble anti-CD3 Ab for 24 hours. As shown in figure 30C, foxp3 transcript levels were significantly increased following 20μM treatment of SB3CT, as compared to vehicle treated cells. During this observation, we also measured the expression of interleukin 10 (IL-10), being that it is a suppressive cytokine predominantly secreted by $CD4^+$ T cells along with a few others. IL-10 has important suppressive functions on immune responses and is involved in the maintenance of tolerance and blocks activation of cytokine synthesis by Th1 cells. MMP9 deficient $CD4^+$ T cells and their wild-type control cells were cultured in the presence or absence of soluble anti-CD3 Ab for 72 hours. Cell culture supernatants were collected and protein

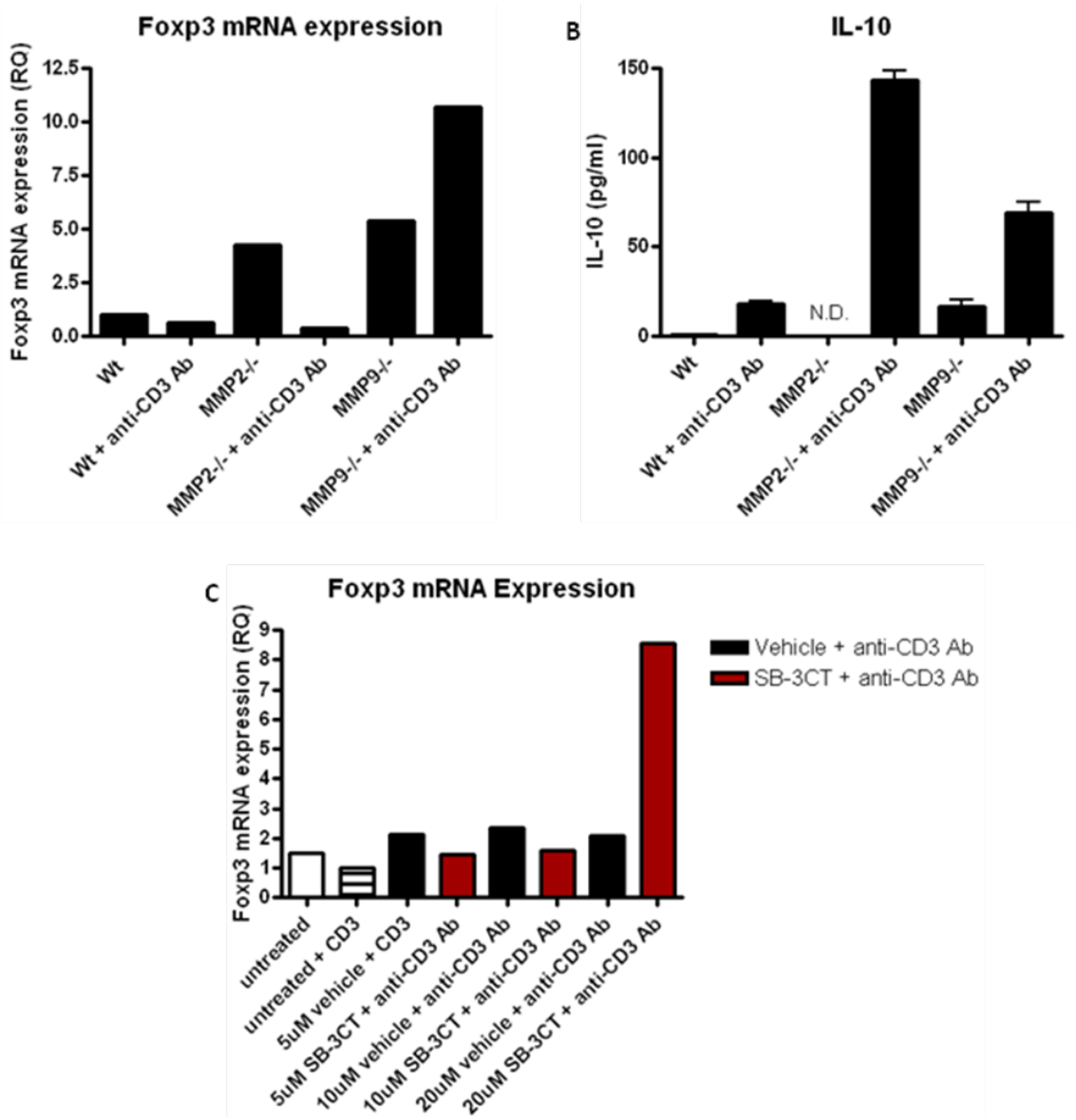

Figure 30. Foxp3 and IL-10 expression is elevated in MMP9 deficient and SB3CT treated CD4$^+$ T cells

Pure splenic CD4$^+$ T cells were isolated from wild-type and MMP2 and MMP9 deficient mice. A) Cells were plated in a 96 well plate in the presence of anti-CD3 Ab (0.5µg/ml) for 72 hours. Cells were collected and foxp3 gene expression was measured by quantitative real-time PCR. B) Culture supernatants were collected and assayed for IL-10 using a Cytometric Bead Array (CBA). The beads were washed and analyzed by flow cytometry. C) CD4$^+$ T cells were treated with varying concentrations of SB3CT (5-20µM) or VCtl for 6 hours. Cells were collected and foxp3 mRNA levels were measured by real-time quantitative PCR. These data are representative of the mean ± SD of one of three separate experiments performed in triplicate (n=3).

expression was analyzed by cytokine bead array. Interestingly, as shown in figure 30B, IL-10 protein expression is significantly elevated in anti-CD3 Ab stimulated MMP2 and MMP9 deficient T cells, suggesting that MMP inhibition may induce cells to exhibit a suppressive nature.

We next wanted to determine if inhibition of MMP9 induces regulatory T cell function, thereby causing a suppressive effect, leading to the decrease in T cell proliferation. To address this concept, suppressor assays [figure 31A] were utilized in which, $CD4^{+}25^{-}$ T cells were treated for 6 hours with 10μM of SB3CT or the vehicle control. These cells were then co-cultured at varying ratios (1:1, 2:1, 4:1, 6:1 treated: untreated) with untreated $CD4^{+}25^{-}$ T cells in the presence of irradiated antigen presenting cells (APCs). Seventy-two hours later we measured the ability of SB3CT treated T cells to inhibit/suppress the proliferative capacity of untreated $CD4^{+}25^{-}$ T cells. As shown in figure 31B, SB3CT treatment at each ratio (1:1-6:1 treated: untreated) inhibited T cell proliferation by 50%. However, as the ratio of SB3CT treated cells increased, T cell proliferation also increased, suggesting that SB3CT treatment does not induce regulatory T cell function. For this to be the case, we would have expected to see that as the number of SB3CT treated cells increased there should have been a significantly larger decrease in T cell proliferation.

Likewise, when $CD4^{+}25^{+}$ T cells [figure 32A] were treated with SB3CT and co-cultured at varying ratios (.5:1 and 1:1 treated:untreated) with untreated $CD4^{+}25^{-}$ T cells in the presence of irradiated APCs, it was found that $CD4^{+}25^{+}$ T cells retained their suppressive function [figure 32B]. Worth noting however is that, SB3CT treated $CD4^{+}25^{+}$ T cells displayed somewhat altered suppressive ability, requiring more treated

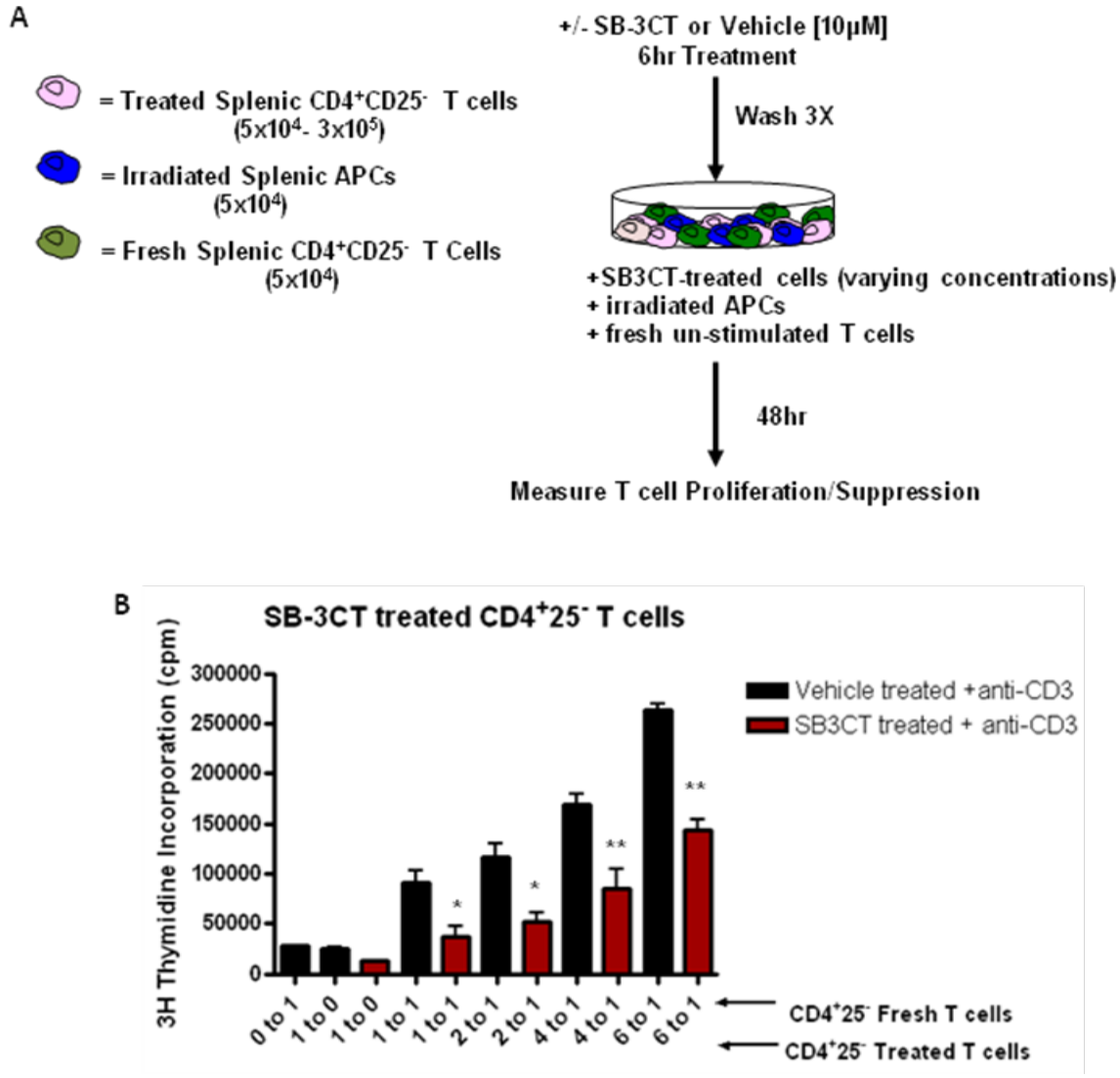

Figure 31. SB3CT treatment does not induce suppressor T cell function
A) Diagram of suppressor assay. B) Pure splenic $CD4^+$ T cells were isolated from C57BL/6 mice. $CD4^+25^-$ T cells were treated with 10µM of SB3CT or VCtl for 6 hours. Cells were then washed in RPMI and plated at varying ratios (1-6:1 treated $CD4^+25^-$:fresh $CD4^+25^-$) in a 96 well plate in the presence of anti-CD3 (0.5µg/ml). 18 hours prior to harvest, 3H thymidine (0.5µCi/well) was added to the culture. T cell proliferation was measured by the amount of 3H thymidine incorporation. These data are representative of the mean ± SD of one of three separate experiments performed in triplicate (n=3). *p<0.01, **p<0.001 as compared to vehicle in each ratio.

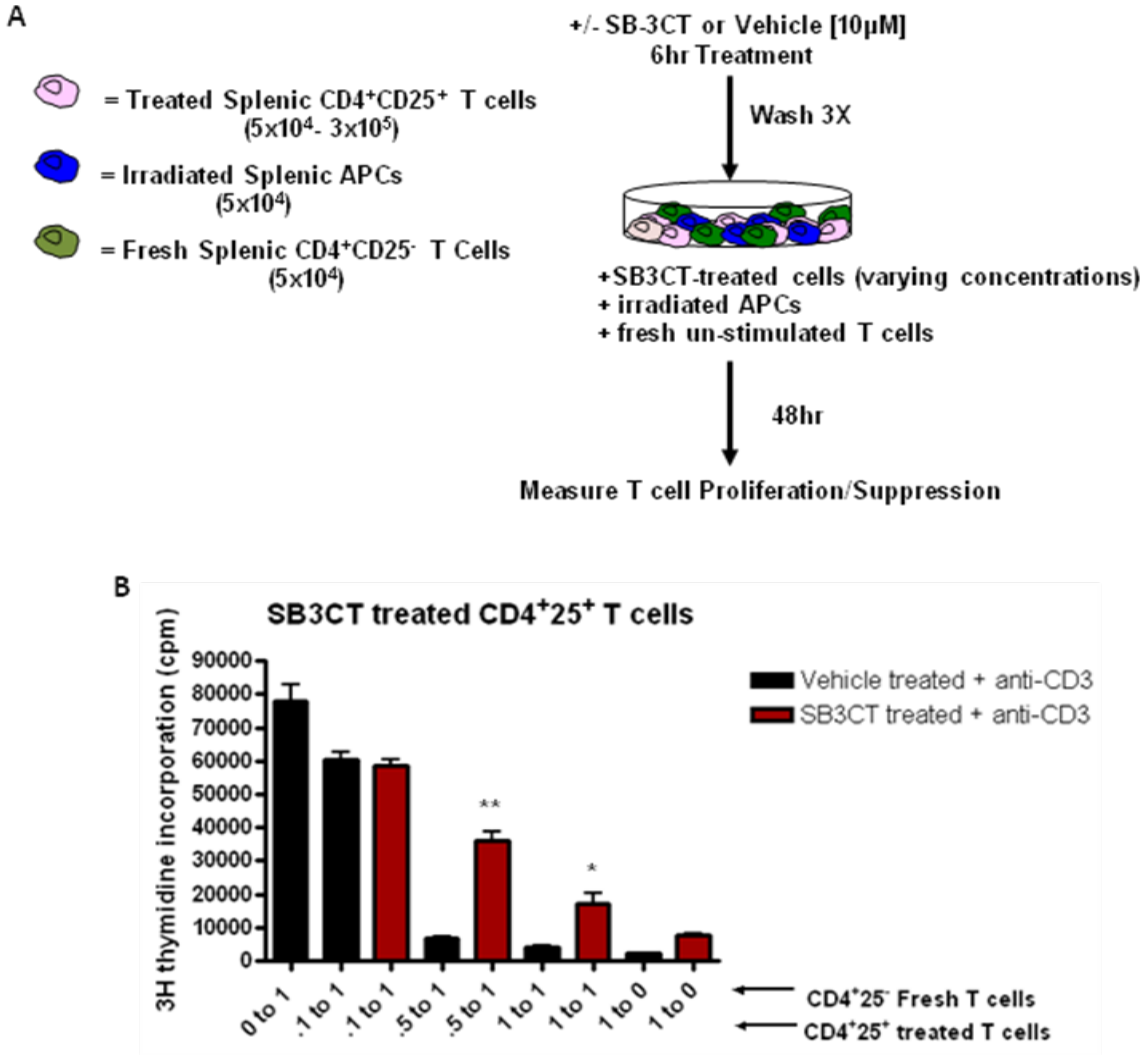

Figure 32. SB3CT treatment does not induce regulatory T cell function

A) Diagram of regulatory T cell assay B) Pure splenic $CD4^+$ T cells were isolated from C57BL/6 mice. $CD4^+25^+$ T cells were treated with 10μM of SB3CT or VCtl for 6 hours. Cells were then washed in RPMI and plated at varying ratios (.5-1:1 treated $CD4^+25^+$:fresh $CD4^+25^-$) in a 96 well plate in the presence of anti-CD3 (0.5μg/ml). 18 hours prior to harvest, 3H thymidine (0.5μCi/well) was added to the culture. T cell proliferation was measured by the amount of 3H thymidine incorporation. These data are representative of the mean ± SD of one of three separate experiments performed in triplicate (n=3). *$p<0.01$, **$p<0.001$ as compared to vehicle in each ratio.

cells to exhibit their suppressive nature [figure 32B]. The reasoning behind the increase in foxp3 and IL-10 levels remains unclear. Taken together, these data suggest that MMP9 inhibition does not induce a mechanism of regulatory T cell function. These data do however suggest MMP9 involvement in foxp3 and IL-10 expression.

J. Production of IL-2, TNF-α and IFN-γ in MMP9 deficient $CD4^+$ and $CD8^+$ T cells

In an effort to further understand how MMP9 regulates intracellular T cell signaling, we sought to examine the effects of MMP9 deficiency on T cell cytokine gene and protein expression. Three cytokines of interest were chosen, IL-2, TNF-α and IFN-γ. IL-2 is produced primarily by antigen activated T cells, and as such it is known to stimulate proliferation in T cells. Therefore changes seen in T cell proliferation may be due to changes in the production of IL-2. IL-2 has also been shown to be a potent inducer of IFN-γ gene expression in T cells (116). TNF-α is a major pro-inflammatory cytokine, that can exert multiple stimulatory activities on activated T cells. TNF-α enhances expression of IL-2 receptors and synergizes with IL-2 with respect to both stimulation of T cell proliferation and production of IFN-γ (117). IFN-γ is the hallmark cytokine of Th1 cells and is expressed in $CD8^+$ T cell (118).

To examine the effects of MMP9 deficiency on T cell cytokine gene production, mRNA expression levels for IL-2, TNF-α and IFN-γ in MMP9 deficient $CD4^+$ and $CD8^+$ T cells and their wild-type littermates were measured by means of real-time PCR. $CD4^+$ and $CD8^+$ T cells were cultured in the presence of soluble anti-CD3 Ab for 72 hours. Cell pellets were then collected and processed for real-time PCR and the supernatants were collected and analyzed by means of cytokine bead array. Gene expression levels in $CD4^+$

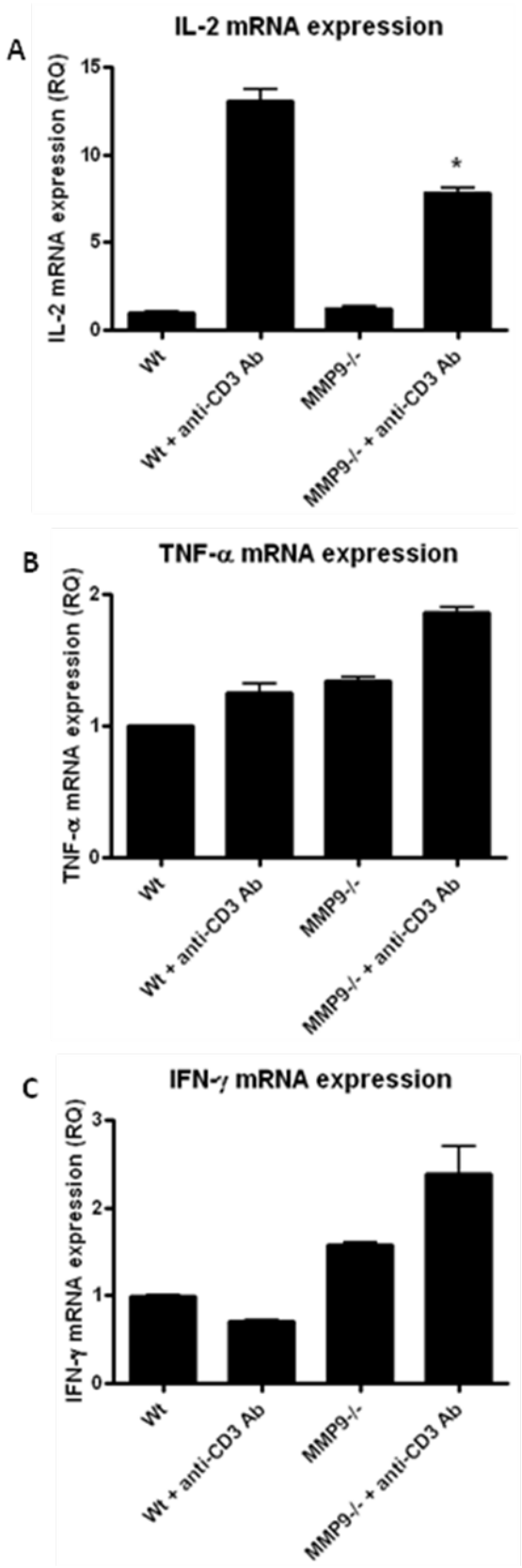

Figure 33. Cytokine gene profile of IL-2, TNF-α and IFN-γ in MMP9 deficient $CD4^+$ T cells

Pure splenic $CD4^+$ T cells were isolated from wild-type and MMP9 deficient mice. Cells were plated at $2x10^6$/tube in 3ml tissue culture tubes in the presence or absence of anti-CD3 Ab (0.5μg/ml) for72 hours. Cells were collected and IL-2, TNFα, and IFN-γ were measured by real-time quantitative PCR. These graphs are representative of one of three separate experiments performed in triplicate (n=3). *$p<0.001$ as compared to stimulated wild-type cells.

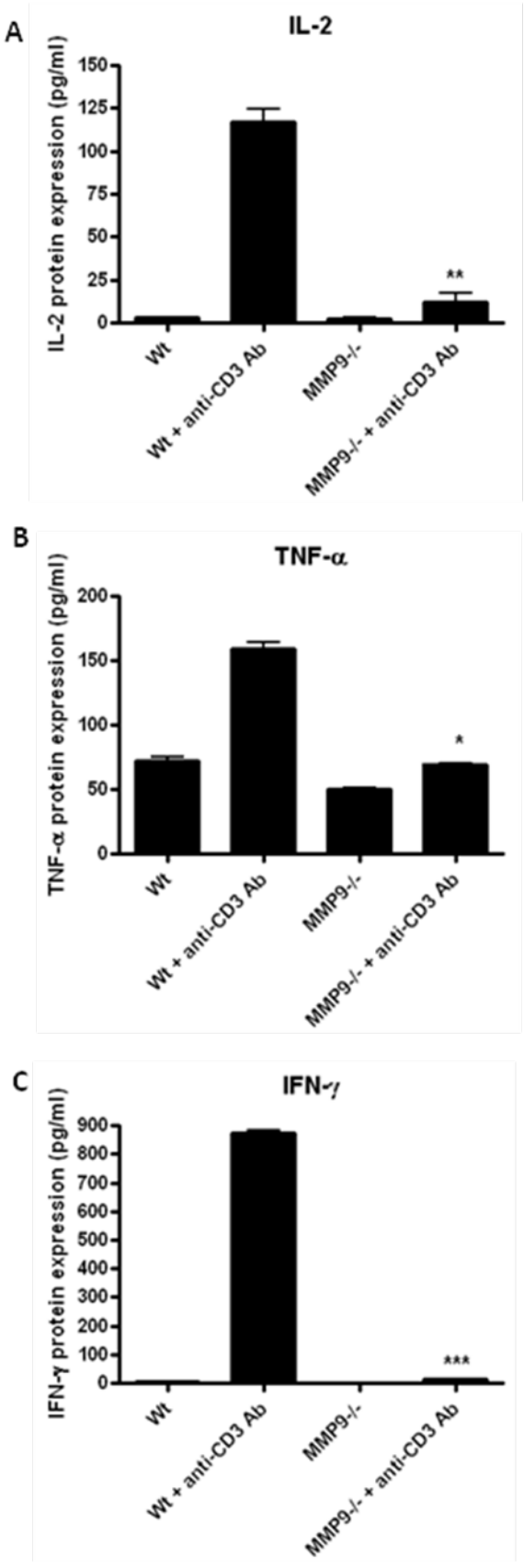

Figure 34. Cytokine protein profile of IL-2, TNF-α and IFN-γ in MMP9 deficient CD4$^+$ T cells

Pure splenic CD4$^+$ T cells were isolated from wild-type and MMP9 deficient mice. Cells were plated at 2x10^6/tube in 3ml tissue culture tubes in the presence or absence of anti-CD3 Ab (0.5μg/ml) for72 hours. Culture supernatants were collected and assayed using a Cytometric Bead Array (CBA). Fifty microliters of supernatant from each sample was added to 50μl of cytokine capture beads and incubated at room temperature for 2 hours. The beads were washed and analyzed by flow cytometry. These graphs are representative of one of two separate experiments performed in triplicate (n=3). *p<0.01, **p<0.001, ***p<0.0001 as compared to stimulated wild-type cells.

MMP9 deficient T cells displayed a significant decrease in IL-2, with a dramatic increase in TNF-α and IFN-γ, as compared to wild-type $CD4^+$ T cells [figure 33A-C]. Strikingly, supernatants from $CD4^+$ MMP9 deficient T cells, as compared to wild-type, showed significantly lower levels of IL-2 [figure 34A], TNF-α [figure 34B] and IFN-γ [figure 34C] protein expression, with IL-2 and TNF-α displaying a 50% decrease and IFN-γ displaying an 80-90% decrease. The discrepancy in the mRNA and protein expression levels of TNF-α and IFN-γ remain unclear. Increasing the replicates in the sample size may clarify this discrepancy.

Examination of mRNA levels in $CD8^+$ MMP9 deficient T cells revealed significantly diminished levels of IL-2, IFN-γ, and to a lesser extent, although still pronounced, TNF-α [figure 35A-C]. In addition, supernatants from $CD8^+$ MMP9 deficient T cells showed diminished levels of TNF-α [figure 36A] and IFN-γ [figure 36B] protein expression very similar to those seen in the $CD4^+$ T MMP9 deficient T cells (due to limited sample size, IL-2 data was not assessed). These results indicate that T cells deficient in MMP9 exhibit altered cytokine production at the mRNA and protein levels. If we combine these results with the previous observation that IL-10 and foxp3 expression were elevated and that NFAT and CD25 expression were diminished in the absence of MMP9, then these findings suggest that although MMP inhibition does not induce Treg function, these cells exhibit regulatory T cell characteristics in response to the absence of MMP9. These data may suggest a role of foxp3 in inhibiting NFAT and repressing cytokine expression as is seen in Tregs.

It has been previously reported that in addition to the alterations in cytokine expression, MMP9 deficient mice display alterations in chemokine expression (95).

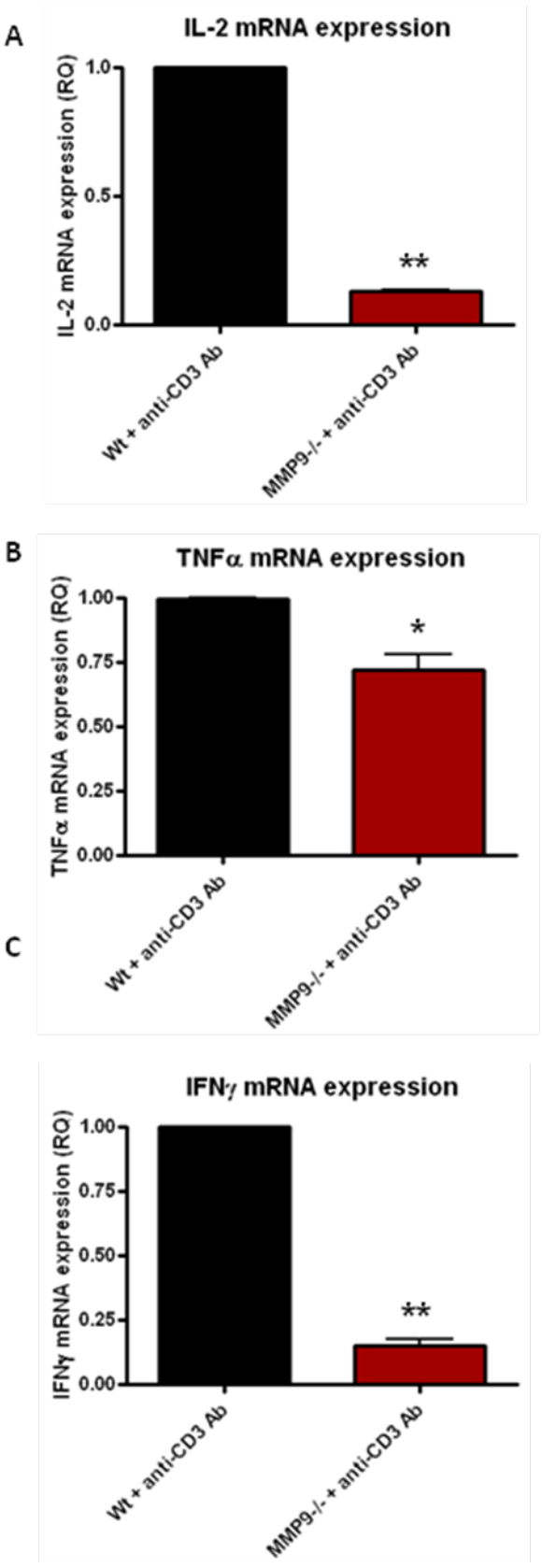

Figure 35. Cytokine gene profile of IL-2, TNF-α and IFN-γ in MMP9 deficient CD8$^+$ T cells

Pure splenic CD8$^+$ T cells were isolated from wild-type and MMP9 deficient mice. Cells were plated at 2x10^6/tube in 3ml tissue culture tubes in the presence or absence of anti-CD3 Ab (0.5μg/ml) for72 hours. Cells were collected and IL-2, TNFα, and IFN-γ were measured by real-time quantitative PCR. These graphs are representative of one of three separate experiments performed in triplicate (n=3). *p<0.01, **p<0.0001 as compared to stimulated wild-type cells.

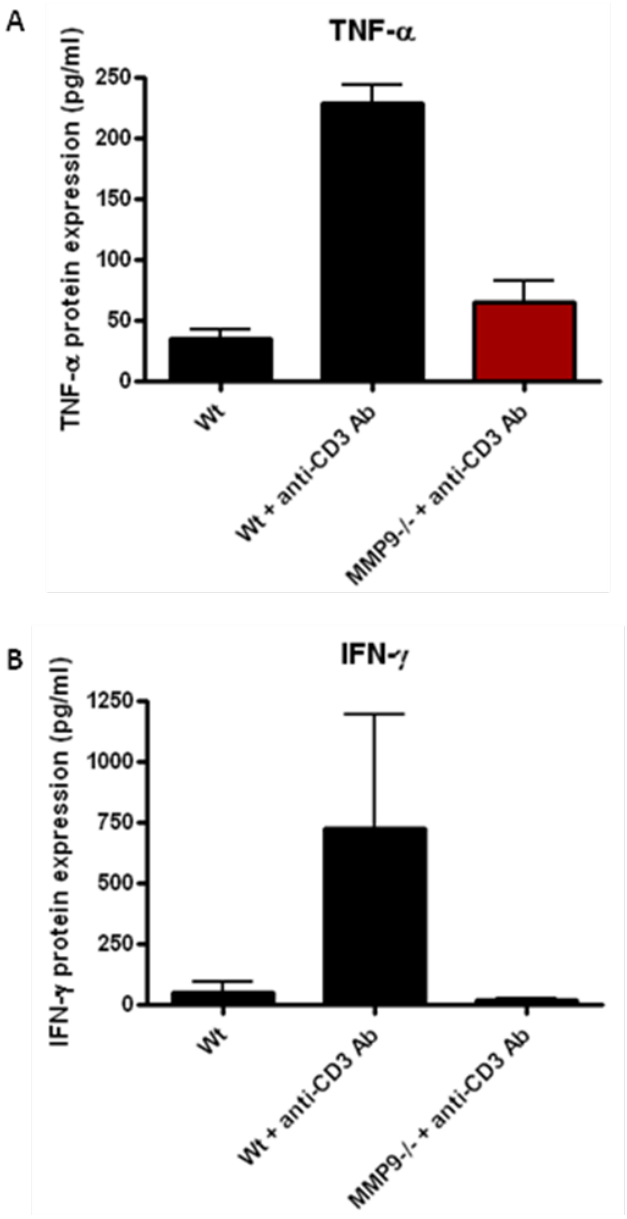

Figure 36. Cytokine protein profile of TNF-α and IFN-γ in MMP9 deficient CD8$^+$ T cells

Pure splenic CD8$^+$ T cells were isolated from wild-type and MMP9 deficient mice. Cells were plated at 2x10^6/tube in 3ml tissue culture tubes in the presence or absence of anti-CD3 Ab (0.5μg/ml) for 72 hours. Culture supernatants were collected and assayed using a Cytometric Bead Array (CBA). Fifty microliters of supernatant from each sample was added to 50μl of cytokine capture beads and incubated at room temperature for 2 hours. The beads were washed and analyzed by flow cytometry. These graphs are representative of one of two separate experiments performed in triplicate (n=2).

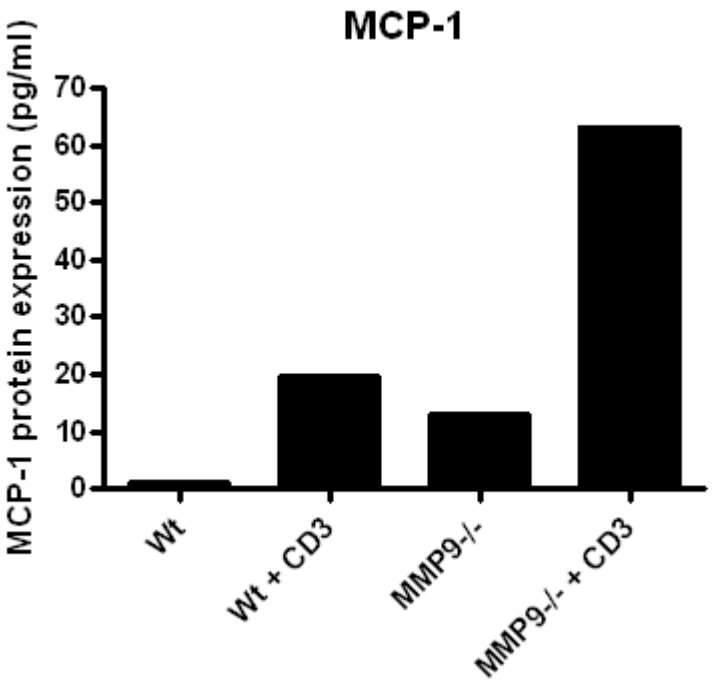

Figure 37. MCP-1 expression is elevated in MMP9 deficient CD4$^+$ T cells
Pure splenic CD4$^+$ T cells were isolated from wild-type and MMP9 deficient mice. Cells were plated at 2x10^6/tube in 3ml tissue culture tubes in the presence or absence of anti-CD3 Ab (0.5µg/ml) for 72 hours. Culture supernatants were collected and assayed using a Cytometric Bead Array (CBA). Fifty microliters of supernatant from each sample was added to 50µl of cytokine capture beads and incubated at room temperature for 2 hours. The beads were washed and analyzed by flow cytometry. This graph is representative of one experiments performed in triplicate (n=1)

Campbell et al. reported an increase in MCP-1, MCP-5 and RANTES (95). To determine if these changes were present in our studies, we examined the expression of MCP-1 from MMP9 deficient T cell supernatant. Our preliminary data also revealed an increase in MCP-1 protein expression in MMP9 deficient T cells following stimulation with anti-CD3 Ab [figure 37]. Although it is not clear, what importance MCP-1 plays in our studies, the increase in MCP-1 may be due to the T cell trying to compensate for the defect in T cell activation. Since MCP-1 is a chemokine important in guiding cellular infiltration or trafficking, its up-regulation in MMP9 deficient T cells may aid in their cellular migration.

K. Production of IL-2, TNF-α, and IFN-γ are reduced in SB3CT treated $CD4^+$ and $CD8^+$ T cells

To determine the effects of MMP9 inhibition by SB3CT on T cell cytokine production and identify any correlation with MMP9 deficiency, mRNA and protein expression levels of IL-2, TNF-α and IFN-γ were measured by means of real-time PCR and a cytokine bead array, respectively. Wild-type $CD4^+$ T cells were treated with SB3CT or the corresponding vehicle control for 6 hours, followed by stimulation with soluble anti-CD3 Ab for varying time points (1-12 hours). The cell pellets were collected and processed for real-time PCR and the supernatants were collected and analyzed by means of a cytokine bead array. In figure 38, vehicle treated $CD4^+$ T cells exhibit increasing levels of IL-2 [figure 38A], TNF-α [figure 38B] and IFN-γ [figure 38C] mRNA expression in relation to time. In response to SB3CT treatment however, mRNA

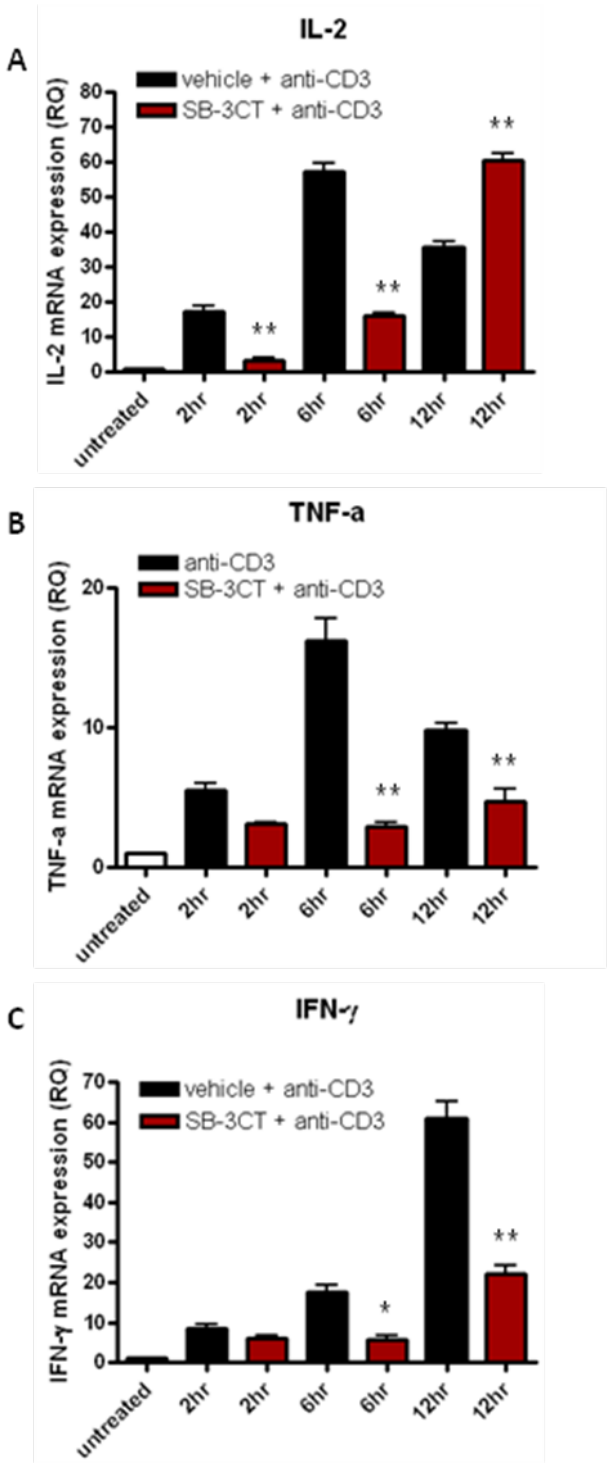

Figure 38. Cytokine mRNA profile of IL-2, TNF-α and IFN-γ expression in SB3CT treated $CD4^+$ T cells

Pure splenic $CD4^+$ T cells were isolated from C57BL/6 mice and treated with 10μM of SB3CT or VCtl for 6 hours. Cells were then washed in RPMI and plated at $2x10^6$/tube in 3ml tissue culture tubes in the presence of anti-CD3 Ab (0.5μg/ml) for 1-12 hours. Cells were collected and IL-2, TNFα and IFN-γ mRNA levels were measured by real-time quantitative PCR. These graphs are representative of one of three separate experiments performed in triplicate (n=3). *p>0.01, **p>0.001 as compared to the corresponding vehicle treated group.

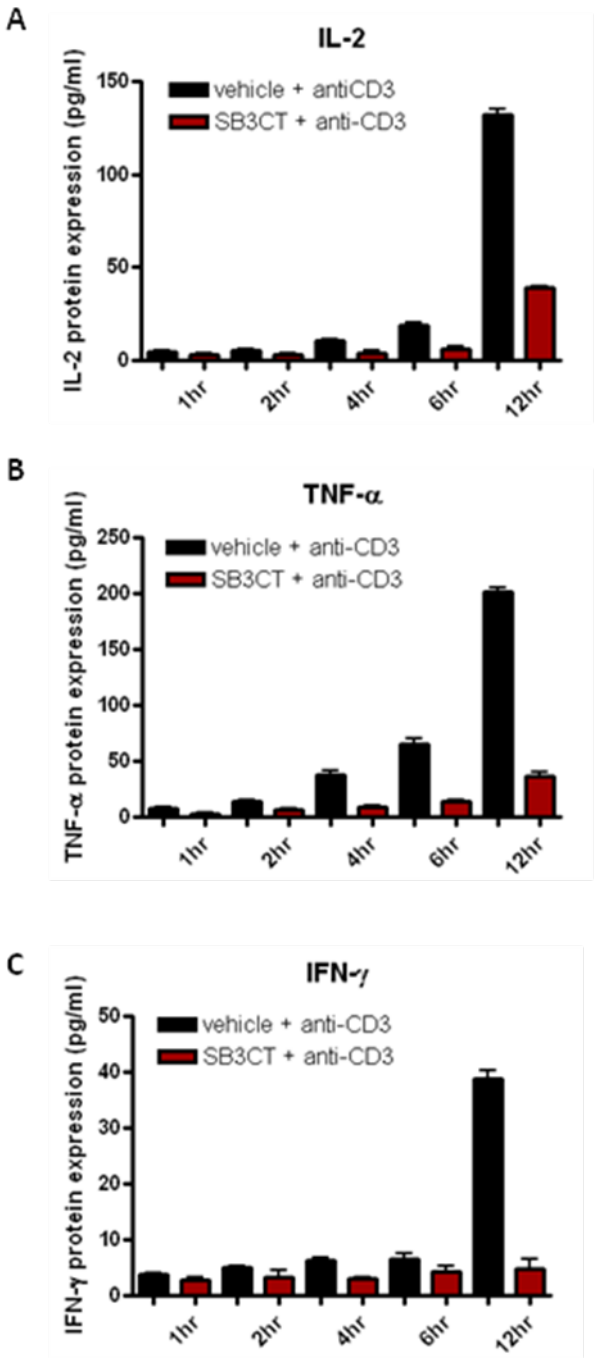

Figure 39. Cytokine protein profile of TNF-α and IFN-γ in SB3CT treated $CD4^+$ T cells

Pure splenic $CD8^+$ T cells were isolated from C57BL/6 mice and treated with 10μM of SB3CT or VCtl for 6 hours. Cells were then washed in RPMI and plated at $2x10^6$/tube in 3ml tissue culture tubes in the presence of anti-CD3 Ab (0.5μg/ml) for 1-12 hours. Culture supernatants were collected and assayed using a Cytometric Bead Array (CBA). Fifty microliters of supernatant from each sample was added to 50μl of A) IL-2, B) TNF-α or C) IFN-γ cytokine capture beads and incubated at room temperature for 2 hours. The beads were washed and analyzed by flow cytometry. These graphs are representative of one of two separate experiments performed in triplicate two experiments (n=2).

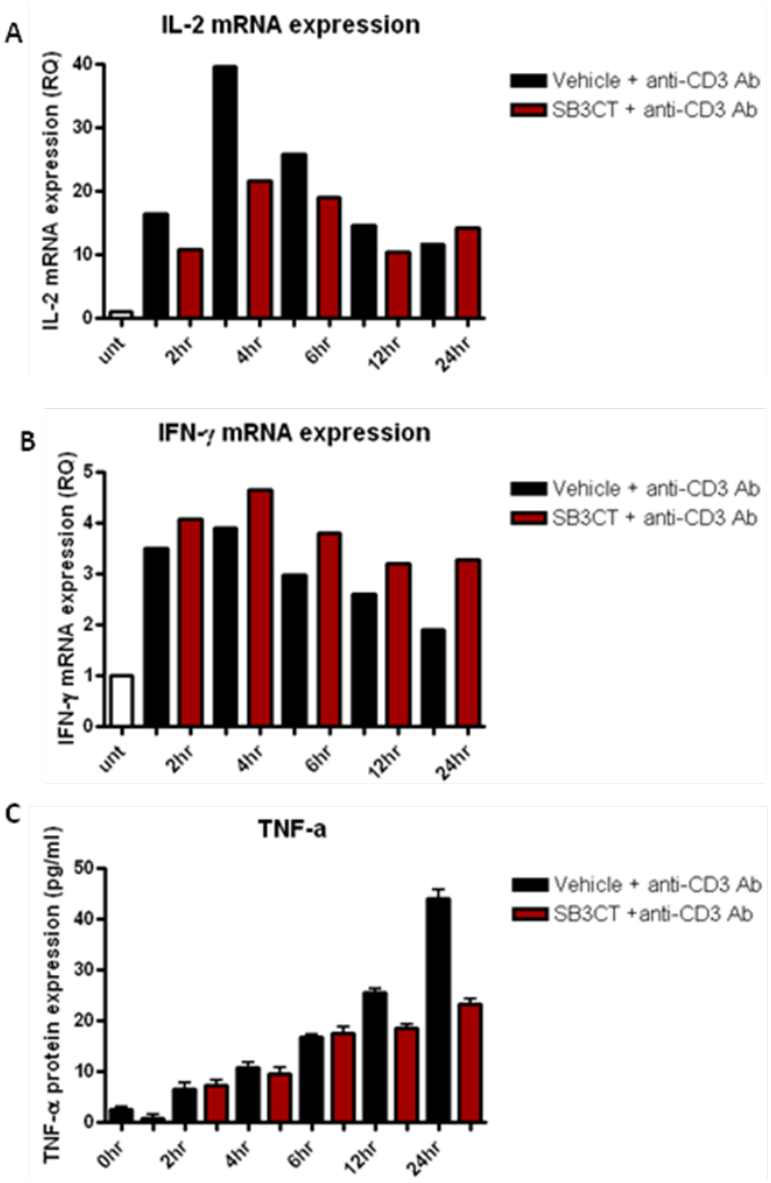

Figure 40. Cytokine gene and protein expression of IL-2, TNF-α and IFN-γ are reduced in SB3CT treated CD8$^+$ T cells

Pure splenic CD8$^+$ T cells were isolated from C57BL/6 mice and treated with 10μM of SB3CT or VCtl for 6 hours. Cells were then washed in RPMI and plated at 2x10^6/tube in 3ml tissue culture tubes in the presence of anti-CD3 Ab (0.5μg/ml) for 1-6 or 1-12 hours. Cells were collected and A) IL-2 and B) IFN-γ mRNA expression levels were measured by real-time quantitative PCR. Culture supernatants were collected and assayed using a Cytometric Bead Array (CBA). Fifty microliters of supernatant from each sample was added to 50μl of C) TNF-α cytokine capture beads and incubated at room temperature for 2 hours. The beads were washed and analyzed by flow cytometry. These graphs are representative of one of two separate experiments performed in triplicate two experiments (n=2).

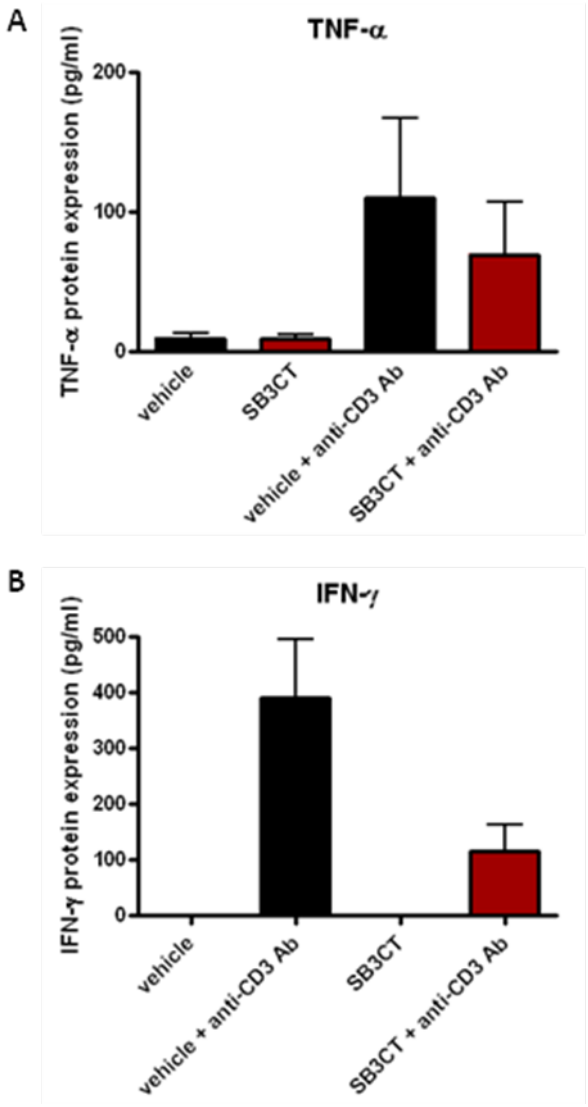

Figure 41. Cytokine protein production of TNF-α and IFN-γ are reduced in SB3CT treated CD8$^+$ T cells

Pure splenic CD8$^+$ T cells were isolated from C57BL/6 mice. Cells were treated with 10μM of SB3CT or Vehicle (VCtl) for 6 hours. Cells were then washed three times in RPMI and plated at 2x10^6/tube in 3ml tissue culture tubes in the presence of anti-CD3 Ab (0.5μg/ml) for 72 hours. Culture supernatants were collected and assayed using a Cytometric Bead Array (CBA). Fifty microliters of supernatant from each sample was added to 50μl of A) TNF-α and B) IFN-γ cytokine capture beads and incubated at room temperature for 2 hours. The beads were washed and analyzed by flow cytometry. These graphs are representative of two experiments (n=2).

levels are dramatically lower, even with the slight increase in IL-2, TNF-α and IFN-γ mRNA expression over time.

Observation of protein expression reveals significantly lower levels of all three cytokines in SB3CT treated $CD4^+$ T cells over the 12 hour period, as compared to protein levels produced from vehicle treated cells [figure 39A-C]. In contrast, examination of vehicle or SB3CT treated $CD8^+$ T cells revealed variable mRNA expression levels. There does not seem to be a distinct trend in the expression levels over time. IL-2 expression appears to peak at 4 hours and then decrease over time, with not much distinction between vehicle or SB3CT treatment [figure 40A]. IFN-γ mRNA expression in SB3CT treated $CD8^+$ T cells appears to plateau over the duration of time, while vehicle treated cells display a slight decrease in expression from 4 to 24 hours [figure 40B]. Due to the limited sample size, TNF-α mRNA expression was not assessed. In examining protein expression, TNF-α protein expression appears to be similar between the vehicle and SB3CT treated T cells until 12 hours, when expression in SB3CT treated cells seems to decline as vehicle treated cells continues to rise [figure 40C] (due to sample size, IL-2 and IFN-γ expression was not assessed). When cell supernatants were analyzed 72 hours after stimulation, TNF-α [figure 41A] and IFN-γ [figure 41B] protein expression were still reduced. Taken together, these data confirm that inhibition of T cell derived MMP9 by SB3CT alters cytokine production at the mRNA and protein levels.

L. MMP9 deficiency alters $CD4^+$ and $CD8^+$ T cell phenotypes

To further characterize the role of T cell derived MMP9, the cell phenotype of MMP9 sufficient T cells, as well as MMP9 deficient T cells were assessed by means of

flow cytometry. A panel of seven cell surface markers were chosen, because their expression is elevated following T cell activation and, as such are T cell activation markers. CD45RO is an isoform of the transmembrane tyrosine phosphatase CD45, present on $CD4^+$ effector cells. CD45 regulates the threshold of T cell antigen receptor (TCR) signaling through dephosphorylation of protein tyrosine kinases (119). CD69 is the earliest inducible cell surface glycoprotein acquired during lymphoid activation, and is involved in lymphocyte proliferation (120). CD25 is the alpha chain of the IL-2 receptor and is a type I transmembrane protein present on activated T cells (121). CD40L is a membrane glycoprotein and differentiation antigen expressed on the surface of T-cells, that co-stimulates proliferation of activated T-cells, accompanied by the production of IFN-γ, TNF-α, and IL-2 (122). CD44 is a cell-surface glycoprotein involved in cell-cell interactions, cell adhesion and migration along with T cell activation (123). CTLA-4 is a member of the immunoglobulin super-family, which is expressed on the surface of T cells and transmits an inhibitory signal to T cells (124). Intracellular CTLA4 is also found in regulatory T cells and may be important to their function. CD62L is a cell adhesion molecule found on leukocytes (125).

$CD4^+$ and $CD8^+$ T cells isolated from wild-type and MMP9 deficient C57BL/6 mice were cultured in the presence or absence of soluble anti-CD3 Ab for 24 hours. Cells were then collected and stained for CD45RO-FITC, CD69-FITC, CD25-PE, CD40L-PE, CD44-PE, CTLA-4-PE and CD62L-APC. Analysis of wild-type $CD4^+$ T cells revealed increased surface expression levels of CD25, CD69, CD62L, and CD44. CTLA-4 and CD40L were also expressed, although at lower levels, while CD45RO expression was significantly diminished [figure 42]. In comparison, analysis of $CD4^+$ T cells from

MMP9 deficient T cells revealed increased surface expression levels of CD62L, CTLA-4 and CD45RO. CD44 and CD40L were expressed as well, although at lower levels. CD25, CD69 and CD40L expression levels were all significantly diminished [figure 42]. These data show that as compared to wild-type CD4+ T cells, MMP9 deficient $CD4^+$ T cells have significantly lower levels of cell surface CD25 and CD69, while expressing higher levels of CD45RO and CTLA-4 [figure 42].

Analysis of cell surface expression in wild-type $CD8^+$ T cells [figure 42] revealed increased levels of CD25, CD62L and CD69, although, CD25 levels were somewhat lower than that seen in wild-type $CD4^+$ T cells. Additionally, CD40L, CD44 and CTLA-4 were expressed although the percent expression was less than or equal to 20%. CD45RO was also expressed at very low levels, not exceeding 5%. Analysis of MMP9 deficient $CD8^+$ T cells as compared to wild-type $CD8^+$ T cells revealed extremely low expression levels of CD69, CD25, CD62L. CD45RO and CD44 surface expression levels remained the same as in wild-type cells. Interestingly, CTLA-4 and CD40L surface expression exhibited slight elevation as compared to wild-type cells [figure 42]. Taken together, these data demonstrate that $CD4^+$ and $CD8^+$ T cells display differential cell surface expression in the absence of MMP9.

M. MMP9 inhibition by SB3CT alters CD4 and CD8 T cell phenotypes

In continuation of the phenotypic analysis of T cells in response to MMP inhibition, we next wanted to determine the phenotype of T cells treated with SB3CT and compare the results to those seen in the MMP9 deficient T cells. Since CD25 and CD69 were significantly diminished in the MMP9 deficient $CD4^+$ and $CD8^+$ T cells, we

	Wt CD4$^+$ T cells	MMP9-/- CD4$^+$ T cells	Wt CD8$^+$ T cells	MMP9-/- CD8$^+$ T cells
CD45RO	17.9%	98.2%	5.0%	5.4%
CD69	88.8%	18.0%	72.8%	3.9%
CD25	92.8%	31.6%	63.8%	11.9%
CD40L	59.9%	50.9%	16.9%	34.6%
CD44	97.6%	77.5%	20.1%	24.0%
CTLA-4	62.3%	96.2%	14.9%	25.1%
CD62L	98.6%	99.4%	91.8%	29.6%

Figure 42. Phenotypic analysis of CD4+ and CD8+ MMP deficient T cells

Pure splenic CD4$^+$ and CD8+ T cells were isolated from wild-type and MMP9 deficient mice. Cells were plated in a 96 well plate in the presence of anti-CD3 (0.5 µg/ml) for 24 hours. Cells were collected and surface expression of CD45RO, CD69, CD25, CD44, CD40L, CD62L, CTLA-4 was analyzed by flow cytometry. These data are representative of the mean ± SD of one of two separate experiments performed in triplicate (n=2).

chose to analyze the surface expression of these two markers in T cells following MMP9 inhibition by SB3CT. $CD4^+$ T cells were isolated from wild-type C57BL/6 mice and treated with varying concentrations of SB3CT (5-20μM) or the corresponding vehicle control for 6 hours. Following treatment, $CD4^+$ T cells were washed and cultured in the presence or absence of soluble anti-CD3 Ab for 24 hours. Cells were then collected and stained for CD69-FITC and CD25-PE. In the absence of anti-CD3 Ab stimulation, cell surface expression levels of CD69 and CD25 were minimal (data not shown).

Analysis of stimulated vehicle-treated $CD4^+$ T cells revealed enhanced CD69 surface expression, which remained elevated as the concentration of vehicle-treatment increased from 5-20μM [figure 43A]. Interestingly, SB3CT-treatment also displayed an increase in CD69 expression, similar to that seen in vehicle-treated cells [figure 43B]. As the concentration of SB3CT increased, however, there was a slight decrease in CD69 expression. Analysis of CD25 surface expression on vehicle-treated cells revealed a slight decrease in CD25 expression as the concentration of vehicle-treatment increased from 5-20μM [figure 44A]. Comparatively, SB3CT treated cells displayed a significant dose-dependent decrease in CD25 surface expression as the concentration of SB3CT increased [figure 44B]. Taken together, these data demonstrate a significant defect in CD25 surface expression thereby confirming results previously shown in MMP9 deficient T cells. These data also strengthen the gene expression data, again confirming MMP9s involvement in regulating CD25 expression, thereby affecting T cell activation and function.

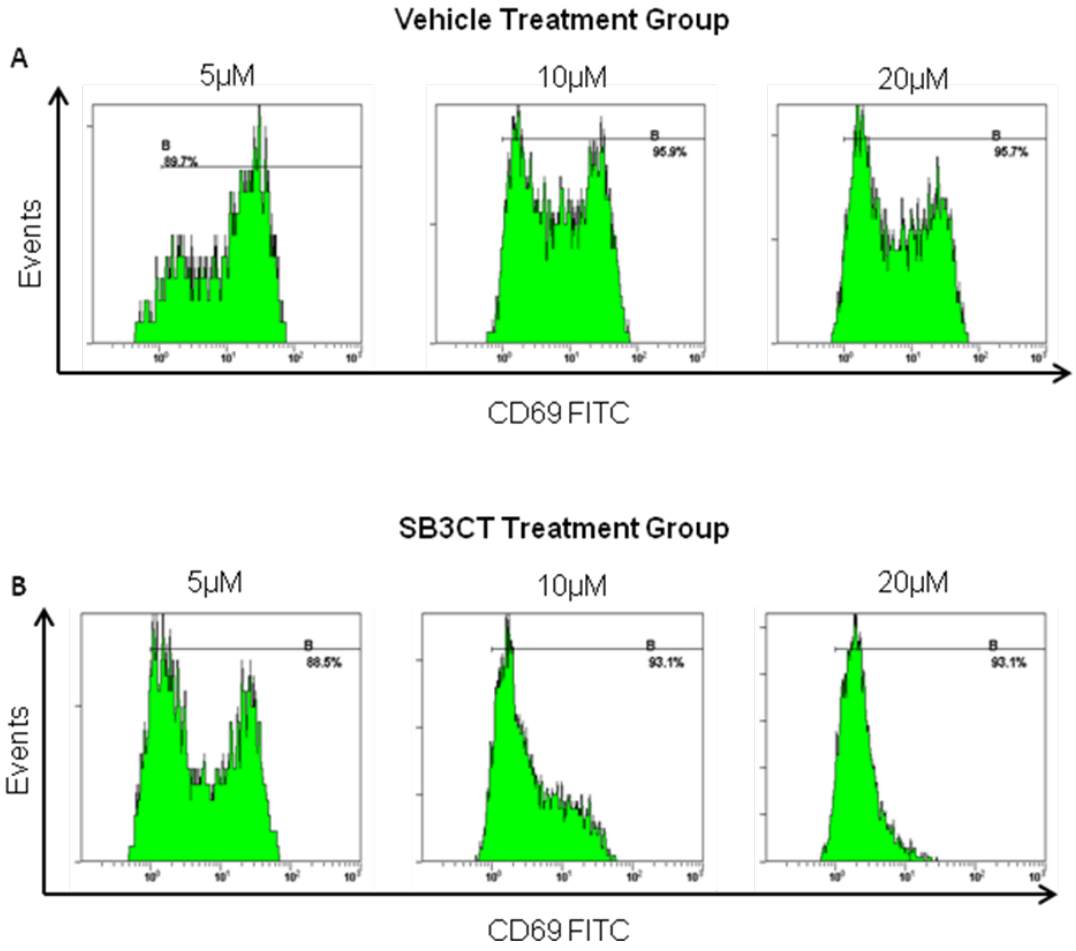

Figure 43. Phenotypic analysis of CD69 on SB3CT treated CD4$^+$ T cells
Pure splenic CD4$^+$ T cells were isolated from wild-type C57BL/6 mice. Cells were treated with varying concentrations of SB3CT (5-10μM). Cells were then plated in a 96 well plate in the presence of anti-CD3 Ab (0.5μg/ml) for 24 hours. Cells were collected and surface expression of CD69 was analyzed by flow cytometry. These data are representative of the mean ± SD of one of two separate experiments performed in triplicate (n=2).

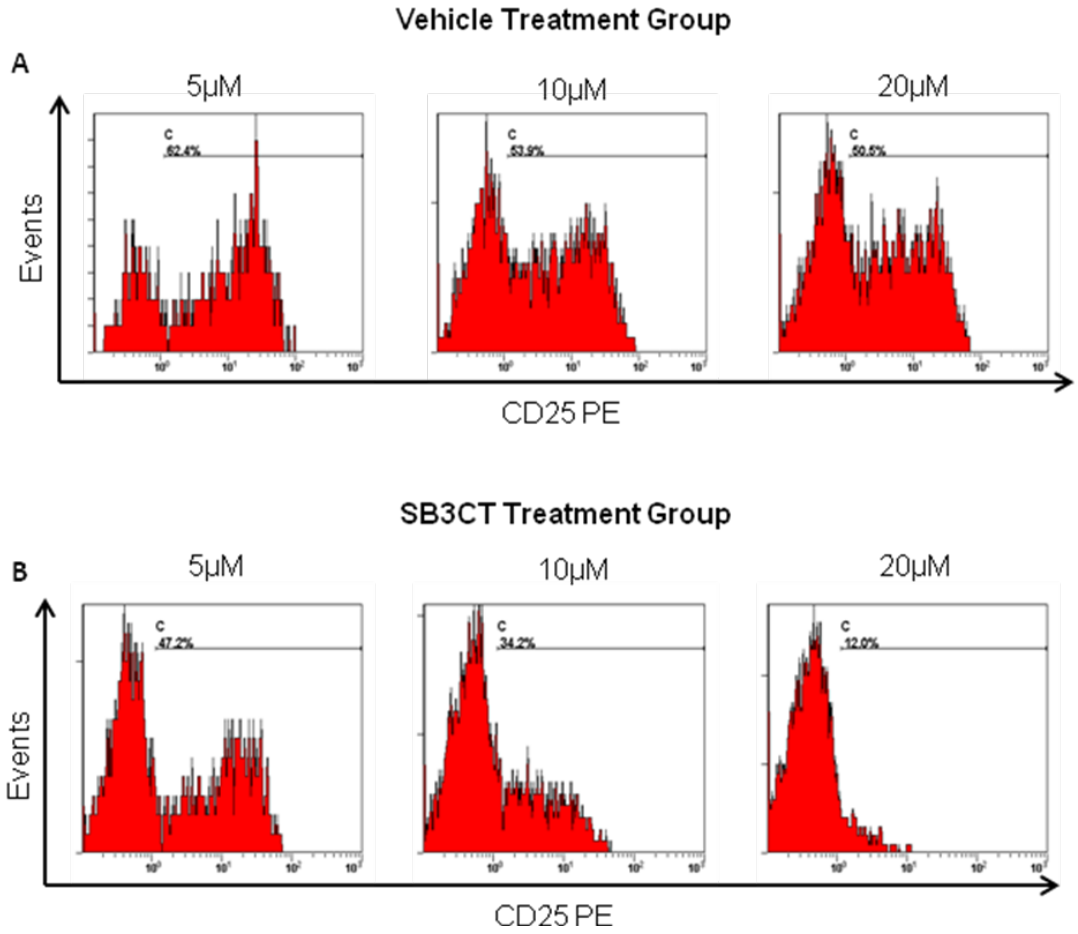

Figure 44. Phenotypic analysis of CD25 on SB3CT treated CD4$^+$ T cells
Pure splenic CD4$^+$ T cells were isolated from wild-type C57BL/6 mice. Cells were treated with varying concentrations of SB3CT (5-10μM). Cells were then plated in a 96 well plate in the presence of anti-CD3 Ab (0.5μg/ml) for 24 hours. Cells were collected and surface expression of CD25 was analyzed by flow cytometry. These data are representative of the mean ± SD of one of two separate experiments performed in triplicate (n=2).

Chapter 3. MMP inhibition in vivo: Model of antigen-specific T cell mediated lung injury

A. Murine model of antigen-specific CD8$^+$ effector T cell mediated lung injury

To investigate the role of MMP inhibition in vivo, we utilized a CC10-OVA model of airway hyperresponsiveness. Our data has demonstrated that CD8$^+$ T cells express significantly elevated levels of MMP9 following anti-CD3 Ab activation. Therefore, studying an in vivo CD8$^+$ T cell dependent model of lung injury will allow us to investigate the role of T cell derived MMP9 in mediating antigen-specific T cell activation in a physiological environment in vivo. Medoff et al. created this model, which was adapted by Shilling et al., such that transgenic mice only express chicken ovalbumin (126) in the lung as a result of ligation of the OVA gene behind the promoter for Clara cell secretory protein (CC10) (127). Since CC10 is specifically expressed by Clara cells, which make up 50-60% of the conducting airways of the lung in mice, this model allows us to specifically assess OVA-induced airway hypersensitivity in the lung (126). To induce lung injury, CD8$^+$ T cells are isolated from OT-1 transgenic mice, which have a TCR specific for the OVA peptide SIINFEKL bound to the class I MHC H-2K^b (128). This murine model provides a means for us to examine the role of antigen-specific T cell mediated lung injury, similar to that seen in lung transplant rejection and bronchiolitis obliterans syndrome (44).

B. MMP9 inhibition by SB3CT abrogates antigen-specific T cell proliferation

To examine the role of MMP inhibition on antigen-specific T cell mediated lung injury in vivo, we first wanted to determine whether specific MMP inhibition by SB3CT

would affect antigen-specific T cell proliferative function. To answer this question, antigen-specific T cell proliferation assays [figure 45] were utilized. Antigen-specific $CD4^+$ and $CD8^+$ T cells from OT-II and OT-1 transgenic C57BL/6 mice, respectively, were treated with varying concentrations of SB3CT (5-20μM) for 6 hours and cultured in the presence of OT-II (ova peptide) or OT-I (SIINFEKL peptide) pulsed antigen-presenting cells, respectively. As shown in figure 46A, untreated or vehicle treated OT-II transgenic $CD4^+$ T cells proliferated in response to OT-II pulsed antigen presenting cells. Interestingly, SB3CT treatment of OT-II transgenic $CD4^+$ T cells completely abrogated the proliferative response to OT-II pulsed antigen presenting cells. Examination of $CD8^+$ T cells from OT-I transgenic mice revealed a similar trend. OT-I transgenic $CD8^+$ T cells treated with SB3CT significantly decreased T cell proliferation in a dose-dependent manner in response to OT-I-pulsed antigen presenting cells, compared to vehicle treatment [figure 46B]. These data suggest that specific MMP inhibition can also abrogates T cell proliferation in an antigen-specific manner. Since anti-CD3 Ab is not a physiological stimulus of cells, we wanted to assess the effects of MMP inhibition on T cell activation in an in vivo model, which allows us to study MMP regulated T cell activation under physiological conditions.

C. Adoptive transfer of SB3CT treated OT-1 $CD8^+$ T cells

To determine whether MMP inhibition had an effect on antigen-specific T cell mediated lung injury in vivo, $CD8^+$ T cells were isolated from OT-1 transgenic mice and treated with 10μM of SB3CT or the corresponding vehicle control for 6 hours [figure 47]. The cells were then cultured in vitro for 5 days in the presence of IL-2, IL-12,

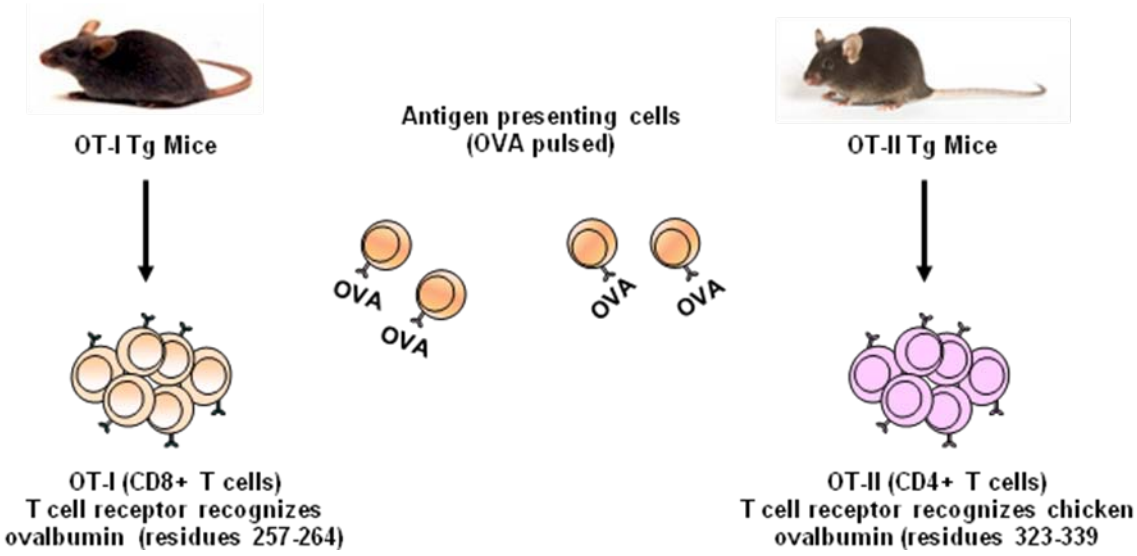

Figure 45. Schematic diagram of antigen specific (OT-I and OT-II) T cell proliferation

OT-II Tg $CD4^+$ T cells were isolated from OT-I Tg mice. OT-II T cells proliferate in response to residues 323-339 of ovalbumin. OT-I Tg $CD8^+$ T cells were isolated from OT-I Tg mice. OT-I T cells proliferate in response to residues 257-264 of ovalbumin.

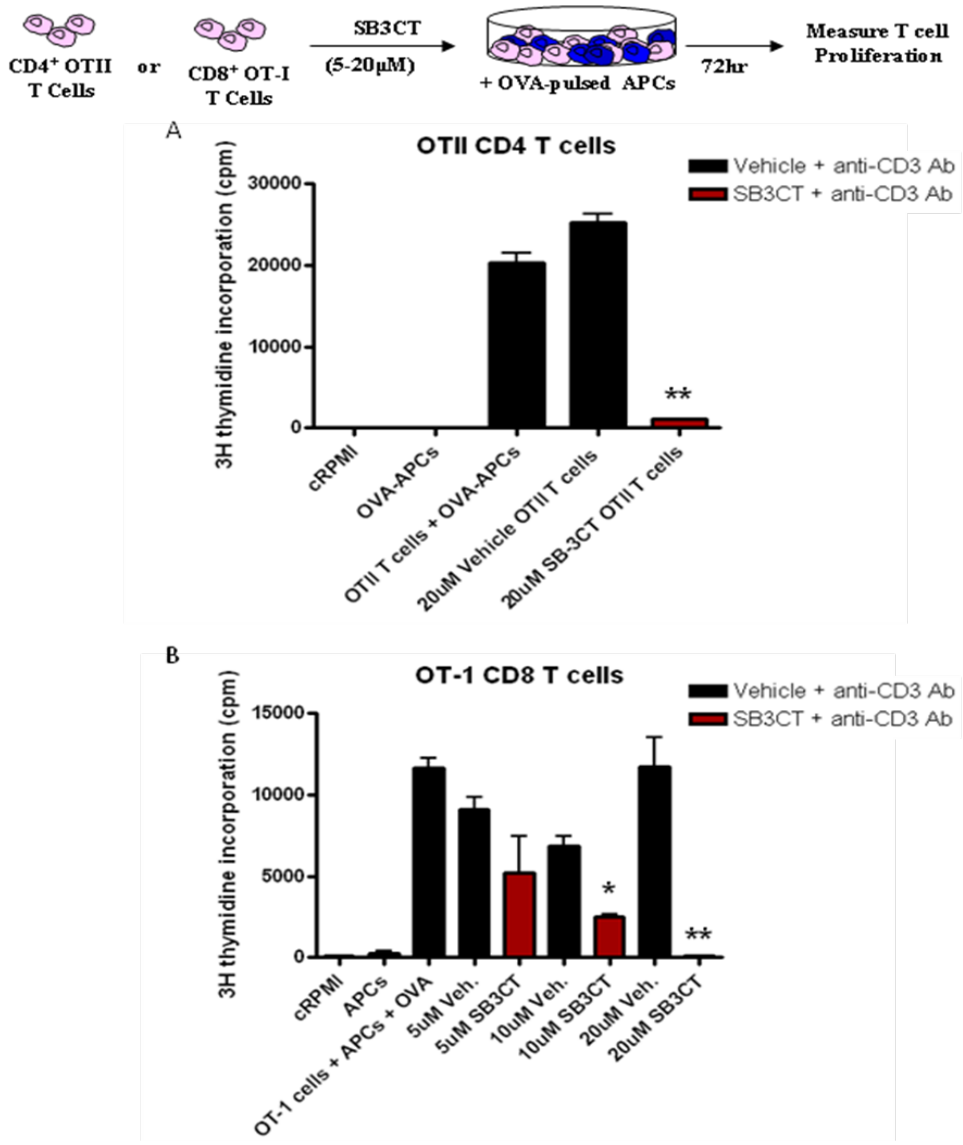

Figure 46. SB3CT treated antigen-specific T cells (OT-I and OT-II) display impairment in proliferative ability

Pure splenic $CD4^+$ and $CD8^+$ T cells were isolated from OTII transgenic and OTI transgenic C57BL/6 mice, respectively. A) OTII Tg $CD4^+$ T cells were treated with 20μM SB3CT or VCtl for 6 hours, and B) OTI Tg $CD8^+$ T cells were treated with varying concentrations of SB-3CT (5-20μM) or VCtl. Cells were then washed three times in RPMI and plated at $1x10^5$/well in a 96 well plate in the presence of OVA-pulsed antigen presenting cells (APCs) for 72 hours. 18 hours prior to harvest, 3H thymidine (0.5μCi/well) was added to the culture. T cell proliferation was measured by the amount of 3H thymidine incorporation. These data are representative of the mean ± SD *P<0.001 of one of two separate experiments performed in triplicate (n=2). *p<0.001, **p<0.0001 as compared to stimulated wild-type cells.

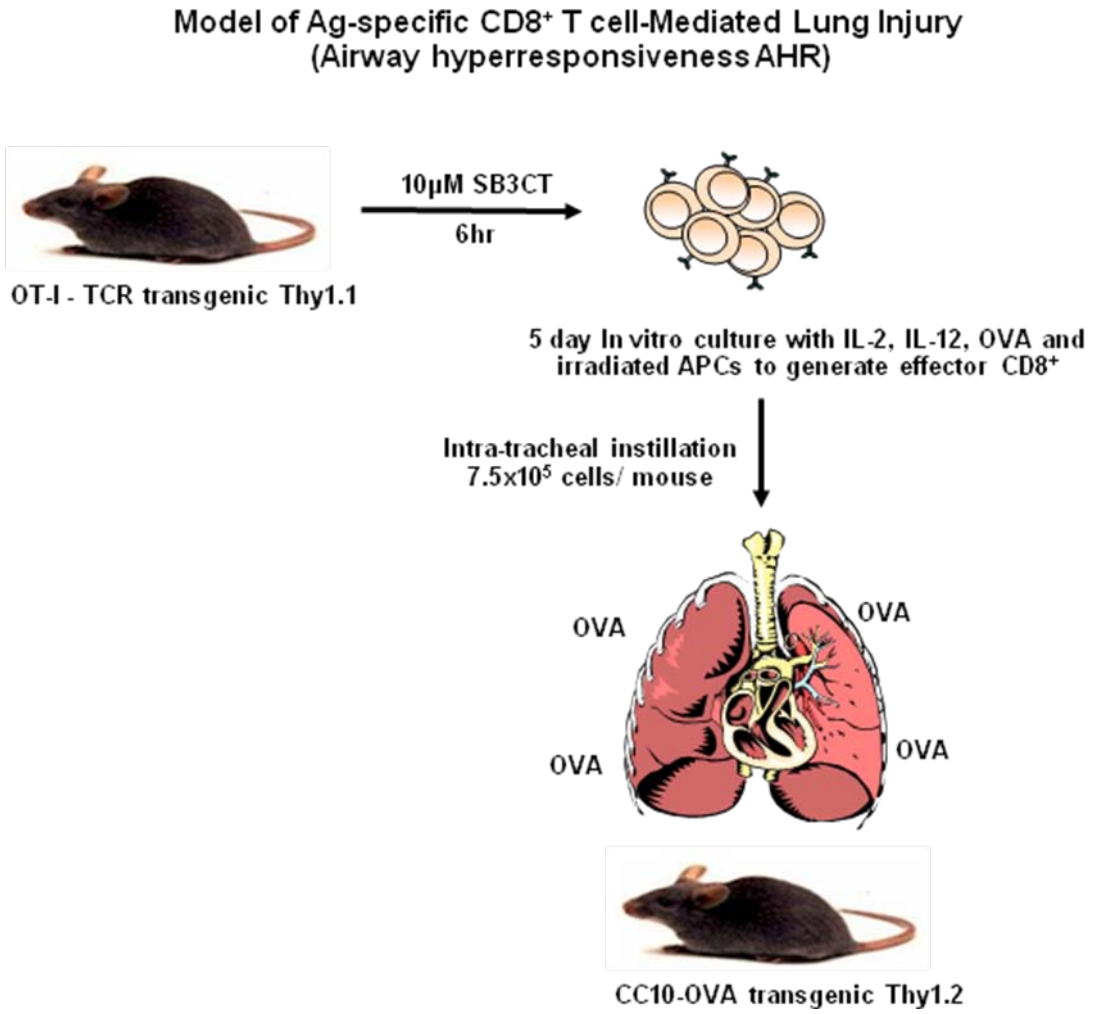

Figure 47. Schematic diagram of adoptive transfer of SB3CT treated OT-I $CD8^+$ T cells into CC10-OVA mice

anti-CD28 Ab, OVA peptide, and irradiated antigen presenting cells to generate effector $CD8^+$ lymphocytes. The cultured OT-1 $CD8^+$ T cells were then intratrachelly transferred into the lungs of CC10-OVA transgenic or non-transgenic wild-type C57BL/6 mice. Analysis of total cell accumulation in bronchoalveolar lavage 7 days after adoptive transfer into wild type mice revealed similar low cell accumulation between the SB3CT treated (MMPI) and vehicle groups [figure 48A]. Additionally, total cell accumulation in the BAL of CC10-OVA transgenic mice 7 days after adoptive transfer displayed similar cell numbers between the SB3CT treated and vehicle groups [figure 48A] (not statistically significant). As expected, total cell accumulation was significantly higher in the BAL from CC10-OVA transgenic mice, as compared to wild-type mice, due to T cell mediated antigen specificity.

Within this animal model, neutrophilic alveolitis is determined by neutrophil accumulation in the BAL, quantified by the percentage of $GR1^+$ staining (126). Analysis of flow cytometry revealed a significantly higher percentage of neutrophilic accumulation in the CC10-OVA transgenic mice, as compared to the non-transgenic wild-type mice following adoptive transfer [figure 48B]. Strikingly, the mice that received SB3CT treated OT-1 cells displayed a significant decrease in neutrophilic accumulation, as compared to the mice that received vehicle-treated OT-1 cells [figure 48B] ($p<0.01$). The OT-1 transgenic mice were on a $Thy1.1^+$ background, providing a means of tracking the transferred cells in the CC10-OVA mice, which were on a $Thy1.2^+$ background. We next wanted to determine if there was a difference in the accumulation of $CD8^+$ $Thy1.1^+$ T cells in the lung between the two CC10-OVA treated groups (vehicle or SB3CT). Interestingly, analysis of the lung revealed a significant impairment of SB3CT treated

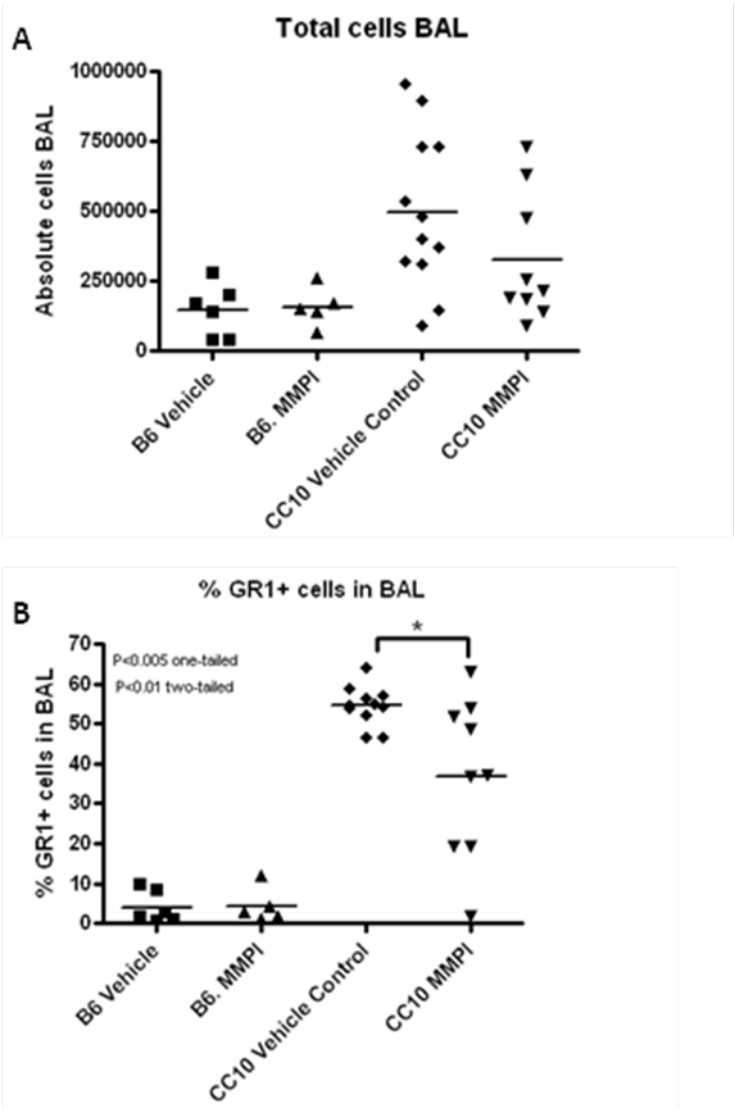

Figure 48. SB3CT treated OT-1 cells dampen neutrophilic accumulation in the BAL
SB3CT or vehicle treated OT-1 $CD8^+$ T cells were cultured for 5 days in vitro then adoptively transferred in the CC10-OVA transgenic (CC10) or non-transgenic (B6) wild-type C57BL/6 mice. Seven days after adoptive transfer, BAL fluid from the CC10-OVA or non-transgenic mice was analyzed and total cells present in the BAL were quantitated and neutrophils were stained with GR1 and analyzed by means of flow cytometry. B6 vehicle or MMPI = vehicle or SB3CT treated OT-I cells into wild-type C57BL/6 mice, respectively. CC10 vehicle or MMPI = vehicle or SB3CT treated OT-I cells into CC10-OVA transgenic mice, respectively. *$p<0.005$ as compared to stimulated wild-type cells. n=10

$CD8^+$ $Thy1.1^+$ T cells to accumulate in the lung compared with vehicle-treated $CD8^+$ $Thy1.1^+$ T cells ($p<0.01$) [figure 49A]. Moreover, analysis of CD25 cell surface expression revealed that of the SB3CT treated $CD8^+$ $Thy1.1^+$ T cells that accumulated in the lung, these cells displayed a lower percentage of CD25 expression (~30%) [figure 49B] and mean fluorescence intensity (MFI) as compared to vehicle-treated $CD8^+$ $Thy1.1^+$ T cells, which were ~50% $CD25^+$ and displayed a higher MFI ($p<0.01$) [figure 49C].

In the BAL fluid, adoptive transfer of OT-I vehicle treated T cells showed an increase in neutrophilic presence, whereas OT-1 SB3CT treated T cells showed a decrease. We hypothesized that this could in part be due to an up-regulation of interleukin 8 (IL-8), known as KC in mice. MMP9 can cleave IL-8 at its N-terminus, causing an increase its chemotactic activity for neutrophils. If MMP9 is inhibited, then this should prevent the cleavage and activation of IL-8, thereby reducing neutrophilic migration or infiltration. Using an KC elisa assay to measure the presence of active IL-8, we unexpectedly discovered that KC levels were not different between the vehicle and SB3CT treatment groups [figure 50]. These data suggest that the changes in neutrophilic recruitment may be IL-8 independent.

Histological analysis of the lung demonstrated varying degrees of perivascular and peribronchial inflammation among the groups. Due to the variability in the histology between mice, we did not achieve statistical significance when comparing the groups. However, the CC10-OVA mice that received vehicle-treated OT-1 $CD8^+$ T cells exhibited severe inflammation, with cells migrating into the vessel wall and lumen causing severe vessel occlusion (arrows point to cellular occlusion) [figure 51].

Strikingly, although some of the CC10-OVA mice that received SB3CT treated OT-1 CD8+ T cells displayed varying degrees of inflammation, the degree of inflammation was significantly dampened. As shown in figure 51, SB3CT treated OT-1 CD8+ T cells did not induce perivascular or perinuclear infiltration following intrapulmonary adoptive transfer into CC10-OVA mice, although there was some cellular accumulation around the vessels (arrows point to the clear vessel lumen). Taken together, these results demonstrate that inhibition of T cell derived MMPs leads to a decrease in the percentage of CD8+ Thy1.1+ cells residing in the lung, along with a decrease in CD25 surface expression. These data clearly demonstrate a role for MMP9 in mediating antigen specific T cell driven lung injury. This injury is then dampened by inhibition of T cell- derived MMPs, which lessening T cell activation, thereby providing a protective response.

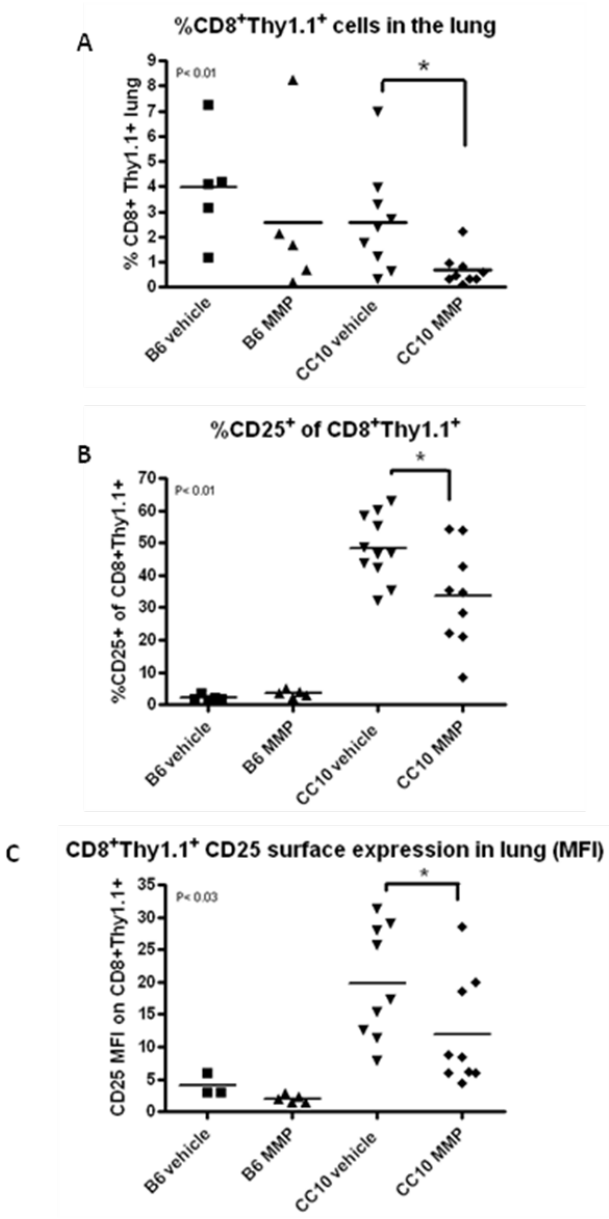

Figure 49. SB3CT treated OT-1 cells abrogated $CD8^{+}Thy1.1^{+}$ T cell accumulation in the lung

Activated OT-1 $CD8^{+}$ T cells were adoptively transferred in the CC10-OVA transgenic or non-transgenic wild-type C57BL/6 mice. $CD8^{+}$ $Thy1.1^{+}$ T cells were isolated from the lung mice following the adoptive transfer of SB3CT or vehicle treated cells. The $CD8^{+}$ $Thy1.1^{+}$ T cells were stained with CD25 and analyzed by means of flow cytometry. *$p<0.01$ as compared to stimulated wild-type cells.

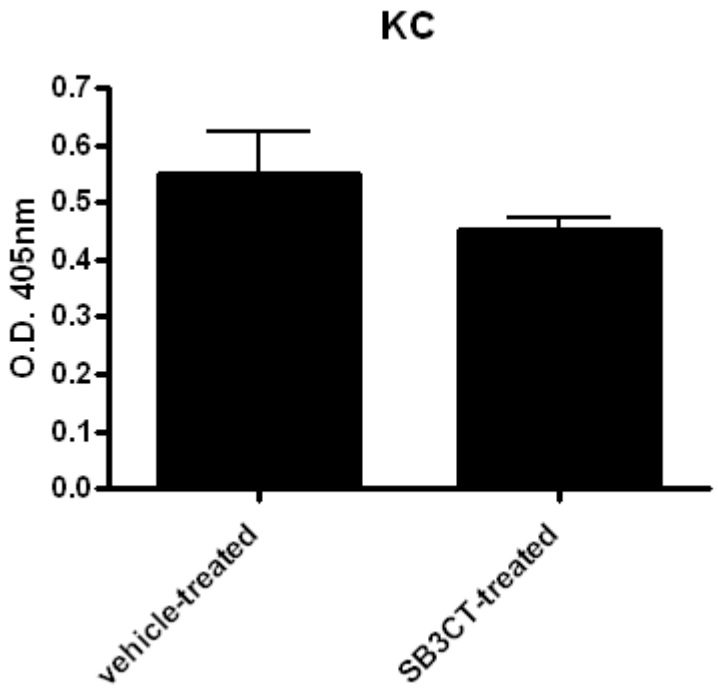

Figure 50. IL-8 (KC) expression in the BAL fluid of vehicle or SB3CT treated OT-1 T cells adoptively transferred into the lungs of CC10 mice

$CD8^+$ T cells were isolated from OT-1 transgenic mice and were treated with 10μM of SB3CT or the corresponding vehicle control for 6 hours. The cells were then washed and cultured in vitro for 5 days in the presence of IL-2, IL-12, anti-CD28, OVA peptide, and irradiated antigen presenting cells to generate effector $CD8^+$ lymphocytes. The cultured OT-1 $CD8^+$ T cells were then adoptively transferred in the CC10-OVA transgenic or non-transgenic wild-type C57BL/6 mice. BAL fluid was collected and assayed for IL-8 expression by elisa. n=8 per group p value=0.04

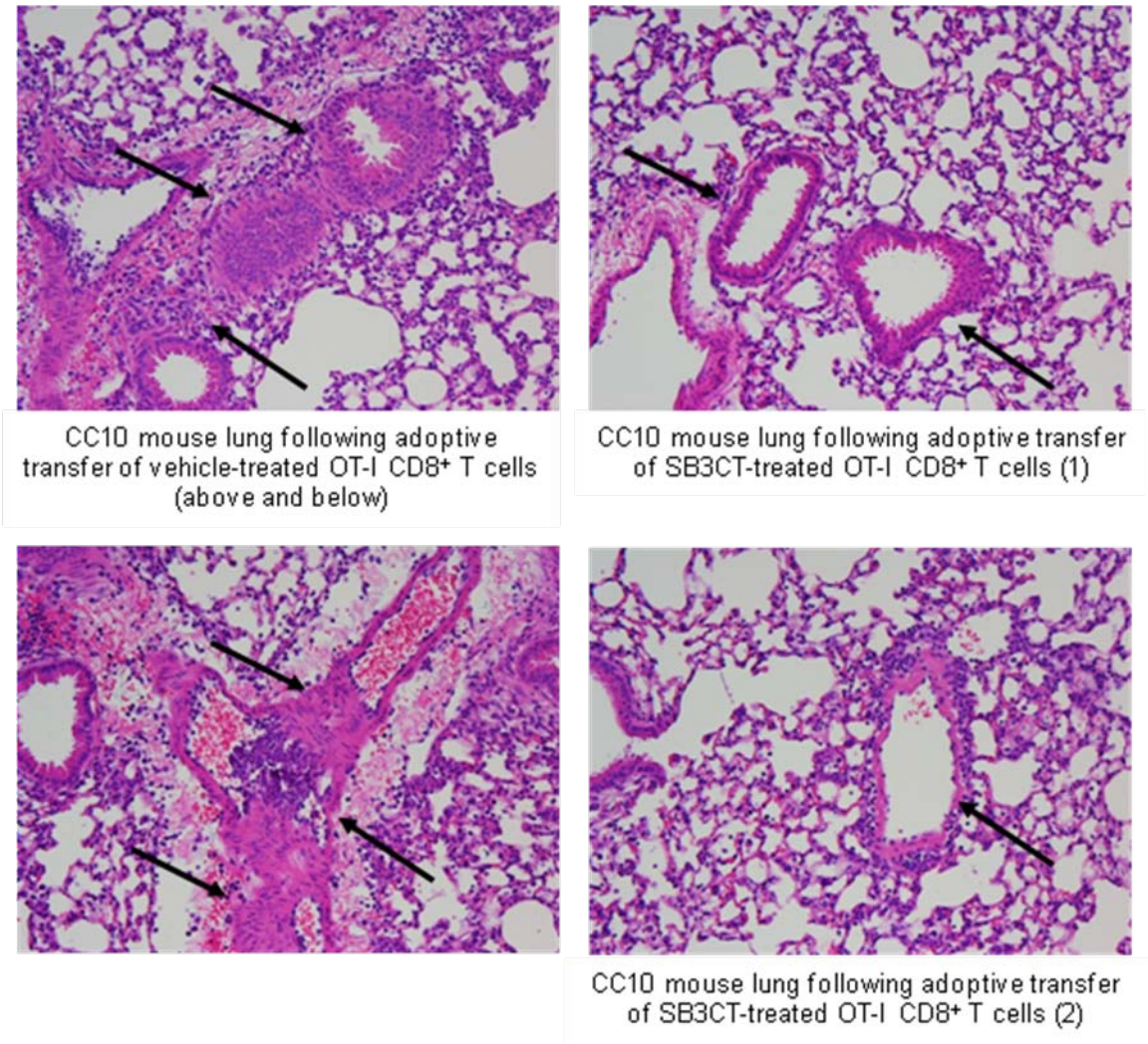

Figure 51. Murine model of antigen-specific $CD8^+$ effector T cell mediated lung injury

$CD8^+$ T cells were isolated from OT-1 transgenic mice and were treated with 10μM of SB3CT or the corresponding vehicle control for 6 hours. The cells were then washed and cultured in vitro for 5 days in the presence of IL-2, IL-12, anti-CD28, OVA peptide, and irradiated antigen presenting cells to generate effector $CD8^+$ lymphocytes. The cultured OT-1 $CD8^+$ T cells were then adoptively transferred in the CC10-OVA transgenic or non-transgenic wild-type C57BL/6 mice. Histology of the lung was evaluated by H&E staining 20X. In vehicle panels, arrows indicate areas of mononuclear cellular infiltrate, along with neutrophilic infiltration. In SB3CT panels, arrows indicate areas that are void of infiltration. n=8 per group

IV. DISCUSSION

A. Summary

Previous reports have demonstrated the importance of MMP in a variety of T cell mediated pulmonary diseases (44, 51). Although many studies have addressed functional aspects of MMPs, such as their involvement in the process of matrix remodeling, cell migration and the processing of other non-matrix substrates, the role of MMPs in regulating T cell activation has not been investigated and therefore remains unknown. The results presented herein demonstrate that MMPs, specifically MMP9 has a functional role in the regulation of T cell activation.

In chapter 1, the effects of MMP inhibition on T cells ($CD4^+$ and $CD8^+$) were examined from a functional standpoint. We first identified the presence of MMP9 within these cells and then assess their functional response to broad spectrum MMP inhibition by assessing their proliferative ability. We reported that broad spectrum MMP inhibition, by treatment with 1,10 phenanthroline and COL-3, abrogated alloantigen- and anti-CD3 Ab-induced T cell proliferative responses. We then continued our studies by assessing the effects of a specific MMP2/MMP9 inhibitor (SB3CT) and discovered that along with abrogating T cell proliferative responses, this pharmacological inhibitor down-regulated MMP9 expression at the level of transcription. Further assessment of SB3CT treated cells revealed that neither IL-2 nor anti-CD3/anti-CD28 Ab co-stimulation was able to fully rescue the proliferative responses. The functional proliferative studies with SB3CT were then confirmed using T cells ($CD4^+$ and $CD8^+$) from MMP2, MMP2/9 and MMP9 deficient mice. We reported that T cells from MMP9 deficient mice displayed the greatest

decrease in proliferation and chose to focus our studies on the effects of MMP9 in T cell activation.

In chapter 2, the effects of MMP inhibition on intracellular T cell signaling events were examined. Our observation began with the evaluation of calcium signaling, since it is an intracellular event proximal to the TCR. We reported that in response to MMP inhibition (SB3CT) or in the absence of MMP9 (MMP9 deficient mice), T cells ($CD4^+$ and $CD8^+$) displayed elevated levels of intracellular calcium release from the ER, as well as, influx of exogenous calcium from the media, following anti-CD3 Ab stimulation. After observing the effects of calcium signaling following specific TCR mediated T cell activation by anti-CD3 Ab, we next examined the effects of non-specific T cell activation on calcium signaling. We reported that following non-specific stimulation, with a phorbol ester (ionomycin), T cells ($CD4^+$ and $CD8^+$) displayed varying levels of intracellular calcium flux in response to MMP inhibition by (SB3CT) or MMP9 deficiency.

Upon further examination of intracellular signaling events, we reported that MEK1/2 total and phosphorylated protein expression were unaffected in response to MMP inhibition. Our investigation continued downstream, where we examined changes in the expression of genes involved in T cell activation. Following MMP inhibition or MMP9 deficiency, NFATc1 and CD25 gene expression were down-regulated. Additionally, we found that foxp3 gene expression and IL-10 protein expression levels were elevated, suggesting regulatory T cell function. However, upon further investigation through T cell suppressor assays, we reported that MMP inhibition did not induce regulatory T cell function. Moreover, analysis of IL-2, TNF-α and IFN-γ cytokine gene and protein expression revealed an overall trend of down-regulation in response to

MMP9 deficiency and MMP9 inhibition. Phenotypic analysis of T cells in response to MMP9 deficiency or MMP9 inhibition, revealed changes in cell surface activation marker expression when compared to T cells from wild-type mice.

In chapter 3, we examine the effects of MMP inhibition in vivo, in a model of antigen-specific T cell (OT-I) mediated lung injury. We first assess the functional response of antigen-specific T cells (OT-I and OT-II) by examining their proliferative ability in response to MMP inhibition (SB3CT). We reported that SB3CT abrogated the proliferative ability of antigen-specific OT-I ($CD8^+$) and OT-II ($CD4^+$) T cells to respond to their corresponding antigen-pulsed APCs. Following this observation, OT-I SB3CT treated T cells, were intratracheally transferred into the lungs of CC10-OVA mice, which express ovalbumin in their lungs. We reported that the number of total cells is the BAL was decreased, and that the percentage of $GR1^+$ cells (neutrophils) were significantly reduced. Additionally, in response to MMP9 inhibition, the percentage of $CD8^+$ $Thy1.1^+$ T cells in the lung of CC10-OVA mice was decreased. Further analysis of CD25 surface expression on $CD8^+$ $Thy1.1^+$ T cells in the lung revealed a dramatic decrease in CD25 surface expression. Histological analysis of lung sections collected from the lungs of CC10-OVA mice, provide further evidence that MMP9 inhibition decreased the degree of inflammation within the lung. These results supported the hypothesis that MMP inhibition significantly impaired the degree of neutrophilic alveolitis, thereby dampening T cell mediated lung injury. Collectively, these data clearly indicate a role for T cell derived MMP9 in the process of T cell activation and in mediating T cell induced lung injury. These findings will be discussed in more detail below.

B. MMP9 expression in T cells

There have been many reports showing the presence of T cell-derived MMP9 following treatment with various stimuli or in abnormal disease states. Human recombinant IL-2 has been shown to up-regulate MMP9 activity in human peripheral blood T cells (105, 129). Additionally, 12-O-tetradecanoylphorbol 13-acetate (TPA), has been shown to induce MMP9 activity in primary human T cells (130), as well as in a human T-lymphoma cell line (HSB) (131). T cell-derived MMP9 expression has also been shown to be up-regulated in a mammary tumor-bearing mouse model. In this model $CD4^+$ and $CD8^+$ T cells both in the periphery (in the spleen) and within the tumor microenvironment expressed high levels of MMP9 (132). Although, these and other studies have confirmed that T cells can express MMPs in humans and mice, the role of MMPs, specifically MMP9, in regulating T cell activation remains unknown.

In the current studies, we demonstrated that MMP9 is expressed in murine splenic $CD4^+$ and $CD8^+$ T cells by protein and mRNA transcript levels. Interestingly, following stimulation with anti-CD3 Ab, there seems to be a diverging effect in mRNA expression [figure 5]. In $CD4^+$ T cells, MMP9 expression is decreased following anti-CD3 Ab stimulation whereas in $CD8^+$ T cells, MMP9 expression levels are significantly elevated. This alteration in gene expression may be due to the different T cell subsets being analyzed. $CD4^+$ T cells are T helper cells, known to "help" in the immune system by activating and directing other immune cells. In contrast, $CD8^+$ T cells are cytotoxic T cells known to "kill" by exhibiting cytotoxic effects on other cells within the immune system. Since $CD8^+$ T cells have the ability to secrete perforin, a cytolytic protein and granzyme B, a serine protease, it is possible that these cells are predisposed to the

induction of MMP9 expression more readily, being that MMP9 itself is a protease. Although the changes in mRNA expression are drastically divergent, observation of protein levels reveal similar expression patterns between $CD4^+$ and $CD8^+$ T cells.

C. SB3CT regulates MMP9 expression at the transcriptional level

Many of the earlier reports studying the role of MMPs in various disease states have used broad-spectrum or global MMPIs, such as batimastat, doxycycline and chemically modified tetracyclines (COL-3), to name a few. These inhibitors function to non-selectively inhibit MMPs by binding to the active site zinc and secondarily to the inactive calcium ion site, causing conformational changes and loss of enzymatic activity. We reported that global MMPIs 1,10 phenanthroline and COL-3 both displayed significant reductions in T cell proliferation in response to alloantigen induced or anti-CD3 Ab-induced stimulation. Global MMPIs non-specifically inhibit MMP activity by functioning as metal chelators (divalent ions). The lack of specificity makes studying individual MMPs challenging. For example, Sandler et al. reported that COL-3 inhibits the activity of protein kinase C (PKC) in mast cells, suggesting that COL-3 functions as more than just an MMPI and can negatively affect cell growth and differentiation (107), thus making it difficult to elucidate the role of MMP9 specifically in T cell activation.

To circumvent these limitations we utilized MMP deficient mice and SB3CT. SB3CT is a mechanism based specific inhibitor that irreversibly inhibits MMP2 and MMP9 by permanently blocking the cysteine switch interaction. Many studies have demonstrated that SB3CT blocks MMP2 and MMP9 activity (133-135). Since SB3CT inhibits MMP2 and MMP9, many of the studies presented herein were paralleled by data

from MMP2, MMP/9 and MMP9 deficient mice to allow for comparison of the effects of MMP2 deficiency on some of the events involved in T cell activation, including the proliferative responses.

In our study of specific MMP inhibition, we examined MMP9 expression in T cells following SB3CT treatment. Unexpectedly, the results demonstrated that SB3CT significantly inhibited the mRNA transcript levels of MMP9. These results suggest that SB3CT functions not only in the catalytic site, but also functions to block MMP9 transcript levels, which in turn will block translation and protein activity. The ability of MMP inhibitors to inhibit mRNA transcript levels is supported by a report showing that COL-3 and doxycycline, two broad spectrum MMPIs, markedly decreased MMP2 mRNA levels in human skin keratinocytes as early as 6 hours which was further decreased 24 hours later (136). Similarly, this report concluded that doxycycline and the chemically modified tetracyclines, in addition to inhibiting MMP activity, also reduced the enzyme expression at the transcriptional level (136). In their studies, it is possible that binding of cations by those broad spectrum MMPIs may result in derangement of some transcriptional and posttranscriptional steps. For example, RNA polymerases require Mg^{2+} or Mn^{2+} for their activity. If the MMPIs chelate divalent ions necessary for polymerase activity, then this would inhibit transcription. In our case however, this is not a likely phenomenon because SB3CT does not function as a chelator, it is a mechanism-based inhibitor of MMP2 and MMP9 by binding to the catalytic site of the enzyme.

In our studies, it could be that translational inhibition of some factors necessary for MMP9 transcription may result in gene down-regulation. The MMP9 promoter contains binding sites for transcription factors AP-1, NF-κB, SP1, AP-2 and Ets (PEA3)

(137). AP-1 and NF- κB have been shown to play important regulatory roles in T cell proliferation (4). SB3CT may also be decreasing the levels of intracellular zinc, which can then lead to the down-regulation of AP-1 (c-fos/c-jun heterodimer) binding to the AP-1 binding site in the MMP9 promoter, causing the down-regulation of MMP9 gene expression. This is to say, MMP9 gene expression may be regulated by its direct cleavage of a nuclear target or indirect induction of a nuclear target. Further studies are needed to elucidate whether SB3CT is acting on the MMP9 promoter, thereby causing a decrease in transcriptional activation. Also, examination of other AP-1 or NFAT target genes in response to SB3CT treatment, would provide insight into the relationship of these genes and the MMP9 promoter.

D. T cell proliferation assays and T cell alloreactivity

In assessing the effects of MMP9 on T cells from a functional perspective, we found that anti-CD3 Ab-induced T cell proliferation was significantly decreased in $CD4^+$ and $CD8^+$ T cells in response to SB3CT treatment (figure 9). Additionally, this anti-proliferative response was not rescued by the addition of exogenous IL-2. This provided evidence that SB3CT treated T cells were not anergic. Moreover, the proliferative response was still abrogated in response to anti-CD3/anti-CD28 co-stimulation; further negating the idea of SB3CT treated T cells exhibiting anergy. Comparison of MMP deficient T cells demonstrated that MMP9 deficient T cells displayed the greatest reduction in proliferative capacity (figure 14) as compared to MMP2 and MMP2/9 deficient T cells (figure 13).

Interestingly, treatment of MMP9 deficient T cells with anti-CD3/anti-CD28 Ab co-stimulation fully rescued the proliferative response and even elevated it (figure 15A). These results suggested that although SB3CT treated cells were not anergic, MMP9 deficient T cells may exhibit cell anergy. This could be further confirmed by performing a T cell proliferation experiment with the addition of exogenous IL-2. If proliferation is rescued, then this would provide further confirmation that MMP9 deficient T cells exhibit T cell anergy.

Another potential explanation for the lack of proliferation seen in SB3CT treated T cells following anti-CD3/anti-CD28 Ab co-stimulation, is that SB3CT could be blocking the CD28 receptor, preventing proper stimulation. Since MMP9 deficient T cells exhibit normal CD28 receptor signaling, we can assess whether or not SB3CT blocks CD28 expression experimentally by utilizing these cells in T cell proliferation assays. If MMP9 deficient T cells are treated with SB3CT, co-stimulated with anti-CD3/anti-CD28 Ab and the proliferative response is not rescued, then this would confirm an additional role for SB3CT in regulating T cell activation.

Recently, reports have begun to show a functional role of MMPs in allograft rejection and their role in T cell alloreactivity. For example, Fernandez et al. reported in a tracheal allograft obstructive airway disease (OAD) model, that increased intragraft expression and activity of MMP2 and MMP9 correlated with OAD development, and host mice that lacked MMP-9 expression did not develop OAD when transplanted with wild-type tracheas, which correlated with significantly lower levels of $CD4^+$ and $CD8^+$ T cells (97). They also reported that alloreactivity was enhanced in MMP9 deficient bulk T cells stimulated with allogeneic BALB/c DCs.

In our studies however, we reported that MMP9 deficiency significantly abrogated T cell activation/ proliferation and that MMP2 deficiency only partially reduced T cell proliferative ability. One reason for these dissimilar results, may be due to the fact that in the study above, they used bulk T cells ($CD3^+$) in the presence of allogeneic DCs, thereby inducing non-specific ($CD4^+$ and $CD8^+$ T cell subsets) T cell activation. In contrast, our studies consisted of culturing MMP9 deficient $CD4^+$ and $CD8^+$ T cells separately in the presence of anti-CD3 Ab, allowing us to individually examine how these two cell populations function in the process of T cell activation. Our results indicated that T cell-derived MMP9 plays a more significant role in T cell activation than does MMP2. It has been reported that T cells and macrophages are important to the development of OAD (138, 139), as studies have shown that mice with a genetic T cell deficiency, such as severe combined immunodeficient (SCID) mice or recombinase activating gene 1-deficient (RAG-/-) do not develop OAD (140). These studies provide strong evidence that T cells are important in the development of OAD and suggest that T cell derived MMP9 may play an important role in this development.

In another study using a mouse model of cardiac allograft rejection to study the role of MMP2 and MMP9 in the pathogenesis of cardiac allograft rejection, Campbell et al. reported that rejection was inhibited in MMP2 deficient host mice, and exacerbated in MMP9 deficient host mice (95). They suggest that the protective effects seen in MMP2 deficient mice were due to an inhibition of mononuclear cellular infiltration into the allograft, resulting in lower levels of collagen deposition and tissue remodeling. Examination of T cell alloreactivity revealed that MMP2 deficient T cells displayed an innate defect in their alloresponsive capacity. These data demonstrate that the absence of

a T cell-derived MMP can alter T cell alloreactivity, which is in essence effecting T cell activation. Taken together, these two studies demonstrate that MMP2 and MMP9 play different roles in the process of activation and expansion of alloreactive T cells during the process of cardiac allograft rejection or OAD. These data highlight the complexity of MMPs in immune responses, and suggest that prevention of T cell derived MMPs can result in decreased T cell activation, which provides protective effects in response to a variety of pathogenic states.

E. Calcium signaling is up-regulated as a compensatory mechanism

It is well known that immediately following T cell receptor activation, there is an initiation of signaling pathways that leads to the up-regulation of a myriad of events including the induction of specific protein tyrosine kinases, activation of protein kinase C and an increase in calcium flux. This influx of intracellular calcium then allows for the activation of calcineurin, which in turn dephosphorylates NFAT, allowing for its nuclear translocation. With our finding that T cell activation was altered in response to MMP inhibition, we investigated events proximal to the TCR that may be altered in response to MMP inhibition. We reported that in response to MMP inhibition (SB3CT) or the absence of MMP (MMP9 deficient mice), $CD4^+$ and $CD8^+$ T cells displayed elevated levels of calcium release from the ER following anti-CD3 Ab stimulation. The experiments were performed in calcium-free, divalent ion reduced media, ensuring that any intracellular calcium flux seen was in fact due to release from the ER.

Since the calcium signaling pathway also involves an influx of exogenous calcium via calcium channels, we wanted to determine if MMP inhibition or MMP

deficiency would affect exogenous calcium influx. Since the patterns of calcium flux were similar between the $CD4^+$ and $CD8^+$ T cells, we chose to examine only $CD8^+$ T cells in this experiment. To ensure that we were able to measure the influx of exogenous calcium, these experiments were performed in calcium containing media (cRPMI). Interestingly, we reported that in response to MMP inhibition, CD8+ T cells displayed elevated levels of intracellular calcium, corresponding to release from the ER as well as an influx of exogenous calcium from calcium containing media following anti-CD3 Ab stimulation. Moreover, the arbitrary units used to measure calcium flux, were doubled in the experiments that contained calcium in the media as compared to the experiments that were only measuring calcium release from the ER. This is to be expected as exogenous influx of calcium would increase overall intracellular calcium influx. These findings suggested that in response to MMP9 inhibition or MMP9 deficiency the increase in calcium influx may be the T cell's way of trying to compensate for the lack of effective activation. MMP9 may function as a tonic down-regulator of calcium mediated events.

Although these results suggest that anti-CD3 Ab mediated stimulation of the TCR was able to induce proximal T cell activation in response to MMP9 inhibition or MMP9 deficiency, this may not be the case. There may be other altered signaling events occurring upstream of calcium that are involved. A report by Denny et al. examined the ability of Fyn (a members of the Src family of tyrosine kinases) to mediate TCR signal transduction in an Lck-deficient T-cell line (JCaM1). Interestingly, Fyn in the absence of Lck was able to induce tyrosine phosphorylation of the TCR and recruitment of the ZAP-70 kinase, but the activation of ZAP-70 was defective (141). The SLP-76 adapter protein was inducibly tyrosine phosphorylated, and both the Ras-mitogen-activated protein kinase

and the phosphatidylinositol 4,5-biphosphate signaling pathways were activated. TCR stimulation of JCaM1/Fyn cells also induced the expression of the CD69 activation marker and the influx of calcium, while displaying reduced proliferative ability, NFAT activation and IL-2 production. Additionally, they reported that the induction of AP-1 DNA binding activity in JCaM1/Fyn cells was defective (141). These results display some similarities with our studies (table 1) and suggest that alterations in signaling events upstream of calcium signaling may also account for changes seen downstream, such as proliferation and IL-2 production.

Wild-type	MMP9-/- or MMP inhibition
normal proliferation	defective proliferation
↑ in calcium release from the ER	↑↑ in calcium release from the ER
↑ in NFAT expression	↓in NFAT expression
↑ in CD25 expression	↓in CD25 expression
↑ in IL-2 expression	↓in IL-2 expression
↑in TNFα expression	↓in TNFα expression
↑in IFN-γ expression	↓in IFN-γ expression
↓in Foxp3 expression	↑in Foxp3 expression
↑in CD69 expression	↓in CD69 expression
↓in IL-10 expression	↑in IL-10 expression

Table 2. Comparison of data compilation from wild-type and MMP9 inhibition/deficiency

To further investigate MMP9's role in calcium flux, we examined the effects of ionomycin on calcium signaling in SB3CT treated or MMP9 deficient T cells. Ionomycin is a calcium ionophore responsible for shuttling calcium across the plasma membrane and the release of calcium from any other intracellular sources (such as the mitochondria). Following ionomycin stimulation, there was no change in calcium release from the ER as compared to wild-type cells in $CD4^+$ and $CD8^+$ MMP9 deficient T cells in calcium-free media. However, in the presence of calcium, as compared to wild-type T cells, $CD4^+$ and

$CD8^+$ MMP9 deficient T cells displayed significant decreases in calcium flux following ionomycin stimulation. In the presence of calcium, the influx typically corresponds to the release from the ER and the influx of exogenous calcium. Additionally, following treatment with SB3CT, intracellular calcium flux decreased in a dose-dependent manner in $CD4^+$ and $CD8^+$ T cells, corresponding to the flux of ER release and exogenous calcium influx. These data suggesting that MMP9 inhibition or its absence effects the ability of ionomycin to transverse the membrane, thereby decreasing calcium influx or that there is a defect in SOCE that cannot be stimulated by ionomycin treatment. Further studies are needed to elucidate the effects seen following ionomycin stimulation.

F. CD25 and NFAT expression and the AP-1 binding site

Following TCR ligation, there is an up-regulation of signaling events, leading to the nuclear translocation of NFAT. We reported that following SB3CT treatment, NFAT gene expression was abrogated, which is likely due to the defect in MMP9 gene transcription. Similar results were observed in MMP9 deficient T cells. Due to the importance of NFAT as a transcription factor involved in T cell activation, it is likely that alteration of NFAT expression alters the expression of other downstream genes that rely on NFAT translocation for their proper function. Of these genes, IL-2Rα (CD25) and L-2 are two pleiotropic genes dependent on NFAT expression for their function.

CD25 induction is controlled at the transcriptional level and its promoter activity is rapidly induced by TCR-mediated signals and many transcription factors, one of which is AP-1 (112). AP-1 has been shown to play a role in CD25 transcription, in addition to its formerly established role for the transactivation of the IL-2 gene. Leonard et al.

suggests that diminished levels of AP-1 correspond to diminished levels of CD25 expression which in turn decreases IL-2 responsiveness, thereby promoting T cell anergy (142, 143). In the current studies, we observed a decrease in CD25 mRNA (figure 29) and surface expression (figure 41 and 43) in MMP9 deficient and SB3CT treated $CD4^+$ or $CD8^+$ T cells. Moreover, when exogenous IL-2 was added to the cultures of SB3CT treated $CD4^+$ and $CD8^+$ T cells, T cell proliferation exhibited partial recovery (figure 11).

Taken together, these findings strongly suggest that MMP inhibition down-regulates NFAT activation, possibly by repressing NFAT transcription, which in turn decreases CD25 and IL-2 expression. The decrease in CD25 expression means that less CD25 will be present on the cell surface, which will limit the number of receptors available to bind IL-2 and induce proliferation, thereby abrogating T cell activation. This explains why the addition of exogenous IL-2 did not recover the proliferative response. An effort was made to examine NFATc1 protein expression and nuclear localization. We probed for nuclear and cytoplasmic NFAT with 3 different NFAT antibodies from three different companies. Our attempts were unsuccessful. Although we cannot rule out an extracellular mechanism responsible for these alterations in T cell activation, these data strongly suggest that MMPs are regulating T cell activation by an intracellular mechanism.

G. Regulatory T cell function, Foxp3 and IL-10 expression and regulation of IL-2 and IFN-γ

We reported that MMP inhibition by SB3CT did not induce regulatory T cell function. We did find however, that foxp3 expression was elevated in SB3CT treated and

MMP9 deficient T cells. Regulatory T cells are considered to be anergic in that they do not produce IL-2 or IFN-γ. In T cells that have adopted the Treg lineage, the inability to produce IL-2 and IFN-γ, seems to be a consequence of transcriptional repression by foxp3. Foxp3 binds to the regulatory regions of endogenous IL-2 and IFN-γ loci in Tregs and inhibits the activation induced IL-2 and IFN-γ production. Foxp3 is known to constitutively occupy the promoters of genes that are constitutively expressed in Tregs such as CTLA-4, CD25, and GITR. Following TCR ligation however, foxp3 can bind to the IL-2 promoter (144, 145). This can occur when NFAT cooperates with foxp3 for binding to composite NFAT-forkhead elements in the antigen receptor response element (ARRE)-2 region of the IL-2 promoter. Under traditional activation conditions, NFAT binds to the ARRE-2 site of the IL-2 promoter to a composite NFAT-AP-1 element. In Tregs, foxp3 inhibits AP-1 DNA binding and takes its place with NFAT at the ARRE-2 site (15, 146). In our studies, foxp3 may be actively repressing IL-2 and IFN-γ gene expression following TCR ligation in response to MMP inhibition, thereby causing a decrease in T cell activation. Since IL-10 is a characteristic immunosuppressive cytokine secreted by Tregs and Tr1 suppressive cells, we assessed IL-10 protein expression in MMP9 deficient T cells. We found that IL-10 was elevated in MMP9 deficient T cells following stimulation with anti-CD3 Ab. This may suggest that the absence of MMP2 or MMP9, leads to the development of a new IL-10 secreting T cell subset that exhibits regulatory T cell characteristics but not regulatory T cell function.

Although we have confirmed that MMP9 inhibition did not induce regulatory T cell function, we did report that Treg function was altered in response to MMP9 inhibition. These cells were still suppressive, but to a lesser extent, requiring more Tregs

to induce the same suppressive effects as in untreated Tregs. One possible explanation for this finding is that SB3CT inhibited MMP9 transcriptional expression. If this expression is a necessary function for normal T cell activation, then it is possible that in Tregs, this transcriptional inhibition led to a decrease in Treg suppressive function. Another possibility is that SB3CT may bind to another substrate present in the cell that is similar in structure to an MMP active site and required for Treg function, causing a decrease in the overall suppressive function. Overall, although the exact mechanism of how MMPs are regulating T cell activation and function is not well understood, these data still demonstrate that T cell derived MMPs play an important role in T cell activation and function. Future studies are necessary to more specifically elucidate the regulation of MMP9 in T cell activation in terms of identifying a potential new T cell subset.

H. Cytokine/Chemokine gene changes in response to MMP9 inhibition

Observation of cytokine/chemokine production in the cardiac allograft rejection model, as well as the OAD model both display abnormal cytokine/chemokine production in the MMP9 deficient recipients (95, 97). Our studies also displayed changes in cytokine production in MMP9 deficient T cells, specifically a reduction in IL-2 and IFN-γ and to a lesser extent, TNF-α at the mRNA and protein levels. With our previous discussion of NFAT and the changes that occur in response to MMP inhibition, it is likely that the decrease seen in IL-2, IFN-γ and TNF-α are due to the decrease in NFAT expression affecting the expression of other downstream genes.

In a heterotopic mouse airway model of OB, Neuringer et al. reported an up-regulation of IL-2, IFN-γ (Th1 cytokines) and IL-10 (Th2 cytokine) and $CD8^+$ cytotoxic

T cell granzyme B gene expression during the early (cellular) phase of allograft rejection (weeks 2-4), in addition to significant T cell infiltration into the allografts (140). These results demonstrated a strong up-regulation of Th1 cytokines, which has also been shown in orthotopic and heterotopic rodent lung transplant models. In orthotopic rat lung models, which develop features of acute rejection, IL-2 and IFN-γ gene expression are elevated in allografts compared with isografts (147). Similar to mouse models, heterotopic rat trachea models mimic OB, and exhibit increased CD25, IL-2, and IFN-γ gene expression in allografts (148). Taken together, these reports demonstrate that Th1 cytokine gene is strongly associated with rejection in many rodent lung allografts. Therefore, our data demonstrating that T cell-derived MMP9 inhibition or deficiency abrogates Th1 cytokine gene expression, support the idea that inhibition of Th1 cytokine expression may protect against T cell mediated injury, including the infiltration seen in early rejection.

I. MMP9 preferentially expressed by TH1 versus TH2 cells

Th1 and Th2 subsets are distinguished by their characteristic production of divergent cytokine profiles. Th1 cells secrete IFN-γ, IL-2 and TNF-α. While Th2 cells secrete IL-4, IL-5, IL-10 and IL-13. The data presented herein showed that IL-2, TNF-α and IFN-γ production were all down-regulated in MMP9 deficient $CD4^+$ T cells following anti-CD3 Ab stimulation. Additionally, in figure 30B, IL-10 protein expression was significantly elevated in MMP9 deficient T cells following anti-CD3 Ab stimulation. It is still not clear why IL-10 levels were elevated, although we can speculate that it is in an effort to exert a suppressive effect. These results show that the absence of MMP9

abrogates the production of Th1 producing cytokines and suggests that MMP9 may play an important role in Th1 cell skewing and possibly in preventing Th2 cell skewing. In support of this idea, Abraham et al. reported that Th1 in comparison to Th2 cells, from both human (healthy subjects and multiple sclerosis (MS) patients) as well as from murine origin, secrete higher levels of MMP-9 following anti-CD3/anti-CD28 Ab co-stimulation (149). Taken together, these results suggest a link between MMP9 and Th1 cell skewing and imply that inhibition of Th1 cell derived MMP9 may regulate Th1 mediated diseases.

Further investigation suggests that STAT proteins may play a role in this Th1 cell skewing process. STATs are a family of transcription factors that regulate a broad range of cellular processes, such as T cell differentiation and proliferation. Of the STAT proteins, STAT4 has been implicated in the induction of $CD4^+$ Th1 T cells. It has been reported that STAT4 deficient mice display impairment in the production of IFN-γ, cellular proliferation and Th1 cell differentiation (150). In MMP9 deficient $CD4^+$ T cells we reported that IFN-γ mRNA and protein production were reduced, which is similar to that seen in STAT4 deficient mice. Taken together, these results suggest a potential link between MMPs and STAT4 induction.

In $CD4^+$ T cells, T-bet is rapidly and specifically induced in developing Th1 but not Th2 cells. T-bet functions as a master regulator of Th1 cell differentiation (151). Some studies have suggested that a regulatory circuit involving IFNγR signaling via STAT1 maintains high-level T-bet expression in developing Th1 cells (152, 153). However, the main role of T-bet regulation is known to be STAT4 dependent. In MMP9 deficient mice, we reported that T-bet expression is elevated, while IFN-γ mRNA and

protein expression is abrogated. Conversely, it has been reported that $CD4^+$ T cells isolated from T-bet-deficient mice failed to produce IFNγ in response to either anti-CD3/anti-CD28 Ab or PMA/ionomycin stimulation. One potential hypothesis for these disparaging results is that in response to MMP9 deficiency, the T cells are desperately trying to overcome the lack of proper activation and as such, are inducing expression of STAT4, which is up-regulating the expression of T-bet. MMP9 may also function at the junction between T-bet signal and IFN-γ production. Another hypothesis may be that STAT4 is not essential in T-bet induction. This idea has been reported in a study demonstrating that STAT4 was not required for T-bet induction and that it was not required to aid T-bet in inducing Th1 identity (154), suggesting that T-bet is upstream of the STAT4 pathway. Further studies are needed to clearly define a role for MMP9 in T-bet signaling.

J. Murine model of antigen-specific T cell mediated lung injury

To investigate the role of MMP inhibition in vivo, we utilized a CC10-OVA model of airway hyperresponsiveness. Our reasoning behind choosing this model was due to the fact that our data demonstrated that MMP9 gene expression was significantly elevated in activated $CD8^+$ T cells. Additionally, because anti-CD3 Ab is not a physiological T cell stimulus, we wanted to study MMP regulation of T cell activation under physiological conditions. This directed our focus to study a $CD8^+$ T cell dependent disease. We first assessed the functional response of antigen-specific T cells (OT-I and OT-II) by examining their proliferative ability in response to MMP inhibition (SB3CT). The findings that SB3CT abrogated the proliferative ability of antigen-specific OT-I and

OT-II T cells, provided proof that SB3CT could reduce antigen specific proliferation and allowed us to move forward in our model. Following adoptive transfer of OT-I MMP inhibitor treated T cells, we reported that the number of total cells in the BAL was decreased, and that the percentage of $GR1^+$ cells (neutrophils) were significantly reduced. These results were exactly what we expected, which demonstrate that MMP inhibition decreases cellular infiltration.

Since the animal model was set up to allow us to discriminate between the OT-1 adoptively transferred cells (Thy1.1) and host CC10 cells (Thy1.2), we were able to track the OT-1 transferred cells and determine their localization. In response to MMP9 inhibition, there was a significant decrease in the percentage of $CD8^+$ $Thy1.1^+$ T cells in the lung of CC10-OVA mice, suggesting that MMP inhibition effects T cell migration, likely by decreasing their activation. Further analysis of CD25 surface expression on $CD8^+$ $Thy1.1^+$ T cells in the lung revealed a dramatic decrease in CD25 surface expression. These results are similar to our previous data demonstrating a significant decrease in CD25 mRNA and cell surface expression in response to MMP inhibition. This may also provide more of an explanation of the lack of neutrophilic infiltration into the BAL and lung. If T cells are non-reactive to the OVA present in the lung as a result of MMP inhibition, then there is no major increase in inflammation, which negates the need for neutrophilic infiltration. This suggests that T cells are mediating this inflammation and that MMPs are regulating the T cells' reactivity.

Additionally, we hypothesized that the decrease in neutrophilic migration was in part due to the decrease in the neutrophil chemotactic property of IL-8. MMP9 can cleave IL-8 at its N-terminus, causing an increase in its chemotactic activity for neutrophils.

Therefore, if MMP9 is inhibited by SB3CT, then this should prevent the cleavage of IL-8, thereby decreasing IL-8 chemotactic activity for neutrophils, preventing neutrophil infiltration. Unfortunately, this hypothesis was disproven with results demonstrating no significant changes in IL-8 expression in the BAL of OVA-CC10 mice adoptively transferred with vehicle treated or SB3CT treated OT-I T cells.

Histological analysis of lung sections collected from the lungs of CC10-OVA mice demonstrated varying degrees of perivascular and perinuclear infiltrates. Following the transfer of vehicle-treated OT-1 cells, mononuclear cellular infiltrate was significantly increased, demonstrating the induction of T cell mediated lung injury. This infiltrate lead to severe occlusion of airway vessels. Following the adoptive transfer of SB3CT treated OT-1 cells, the mononuclear cellular infiltration was minimal, suggesting that MMP9 inhibition dampened the degree of inflammation within the lung, thus significantly impairing the degree of T cell mediated lung injury. These results suggest that it would be beneficial to examine the expression of chemokines being that they are important in cell infiltration and trafficking in tissues. We found in our preliminary data that MCP-1 expression was elevated in MMP9 deficient $CD4^+$ T cells following stimulation with anti-CD3 Ab [figure 51]. Other chemokines such as RANTES would also be of interest. It would also be useful to perform lung function studies, thus allowing us to obtain more physiological evidence of the beneficial effect of SB3CT treatment in abrogating T cell mediated lung injury.

K. Potential intracellular role for MMP9

Although we cannot say with absolute certainty that MMP9 intracellularly regulates T cell activation, our results strongly indicate that MMP9 plays a definite role in T cell activation and are suggestive that this role is intracellular by regulation /modulation of mRNA and protein expression under normal homeostatic conditions. In this regard, Kwan et al., reported the presence of an active form of MMP2 within the nucleus of cardiac myocytes, suggesting a possible biological role for MMPs in the nucleus (99). Si-Tayeb et al. reported the presence of an active form of MMP3 in the nucleus of a human hepatocellular carcinoma cell line (HepG2) and hepatocellular carcinoma patient samples, and identified a nuclear localization signal (100). These studies clearly demonstrate an intracellular role for MMPs.

Proteolytic processing of inflammatory mediators in vitro has provided important functional information about the possible biochemical behavior of molecules as sites of inflammation, however little is known about the relevant in vivo substrates of MMPs, particularly MMP2 and MMP9. As mentioned earlier, new proteomic studies are beginning to elucidate potential intracellular substrates for MMP2 and MMP9 (36). Further studies aimed to better define the intracellular signaling mechanisms responsible for the regulation of MMP9 in T cell activation under homeostatic conditions may provide useful for understanding how these cells function normally and how regulation of T cells early in the process of lung disease may provide a novel therapeutic to arbitrate T cell mediated lung disease.

Towards this, VDIPEN, a peptide fragment of aggrecan (the interglobular domain) has been identified that is specific for MMP9 cleavage, along with 5 other

MMPs (MMP-1, -2, -3, -7 and -8) (155). An antibody has been designed that specifically recognizes this cleavage site. This antibody has been identified for its uses in studying MMP destruction of articular cartilage in immune inflammatory arthritic disease (155).We were interested in using this antibody in hopes of identifying potential intracellular MMP cleavage sites that may provide information to potential intracellular MMP2 and MMP9 substrates. This would provide valuable information as to identifying a new functional intracellular role for MMPs in T cell activation.

V. CONCLUSIONS

In normal T cell activation, ligation of the TCR by anti-CD3 Ab stimulates a myriad of signaling events leading to the production of inositol 1, 4, 5-triphosphate (IP_3). IP_3 is then able to bind to its receptor, stimulating the release of intracellular calcium from the endoplasmic reticulum (ER). This leads to store operated calcium entry (SOCE) as a result of calcium channels opening, thereby allowing an influx of exogenous calcium into the cell. This increase in calcium influx allows for activation of the serine/threonine phosphatase, calcineurin. Activated calcineurin dephosphorylates NFAT allowing for its nuclear translocation. NFAT expression in turn activates the expression of other pleiotropic genes such as CD25 and IL-2. CD25 is then expressed on the surface of the T cell, which in turn, can bind IL-2. This interaction of CD25 and IL-2 leads proper T cell activation and proliferation.

In our study of T cell activation, we discovered that MMP9 inhibition by SB3CT or absence by MMP9 deficiency altered proper T cell activation. We found that upon ligation of the TCR with anti-CD3 Ab, there was an increase in intracellular calcium released from the ER. Moreover, SOCE was increased as demonstrated by the influx of exogenous calcium. In contrast, NFAT expression was down-regulated, which also corresponded with the down regulation of CD25 and IL-2 expression. Cell surface CD25 expression was also down-regulated. Additionally, Foxp3 and IL-10 expression levels were increased, which is characteristic of regulatory T cell and suppressor T cell function. However, functional T cell suppressor studies ruled out the induction of a

regulatory T cell. These results support the hypothesis that MMP9 regulates T cell activation.

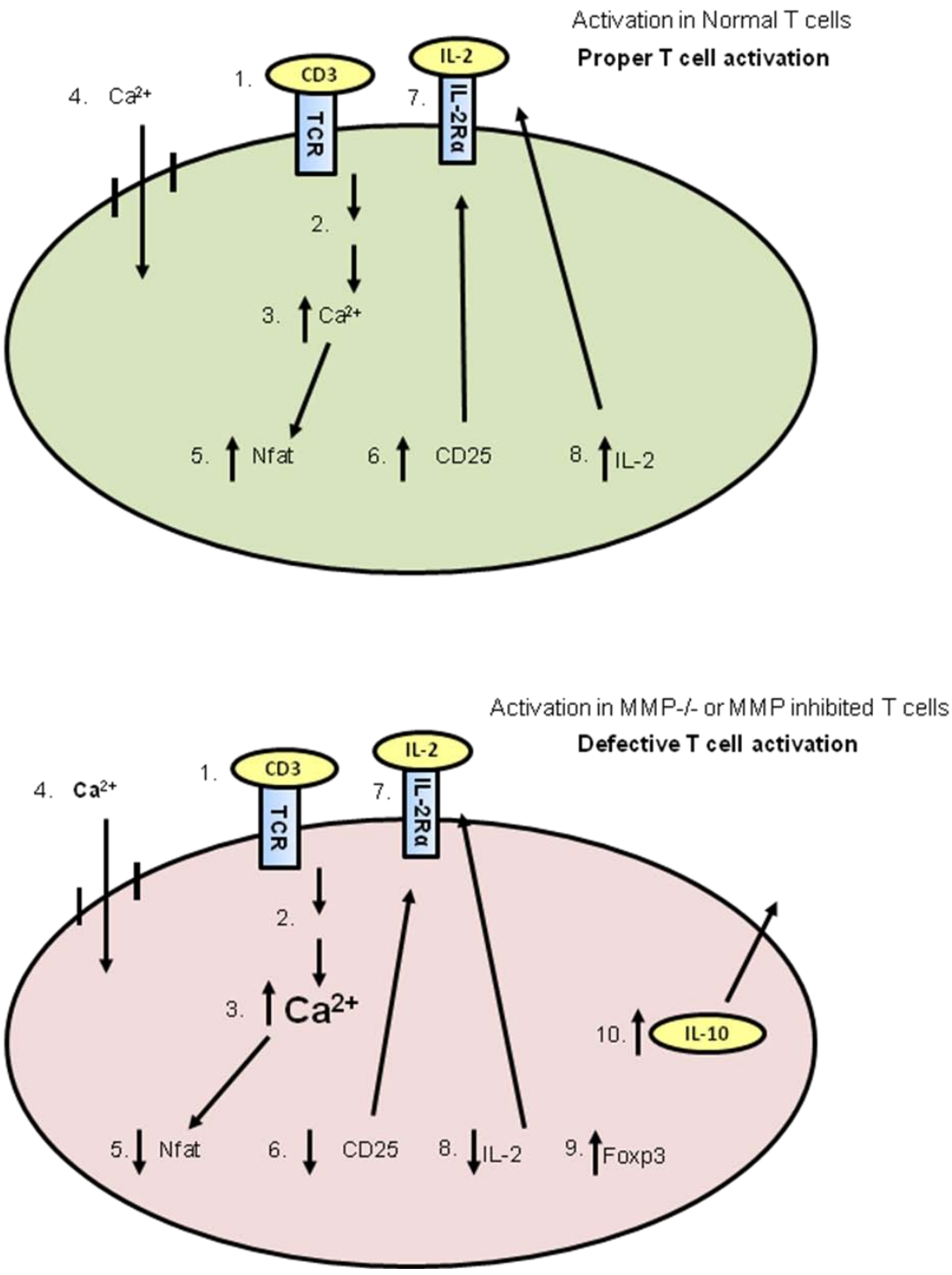

Figure 52. Schematic diagram of differences in T cell activation in response to MMP inhibition (SB3CT) or absence (MMP9 deficiency)

VI. FUTURE STUDIES

The discovery that matrix metalloproteinases, particularly MMP9, regulates T cell activation and that the potential regulatory targets may be intracellular are novel findings. There are however, a number of future studies that are needed to further elucidate the exact mechanism of action by which this regulation is occurring. One of the studies that would provide further evidence of MMPs regulatory role in vivo, would be to revisit the CC10-OVA airway-hyperresponsiveness model. To confirm our report that MMP inhibition by SB3CT dampened the T cell mediated lung injury, it would be interesting to adoptively transfer MMP9 deficient T cells into the airway of CC10-OVA mice, to determine if MMP9 deficiency further dampens airway hyperresponsiveness. One caveat to this approach is that in order to adoptively transfer antigen-specific MMP9 deficient T cells, OT-1 transgenic mice would need to be crossed with MMP9 deficient mice to provide a mouse that is OT-1 specific and MMP9 deficient. If these mice are created, then they will also provide another platform in which to study antigen-specific, MMP deficient T cell mediated events. These studies would shed light on T cell mediated disease under physiological conditions and allow for the study of a specific set of T cells that only respond to a particular antigen. This model could be used to study T cell mediated disease in any organ system.

In trying to identify intracellular MMP2 and MMP9 targets, it would be interesting to generate a mouse model of asthma, which is a T cell mediated lung disease and determine if any of the newly identified in vivo substrates (Ym1, S100A8 and S100A9) are expressed in T cells under inflammatory conditions. Additionally, VDIPEN could also be used to identify any MMP cleavage sites. If any of these proteins or cleavage sites are found to be present, then this would provide evidence of MMP2 and/or MMP9 activity in a T cell and support our hypothesis of T cell derived MMPs working inside the cell to regulate cellular signals, which can result in alterations in activation patterns. These substrates can be identified by performing quantitative RT-PCR to identify gene expression, or western blotting to identify protein expression.

Another aspect of this project that requires further investigation is the calcium signaling cascade in response to MMP inhibition. Identification of intracellular potential targets responsible for the increase in intracellular calcium signaling and consistent decrease in T cell activation would help us understand where MMPs could be acting inside the cell to regulate this pathway. Further experiments are also needed to elucidate the mechanism or mechanisms responsible for the differences in calcium flux between TCR mediated activation and non-specific, ionomycin-induced T cell activation. During our calcium assays, it was discovered that the assay buffer we were using contained traces of divalent ions, such as Mg^{2+} and Cu^{2+}. These divalent ions prevented us from demonstrating the traditional calcium curve that is seen due to the fact that the divalent ions present in the media are quenched by the dye and therefore display some fluorescence. It would also be useful to repeat some of the calcium studies using an assay buffer that contains no divalent ions that interact with fluor-4 dye, which is used to

measure calcium flux. Collectively, the most important next step in this project would be to identify an intracellular MMP2 and MMP9 substrate in T cells responsible for T cell activation, thus proving the hypothesis that MMPs regulate T cell activation by an intracellular mechanism.

VII. REFERENCES

1. Jenkins MK, Khoruts A, Ingulli E, Mueller DL, McSorley SJ, Reinhardt RL, et al. In vivo activation of antigen-specific CD4 T cells. Annual Review of Immunology. 2001;19:23-45.

2. Steinman L. A brief history of TH17, the first major revision in the TH1/TH2 hypothesis of T cell-mediated tissue damage. Nat Med. 2007;13(2):139-45.

3. Cantrell D. T cell antigen receptor signal transduction pathways. Annual Review of Immunology. 1996;14(1):259-74.

4. Qian D, Weiss A. T cell antigen receptor signal transduction. Current Opinion in Cell Biology. 1997;9(2):205-12.

5. Chan AC, Iwashima M, Turck CW, Weiss A. ZAP-70: A 70 kd protein-tyrosine kinase that associates with the TCR [zeta] chain. Cell. 1992;71(4):649-62.

6. Rapecki S, Allen R. Inhibition of Human T Cell Activation by Novel Src Kinase Inhibitors Is Dependent upon the Complexity of the Signal Delivered to the Cell. J Pharmacol Exp Ther. 2002;303(3):1325-33.

7. Koretzky GA, Abtahian F, Silverman MA. SLP76 and SLP65: complex regulation of signalling in lymphocytes and beyond. Nat Rev Immunol. 2006;6(1):67-78.

8. Zhang W, Sloan-Lancaster J, Kitchen J, Trible RP, Samelson LE. LAT: The ZAP-70 Tyrosine Kinase Substrate that Links T Cell Receptor to Cellular Activation. Cell. 1998;92(1):83-92.

9. Connie L. Sommers, Lawrence E. Samelson, Paul E. Love. LAT: a T lymphocyte adapter protein that couples the antigen receptor to downstream signaling pathways. BioEssays. 2004;26(1):61-7.

10. Zhang W, Sommers CL, Burshtyn DN, Stebbins CC, DeJarnette JB, Trible RP, et al. Essential Role of LAT in T Cell Development. Immunity. 1999;10(3):323-32.

11. Liu SK, Fang N, Koretzky GA, Jane McGlade C. The hematopoietic-specific adaptor protein Gads functions in T-cell signaling via interactions with the SLP-76 and LAT adaptors. Current Biology. 1999;9(2):67-75.

12. Genot E, Cantrell DA. Ras regulation and function in lymphocytes. Current Opinion in Immunology. 2000;12(3):289-94.

13. Savignac M, Mellström B, Naranjo J. Calcium-dependent transcription of cytokine genes in T lymphocytes. Pflügers Archiv European Journal of Physiology. 2007;454(4):523-33.

14. Macián F, GarcIa-Cózar F, Im S-H, Horton HF, Byrne MC, Rao A. Transcriptional Mechanisms Underlying Lymphocyte Tolerance. Cell. 2002;109(6):719-31.

15. Wu Y, Borde M, Heissmeyer V, Feuerer M, Lapan AD, Stroud JC, et al. FOXP3 Controls Regulatory T Cell Function through Cooperation with NFAT. Cell. 2006;126(2):375-87.

16. Qin H, Wang L, Elson CO, Niyongere SA, Lee SJ, Benveniste EN, et al. 119 TGF-[beta] promotes Th17 cell development through inhibition of SOCS-3. Cytokine. 2008;43(3):264.

17. O'Shea JJ, Steward-Tharp SM, Laurence A, Watford WT, Wei L, Adamson AS, et al. Signal transduction and Th17 cell differentiation. Microbes and Infection. 2009;11(5):599-611.

18. Creemers EEJM, Cleutjens JPM, Smits JFM, Daemen MJAP. Matrix Metalloproteinase Inhibition After Myocardial Infarction: A New Approach to Prevent Heart Failure? Circ Res. 2001;89(3):201-10.

19. Nagase H, Woessner JFJ. Matrix Metalloproteinases. J Biol Chem. 1999;274(31):21491-4.

20. Egeblad M, Werb Z. New functions for the matrix metalloproteinases in cancer progression. Nat Rev Cancer. 2002;2(3):161-74.

21. Cataldo D, Munaut C, Noël A, Frankenne F, Bartsch P, Foidart J, et al. MMP-2- and MMP-9-Linked Gelatinolytic Activity in the Sputum from Patients with Asthma and Chronic Obstructive Pulmonary Disease Int Arch Allergy Immunol 2000;123:*259-67*.

22. Inaki NT, Yoshio; Kawakami, Kazuyuki; Sato, Hiroshi; Takino, Takahisa; Oda, Makoto; Watanabe, Go. Increased matrix metalloproteinase-2 and membrane type 1 matrix metalloproteinase activity and expression in heterotopically transplanted murine tracheas. Journal of Heart & Lung Transplantation. 2004 Feb;23(2):218-27.

23. Cuzner M, Opdenakker G. Plasminogen activators and matrix metalloproteases, mediators of extracellular proteolysis in inflammatory demyelination of the central nervous system. J Neuroimmunol. 1999;94:1-14.

24. Opdenakker G, Van den Steen PE, Dubois B, Nelissen I, Van Coillie E, Masure S, et al. Gelatinase B functions as regulator and effector in leukocyte biology. J Leukoc Biol. 2001;69(6):851-9.

25. Opdenakker G, Van-den-Steen P, Van-Damme J. Gelatinase B: a tuner and amplifier of immune functions. Trends in Immunology 2001; 22(10):571-9.

26. Van den Steen PE, Opdenakker G, Wormald MR, Dwek RA, Rudd PM. Matrix remodelling enzymes, the protease cascade and glycosylation. Biochimica et Biophysica Acta (BBA) - General Subjects. 2001;1528(2-3):61-73.

27. Allan JA, Docherty AJ, Barker PJ, Huskisson NS, Reynolds JJ, Murphy G. Binding of gelatinases A and B to type-I collagen and other matrix components. Biochem J. 1995 309(Pt 1):299-306.

28. Steffensen B, Bigg HF, Overall CM. The Involvement of the Fibronectin Type II-like Modules of Human Gelatinase A in Cell Surface Localization and Activation. The Journal of Biological Chemistry. 1998 273:20622-8.

29. Murphy G, Docherty A. The matrix metalloproteinases and their inhibitors. American journal of respiratory cell and molecular biology. 1992;7(2):120-5.

30. Yu Q, Stamenkovic I. Cell surface-localized matrix metalloproteinase-9 proteolytically activates TGF-β and promotes tumor invasion and angiogenesis. Genes Dev 2000 14(2):163-76.

31. Van den Steen PE, Proost P, Wuyts A, Van Damme J, Opdenakker G. Neutrophil gelatinase B potentiates interleukin-8 tenfold by aminoterminal processing, whereas it degrades CTAP-III, PF-4, and GRO-alpha and leaves RANTES and MCP-2 intact. Blood. 2000;96(8):2673-81.

32. Liu Z, Zhou X, Shapiro SD, Shipley JM, Twining SS, Diaz LA, et al. The Serpin [alpha]1-Proteinase Inhibitor Is a Critical Substrate for Gelatinase B/MMP-9 In Vivo. Cell. 2000;102(5):647-55.

33. Engsig MT, Chen Q-J, Vu TH, Pedersen A-C, Therkidsen B, Lund LR, et al. Matrix Metalloproteinase 9 and Vascular Endothelial Growth Factor Are Essential for Osteoclast Recruitment into Developing Long Bones. J Cell Biol. 2000;151(4):879-90.

34. Kheradmand F, Werner E, Tremble P, Symons M, Werb Z. Role of Rac1 and Oxygen Radicals in Collagenase-1 Expression Induced by Cell Shape Change. Science. 1998;280(5365):898-902.

35. McQuibban GA, Gong J-H, Wong JP, Wallace JL, Clark-Lewis I, Overall CM. Matrix metalloproteinase processing of monocyte chemoattractant proteins generates CC chemokine receptor antagonists with anti-inflammatory properties in vivo. Blood. 2002;100(4):1160-7.

36. Greenlee KJ, Corry DB, Engler DA, Matsunami RK, Tessier P, Cook RG, et al. Proteomic Identification of In Vivo Substrates for Matrix Metalloproteinases 2 and 9 Reveals a Mechanism for Resolution of Inflammation. J Immunol. 2006;177(10):7312-21.

37. Liu Q, Cheng LI, Yi L, Zhu N, Wood A, Changpriroa CM, et al. p47phox Deficiency Induces Macrophage Dysfunction Resulting in Progressive Crystalline Macrophage Pneumonia. Am J Pathol. 2009;174(1):153-63.

38. Ryckman C, Vandal K, Rouleau P, Talbot M, Tessier PA. Proinflammatory Activities of S100: Proteins S100A8, S100A9, and S100A8/A9 Induce Neutrophil Chemotaxis and Adhesion. J Immunol. 2003;170(6):3233-42.

39. Nacken W, Roth J, Sorg C, Kerkhoff C. S100A9/S100A8: Myeloid representatives of the S100 protein family as prominent players in innate immunity. Microscopy Research and Technique. 2003;60(6):569-80.

40. Takahashi K, Akagi T, Ohtsuki Y, Sonobe H, Yamaguchi H. An immunohistochemical study on the distribution of histiocytes containing S-100 protein-like antigen in cutaneous T-cell lymphoma/leukemia; a preliminary report. Cellular and Molecular Life Sciences. 1982;38(11):1349-51.

41. Bannikov GA, Karelina TV, Collier IE, Marmer BL, Goldberg GI. Substrate binding of gelatinase B induces its enzymatic activity in the presence of intact propeptide. J Biol Chem 2002;277(18):16022-7.

42. Van Wart HE, Birkedal-Hansen H. The cysteine switch: a principle of regulation of metalloproteinase activity with potential applicability to the entire matrix metalloproteinase gene family. Proceedings of the National Academy of Sciences of the United States of America. 1990;87(14):5578-82.

43. Taghavi S, Krenn K, Jaksch P, Klepetko W, Aharinejad S. Broncho-alveolar Lavage Matrix Metalloproteases as a Sensitive Measure of Bronchiolitis Obliterans. American Journal of Transplantation. 2005;5(6):1548-52.

44. Hubner RH, Meffert S, Mundt U, Bottcher H, Freitag S, El Mokhtari NE, et al. Matrix metalloproteinase-9 in bronchiolitis obliterans syndrome after lung transplantation. European Respiratory Journal. 2005 25(3):494-501.

45. Amoscato A, Alexander J, Babcock G. Surface aminopeptidase activity of human lymphocytes. I. Biochemical and biologic properties of intact cells. J Immunol. 1989;142(4):1245-52.

46. Moon S-K, Cha B-Y, Kim C-H. ERK1/2 mediates TNF-alpha-induced matrix metalloproteinase-9 expression in human vascular smooth muscle cells via the regulation of NF-kappaB and AP-1: Involvement of the ras dependent pathway. Journal of Cellular Physiology. 2004;198(3):417-27.

47. Tao P, Fisher JF, Mobashery S, Schlegel HB. DFT Studies of the Ring-Opening Mechanism of SB-3CT, a Potent Inhibitor of Matrix Metalloproteinase 2. Organic Letters. 2009;11(12):2559-62.

48. Brown S, Bernardo MM, Li Z-H, Kotra LP, Tanaka Y, Fridman R, et al. Potent and Selective Mechanism-Based Inhibition of Gelatinases. Journal of the American Chemical Society. 2000;122(28):6799-800.

49. Atkinson J, Senior R. Matrix metalloproteinase-9 in lung remodeling. Am J Respir Cell Mol Biol. 2003;28:12 - 24.

50. Legrand C, Gilles C, Zahm J-M, Polette M, Buisson A-C, Kaplan H, et al. Airway Epithelial Cell Migration Dynamics: MMP-9 Role in Cell–Extracellular Matrix Remodeling. J Cell Biol. 1999;146(2):517-29.

51. Vermaelen KY, Cataldo D, Tournoy K, Maes T, Dhulst A, Louis R, et al. Matrix Metalloproteinase-9-Mediated Dendritic Cell Recruitment into the Airways Is a Critical Step in a Mouse Model of Asthma. J Immunol. 2003;171(2):1016-22.

52. Deryugina E, Quigley J. Matrix metalloproteinases and tumor metastasis. Cancer and Metastasis Reviews. 2006;25(1):9-34.

53. Nakajima M, Welch DR, Wynn DM, Tsuruo T, Nicolson GL. Serum and Plasma Mr 92,000 Progelatinase Levels Correlate with Spontaneous Metastasis of Rat 13762NF Mammary Adenocarcinoma. Cancer Res. 1993;53(23):5802-7.

54. Fridman R, Toth M, Pena D, Mobashery S. Activation of Progelatinase B (MMP-9) by Gelatinase A (MMP-2). Cancer Res. 1995;55(12):2548-55.

55. Hrabec E, Strek M, Nowak D, Greger J, Suwalski M, Hrabec Z. Activity of type IV collagenases (MMP-2 and MMP-9) in primary pulmonary carcinomas: a quantitative analysis. Journal of Cancer Research and Clinical Oncology. 2002;128(4):197-204.

56. Warner RL, Beltran L, Younkin EM, Lewis CS, Weiss SJ, Varani J, et al. Role of Stromelysin 1 and Gelatinase B in Experimental Acute Lung Injury. Am J Respir Cell Mol Biol. 2001;24(5):537-44.

57. Knight DA, Holgate ST. The airway epithelium: Structural and functional properties in health and disease. Respirology. 2003;8(4):432-46.

58. Cohn L, Elias JA, Chupp GL. Asthma: Mechanisms of Disease Persistence and Progression. Annual Review of Immunology. 2004;22(1):789-815.

59. Corry DB, Kiss A, Song L-Z, Song L, Xu J, Lee S-H, et al. Overlapping and independent contributions of MMP2 and MMP9 to lung allergic inflammatory cell egression through decreased CC chemokines. FASEB J. 2004:03-1412fje.

60. McMillan SJ, Kearley J, Campbell JD, Zhu X-W, Larbi KY, Shipley JM, et al. Matrix Metalloproteinase-9 Deficiency Results in Enhanced Allergen-Induced Airway Inflammation. J Immunol. 2004;172(4):2586-94.

61. Belleguic C, Corbel M, Germain N, Léna H, Boichot E, Delaval P, et al. Increased release of matrix metalloproteinase 2 and 9 in the plasma of acute severe asthmatic patients. Clinical & Experimental Allergy. 2002;32(2):217-23.

62. Cataldo DD, Tournoy KG, Vermaelen K, Munaut C, Foidart J-M, Louis R, et al. Matrix Metalloproteinase-9 Deficiency Impairs Cellular Infiltration and Bronchial Hyperresponsiveness during Allergen-Induced Airway Inflammation. Am J Pathol. 2002;161(2):491-8.

63. Corry DB, Rishi K, Kanellis J, Kiss A, Song L-z, Xu J, et al. Decreased allergic lung inflammatory cell egression and increased susceptibility to asphyxiation in MMP2-deficiency. Nat Immunol. 2002;3(4):347-53.

64. Fletcher CM, Pride NB. Definitions of emphysema, chronic bronchitis, asthma, and airflow obstruction: 25 years on from the Ciba symposium. Thorax. 1984;39(2):81-5.

65. Cosio MG, Guerassimov A. Chronic Obstructive Pulmonary Disease . Inflammation of Small Airways and Lung Parenchyma. Am J Respir Crit Care Med. 1999;160(5):S21-5.

66. Barnes PJ, Cosio MG. Characterization of T Lymphocytes in Chronic Obstructive Pulmonary Disease. PLoS Med. 2004;1(1):e20.

67. Saetta M, DiStefano A, Facchini FM, Corbino L, Turato G, Mapp CE, et al. CD8+ T-Lymphocytes in Peripheral Airways of Smokers with Chronic Obstructive Pulmonary Disease. Am J Respir Crit Care Med. 1998;157(3):822-6.

68. Saetta M, Baraldo S, Corbino L, Turato G, Braccioni F, Rea F, et al. CD8+ Cells in the Lungs of Smokers with Chronic Obstructive Pulmonary Disease. Am J Respir Crit Care Med. 1999;160(2):711-7.

69. Lee S-H, Goswami S, Grudo A, Song L-z, Bandi V, Goodnight-White S, et al. Antielastin autoimmunity in tobacco smoking-induced emphysema. Nat Med. 2007;13(5):567-9.

70. Gueders MM, Foidart J-M, Noel A, Cataldo DD. Matrix metalloproteinases (MMPs) and tissue inhibitors of MMPs in the respiratory tract: Potential implications in asthma and other lung diseases. European Journal of Pharmacology. 2006;533(1-3):133-44.

71. Segura-Valdez L, Pardo A, Gaxiola M, Uhal BD, Becerril C, Selman M. Upregulation of gelatinases A and B, collagenases 1 and 2, and increased parenchymal cell death in COPD. Chest. 2000;117(3):684-94.

72. Maisi P, Sorsa T, Raulo SM, Prikk K, Sepper R, McGorum B, et al. INCREASED MATRIX METALLOPROTEINASE (MMP)-9 IN THE AIRWAY AFTER ALLERGEN CHALLENGE. Am J Respir Crit Care Med. 2001;164(9):1740a-1.

73. Mautino G, Henriquet C, Jaffuel D, Bousquet J, Capony F. Tissue Inhibitor of Metalloproteinase-1 Levels in Bronchoalveolar Lavage Fluid from Asthmatic Subjects. Am J Respir Crit Care Med. 1999;160(1):324-30.

74. Ratjen F, Döring G. Cystic fibrosis. The Lancet. 2003;361(9358):681-9.

75. Michael W. Konstan, Melvin Berger. Current understanding of the inflammatory process in cystic fibrosis: Onset and etiology. Pediatric Pulmonology. 1997;24(2):137-42.

76. Ratjen F, Hartog CM, Paul K, Wermelt J, Braun J. Matrix metalloproteases in BAL fluid of patients with cystic fibrosis and their modulation by treatment with dornase alpha. Thorax. 2002;57(11):930-4.

77. Scott D. Sagel, Robert K. Kapsner, Iris Osberg. Induced sputum matrix metalloproteinase-9 correlates with lung function and airway inflammation in children with cystic fibrosis. Pediatric Pulmonology. 2005;39(3):224-32.

78. Crouch E. Pathobiology of pulmonary fibrosis. Am J Physiol Lung Cell Mol Physiol. 1990;259(4):L159-84.

79. Katzenstein AL, Myers JL. Idiopathic pulmonary fibrosis clinical relevance of pathologic classification. Am J Respir Crit Care Med. 1998;157:1301-15.

80. Marimoto DY, Kim H, Oyabu T, Hirohashi M, Nagatomo H, Ogami A, et al. Effect of Long-Term Inhalation of Toner on Extracellular Matrix in the Lungs of Rats In Vivo. Inhalation Toxicology. 2005;17(3):153-9.

81. Yaguchi T, Fukuda Y, Ishizaki M, Yamanaka N. Immunohistochemical and gelatin zymography studies for matrix metalloproteinases in bleomycin-induced pulmonary fibrosis. Pathol Int. 1998;48:954-63.

82. Swiderski R, Dencoff J, Floerchinger C, Shapiro S, Hunninghake G. Differential expression of extracellular matrix remodeling genes in a murine model of bleomycin-induced pulmonary fibrosis. Am J Pathol. 1998;152:821-8.

83. Kim JY, Choeng HC, Ahn C, Cho SH. Early and Late Changes of MMP-2 and MMP-9 in Bleomycin-Induced Pulmonary Fibrosis. Yonsei Medical Journal. 2009;50(1):68 - 77.

84. Manoury B, Nenan S, Leclerc O, Guenon I, Boichot E, Planquois J-M, et al. The absence of reactive oxygen species production protects mice against bleomycin-induced pulmonary fibrosis. Respiratory Research. 2005;6(1):11.

85. Trulock E, Edwards L, Taylor D, et al. The Registry of the International Society for Heart and Lung Transplantation: Twentieth official adult lung and heart-lung transplant report 2003. J Heart Lung Transplant 2003;22:625-35.

86. Trello CA, Williams DA, Keller CA, Crim C, Webster RO, Ohar JA. Increased Gelatinolytic Activity in Bronchoalveolar Lavage Fluid in Stable Lung Transplant Recipient. Am J Respir Crit Care Med. 1997;156:1978-86.

87. Boehler A, Estenne M. Post-transplant bronchiolitis obliterans. Eur Repir J 2003;22:1007-18.

88. Boehler A, Kesten S, Weder W, Speich R. Bronchiolitis Obliterans after lung transplantation. Chest 1998;114:1411.

89. Boehler A KS, Weder W, Speich R. . Bronchiolitis Obliterans after lung transplantation. Chest 1998;114:1411.

90. Mamessier E, Milhe F, Badier M, Thomas P, Magnan A, Reynaud-Gaubert M. Comparison of Induced Sputum and Bronchoalveolar Lavage in Lung Transplant Recipients. The Journal of Heart and Lung Transplantation. 2006;25(5):523-32.

91. Boehler A EM. Post-transplant bronchiolitis obliterans. . Eur Repir J 2003;22:1007-18.

92. Soccal PM, Gasche Y, Miniati DN, Hoyt G, Berry GJ, Doyle RL, et al. Matrix metalloproteinase inhibition decreases ischemia-reperfusion injury after lung transplantation. American Journal of Transplantation. 2004 Jan;4(1):41-50.

93. Yoshida S, Iwata T, Chiyo M, Smith GN, Foresman BH, Mickler EA, et al. Metalloproteinase Inhibition Has Differential Effects on Alloimmunity, Autoimmunity, and Histopathology in the Transplanted Lung. Transplantation. 2007;83(6):799-808.

94. Trello CA WD, Keller CA, Crim C, Webster RO, Ohar JA. . Increased Gelatinolytic Activity in Bronchoalveolar Lavage Fluid in Stable Lung Transplant Recipient. . Am J Respir Crit Care Med. 1997;156:1978-86.

95. Campbell LG, Ramachandran S, Liu W, Shipley JM, Itohara S, Rogers JG, et al. Different Roles for Matrix Metalloproteinase-2 and Matrix Metalloproteinase-9 in the Pathogenesis of Cardiac Allograft Rejection. American Journal of Transplantation. 2005;5(3):517-28.

96. Iwata T, Chiyo M, Yoshida S, Smith GNJ, Mickler EA, Presson RJ, et al. Lung Transplant Ischemia Reperfusion Injury: Metalloprotease Inhibition Down-regulates Exposure of Type V Collagen, Growth-Related Oncogene-Induced Neutrophil Chemotaxis, and Tumor Necrosis Factor-[alpha] Expression. Transplantation. 2008;85(3):417-26.

97. Fernandez FG, Campbell LG, Liu W, Shipley JM, Itohara S, Patterson GA, et al. Inhibition of obliterative airway disease development in murine tracheal allografts by matrix metalloproteinase-9 deficiency. American Journal of Transplantation. 2005 Apr;5(4 Pt 1):671-83.

98. Luo D, Mari B, Stoll I, Anglard P. Alternative splicing and promoter usage generates an intracellular stromelysin-3 isoform directly translated as an active matrix metalloproteinase. J Biol Chem. 2002:M202494200.

99. Kwan JA, Schulze CJ, Wang W, Leon H, Sariahmetoglu M, Sung M, et al. Matrix metalloproteinase-2 (MMP-2) is present in the nucleus of cardiac myocytes and is capable of cleaving poly (ADP-ribose) polymerase PARP in vitro. FASEB J. 2004:02-1202fje.

100. Si-Tayeb K, Monvoisin A, Mazzocco C, Lepreux S, Decossas M, Cubel G, et al. Matrix Metalloproteinase 3 Is Present in the Cell Nucleus and Is Involved in Apoptosis. Am J Pathol. 2006;169(4):1390-401.

101. Shilling RA, Clay BS, Tesciuba AG, Berry EL, Lu T, Moore TV, et al. CD28 and ICOS play complementary non-overlapping roles in the development of Th2 immunity in vivo. Cellular Immunology.In Press, Corrected Proof.

102. Graesser D, Mahooti S, Madri JA. Distinct roles for matrix metalloproteinase-2 and [alpha]4 integrin in autoimmune T cell extravasation and residency in brain parenchyma during experimental autoimmune encephalomyelitis. Journal of Neuroimmunology. 2000;109(2):121-31.

103. Dell'Agli M, Galli GV, Bosisio E, D'Ambrosio M. Inhibition of NF-kB and metalloproteinase-9 expression and secretion by parthenolide derivatives. Bioorganic & Medicinal Chemistry Letters. 2009;19(7):1858-60.

104. Miltenburg A, Lacraz S, Welgus H, Dayer J. Immobilized anti-CD3 antibody activates T cell clones to induce the production of interstitial collagenase, but not tissue inhibitor of metalloproteinases, in monocytic THP-1 cells and dermal fibroblasts. J Immunol. 1995;154(6):2655-67.

105. Leppert D, Waubant E, Galardy R, Bunnett N, Hauser S. T cell gelatinases mediate basement membrane transmigration in vitro. J Immunol. 1995;154(9):4379-89.

106. Yoshida S, Iwata T, Chiyo M, Smith GN, Foresman BH, Mickler EA, et al. Metalloproteinase Inhibition Has Differential Effects on Alloimmunity, Autoimmunity, and Histopathology in the Transplanted Lung. Transplantation. 2007 Mar;83(6):799-808.

107. Sandler C, Ekokoski E, Lindstedt KA, Vainio PJ, Finel M, Sorsa T, et al. Chemically modified tetracycline (CMT)-3 inhibits histamine release and cytokine production in mast cells: possible involvement of protein kinase C. Inflammation Research. 2005 Jul;54(7):304-12.

108. Hall SR, Rhodes J. Schiff base-mediated co-stimulation primes the T-cell-receptor-dependent calcium signalling pathway in CD4 T cells. Immunology. 2001;104(1):50-7.

109. Zitt C, Strauss B, Schwarz EC, Spaeth N, Rast G, Hatzelmann A, et al. Potent Inhibition of Ca2+ Release-activated Ca2+ Channels and T-lymphocyte Activation by the Pyrazole Derivative BTP2. J Biol Chem. 2004;279(13):12427-37.

110. Rosen LB, Ginty DD, Weber MJ, Greenberg ME. Membrane depolarization and calcium influx stimulate MEK and MAP kinase via activation of Ras. Neuron. 1994;12(6):1207-21.

111. Yoshida H, Nishina H, Takimoto H, Marengère LEM, Wakeham AC, Bouchard D, et al. The Transcription Factor NF-ATc1 Regulates Lymphocyte Proliferation and Th2 Cytokine Production. Immunity. 1998;8(1):115-24.

112. Schuh K, Twardzik T, Kneitz B, Heyer J, Schimpl A, Serfling E. The Interleukin 2 Receptor alpha Chain/CD25 Promoter Is a Target for Nuclear Factor of Activated T Cells. J Exp Med. 1998;188(7):1369-73.

113. Rao A. L, C. and Hogan,P.G. Transcription factors of the NFAT family: regulation and function. Annual Review of Immunology

1997;15:707-47.

114. Thornton AM, Shevach EM. CD4+CD25+ Immunoregulatory T Cells Suppress Polyclonal T Cell Activation In Vitro by Inhibiting Interleukin 2 Production. J Exp Med. 1998;188(2):287-96.

115. Schubert LA, Jeffery E, Zhang Y, Ramsdell F, Ziegler SF. Scurfin (FOXP3) Acts as a Repressor of Transcription and Regulates T Cell Activation. J Biol Chem. 2001;276(40):37672-9.

116. Ye J, Ortaldo J, Conlon K, Winkler-Pickett R, Young H. Cellular and molecular mechanisms of IFN-gamma production induced by IL-2 and IL-12 in a human NK cell line. J Leukoc Biol. 1995;58(2):225-33.

117. Scheurich P, Thoma B, Ucer U, Pfizenmaier K. Immunoregulatory activity of recombinant human tumor necrosis factor (TNF)-alpha: induction of TNF receptors on human T cells and TNF-alpha- mediated enhancement of T cell responses. J Immunol. 1987;138(6):1786-90.

118. Schroder K, Hertzog PJ, Ravasi T, Hume DA. Interferon-{gamma}: an overview of signals, mechanisms and functions. J Leukoc Biol. 2004;75(2):163-89.

119. Irie-Sasaki J, Sasaki T, Penninger JM. CD45 Regulated Signaling Pathways. Current Topics in Medicinal Chemistry. 2003;3:783-96.

120. Feng C, Woodside KJ, Vance BA, El-Khoury D, Canelles M, Lee J, et al. A potential role for CD69 in thymocyte emigration. Int Immunol. 2002;14(6):535-44.

121. Stauber DJ, Debler EW, Horton PA, Smith KA, Wilson IA. Crystal structure of the IL-2 signaling complex: Paradigm for a heterotrimeric cytokine receptor. Proceedings of the National Academy of Sciences of the United States of America. 2006;103(8):2788-93.

122. Leo E, Welsh K, Matsuzawa S-i, Zapata JM, Kitada S, Mitchell RS, et al. Differential Requirements for Tumor Necrosis Factor Receptor-associated Factor Family Proteins in CD40-mediated Induction of NF-kappa B and Jun N-terminal Kinase Activation. J Biol Chem. 1999;274(32):22414-22.

123. Bourguignon LYW, Zhu H, Shao L, Chen Y-W. CD44 Interaction with c-Src Kinase Promotes Cortactin-mediated Cytoskeleton Function and Hyaluronic Acid-dependent Ovarian Tumor Cell Migration. J Biol Chem. 2001;276(10):7327-36.

124. Baroja ML, Vijayakrishnan L, Bettelli E, Darlington PJ, Chau TA, Ling V, et al. Inhibition of CTLA-4 Function by the Regulatory Subunit of Serine/Threonine Phosphatase 2A. J Immunol. 2002;168(10):5070-8.

125. Ivetic A, Ridley AJ. The telling tail of L-selectin. Biochem Soc Trans. 2004;32(Pt 6):1118-21.

126. Medoff BD, Seung E, Wain JC, Means TK, Campanella GSV, Islam SA, et al. BLT1-mediated T cell trafficking is critical for rejection and obliterative bronchiolitis after lung transplantation. J Exp Med. 2005;202(1):97-110.

127. Stripp B, Sawaya P, Luse D, Wikenheiser K, Wert S, Huffman J, et al. cis-acting elements that confer lung epithelial cell expression of the CC10 gene. J Biol Chem. 1992;267(21):14703-12.

128. Carbone F, Bevan M. Induction of ovalbumin-specific cytotoxic T cells by in vivo peptide immunization. J Exp Med. 1989;169(3):603-12.

129. Montgomery AM SH, Reisfeld RA. . Production and regulation of gelatinase B by human T-cells. Biochimica et biophysica acta. 1993;1176(3):265-8.

130. Weeks BS, Schnaper HW, Handy M, Holloway E, Kleinman HK. Human T lymphocytes synthesize the 92 kDa type IV collagenase (gelatinase B). Journal of Cellular Physiology. 1993;157(3):644-9.

131. Zhou H, Bernhard EJ, Fox FE, Billings PC. Induction of metalloproteinase activity in human T-lymphocytes. Biochimica et Biophysica Acta (BBA) - Molecular Cell Research. 1993;1177(2):174-8.

132. Owen JL, Iragavarapu-Charyulu V, Gunja-Smith Z, Herbert LM, Grosso JF, Lopez DM. Up-Regulation of Matrix Metalloproteinase-9 in T Lymphocytes of Mammary Tumor Bearers: Role of Vascular Endothelial Growth Factor. J Immunol. 2003;171(8):4340-51.

133. Kruger A, Arlt MJE, Gerg M, Kopitz C, Bernardo MM, Chang M, et al. Antimetastatic Activity of a Novel Mechanism-Based Gelatinase Inhibitor. Cancer Res. 2005;65(9):3523-6.

134. He Z, Wang T, Huang Z, Zou Z, Chen X. Abstract 2058 Expression of Brain MMP9 in a Rat Model of Cardiopulmonary Resuscitation Treated with SB3CT. Circulation. 2008;118(18 MeetingAbstracts):S665.

135. Yu F, Kamada H, Niizuma K, Endo H, Chan PH. Induction of MMP-9 Expression and Endothelial Injury by Oxidative Stress after Spinal Cord Injury. Journal of Neurotrauma. 2008;25(3):184-95.

136. Uitto V-J, Firth JD, Nip L, Golub LM. Doxycycline and Chemically Modified Tetracyclines Inhibit Gelatinase A (MMP-2) Gene Expression in Human Skin Keratinocytes. Annals of the New York Academy of Sciences. 1994;732(Inhibition of Matrix Metalloproteinases: Therapeutic Potential):140-51.

137. Benbow U, Brinckerhoff CE. The AP-1 site and MMP gene regulation: What is all the fuss about? Matrix Biology. 1997;15(8-9):519-26.

138. Kelly KE, Hertz MI, Mueller DL. T-Cell and Major Histocompatibility Complex Requirements for Obliterative Airway Disease in Heterotopically Transplanted Murine Tracheas1. Transplantation. 1998;66(6):764-71.

139. Neuringer IP, Walsh SP, Mannon RB, Gabriel S, Aris RM. Enhanced T cell cytokine gene expression in mouse airway obliterative bronchiolitis. Transplantation. 2000;69(3):399-405.

140. Neuringer IP, Mannon RB, Coffman TM, Parsons M, Burns K, Yankaskas JR, et al. Immune Cells in a Mouse Airway Model of Obliterative Bronchiolitis. Am J Respir Cell Mol Biol. 1998;19(3):379-86.

141. Denny MF, Patai B, Straus DB. Differential T-Cell Antigen Receptor Signaling Mediated by the Src Family Kinases Lck and Fyn. Mol Cell Biol. 2000;20(4):1426-35.

142. Kim H-P, Leonard WJ. The basis for TCR-mediated regulation of the IL-2 receptor α chain gene: role of widely separated regulatory elements. The EMBO Journal. 2002;21(12):3051-9.

143. Grundstrom S, Dohlsten M, Sundstedt A. IL-2 Unresponsiveness in Anergic CD4+ T Cells Is Due to Defective Signaling Through the Common {gamma}-Chain of the IL-2 Receptor. J Immunol. 2000;164(3):1175-84.

144. Chen C, Rowell EA, Thomas RM, Hancock WW, Wells AD. Transcriptional Regulation by Foxp3 Is Associated with Direct Promoter Occupancy and Modulation of Histone Acetylation. J Biol Chem. 2006;281(48):36828-34.

145. Marson A, Kretschmer K, Frampton GM, Jacobsen ES, Polansky JK, MacIsaac KD, et al. Foxp3 occupancy and regulation of key target genes during T-cell stimulation. Nature. 2007;445(7130):931-5.

146. Lee S-M, Gao B, Fang D. FoxP3 maintains Treg unresponsiveness by selectively inhibiting the promoter DNA-binding activity of AP-1. Blood. 2008;111(7):3599-606.

147. Zuo X-J, Matsumura Y, Prehn J, Saito R, Marchevesky A, Matloff J, et al. Cytokine gene expression in rejecting and tolerant rat lung allograft models: analysis by RT-PCR. Transplant Immunology. 1995;3(2):151-61.

148. Boehler A, Bai Xao H, Liu M, Cassivi S, Chamberlain D, Slutsky Arthur S, et al. Upregulation of T-Helper 1 Cytokines and Chemokine Expression in Post-transplant Airway Obliteration. Am J Respir Crit Care Med. 1999;159(6):1910-7.

149. Abraham M, Shapiro S, Karni A, Weiner HL, Miller A. Gelatinases (MMP-2 and MMP-9) are preferentially expressed by Th1 vs. Th2 cells. Journal of Neuroimmunology. 2005;163(1-2):157-64.

150. Kaplan MH, Sun Y-L, Hoey T, Grusby MJ. Impaired IL-12 responses and enhanced development of Th2 cells in Stat4-deficient mice. Nature. 1996;382(6587):174-7.

151. Szabo SJ, Sullivan BM, Peng SL, Glimcher LH. Moleular Mechanisms Regulating Th1 Immune Responses. Annual Review of Immunology. 2003;21(1):713-58.

152. Lighvani AA, Frucht DM, Jankovic D, Yamane H, Aliberti J, Hissong BD, et al. T-bet is rapidly induced by interferon-Î³ in lymphoid and myeloid cells. Proceedings of the National Academy of Sciences of the United States of America. 2001;98(26):15137-42.

153. Afkarian M, Sedy JR, Yang J, Jacobson NG, Cereb N, Yang SY, et al. T-bet is a STAT1-induced regulator of IL-12R expression in naive CD4+ T cells. Nat Immunol. 2002;3(6):549-57.

154. Mullen AC, High FA, Hutchins AS, Lee HW, Villarino AV, Livingston DM, et al. Role of T-bet in Commitment of TH1 Cells Before IL-12-Dependent Selection. Science. 2001;292(5523):1907-10.

155. Hughes CE, Caterson B, Fosang AJ, Roughley PJ, Mort JS. Monoclonal antibodies that specifically recognize neoepitope sequences generated by 'aggrecanase' and matrix metalloproteinase cleavage of aggrecan: application to catabolism in situ and in vitro. Biochem J. 1995 305(3):799-804.

CURRICULUM VITAE

Heather Lynette Benson

Education

8/1998-12/2002	B.S.	Interdisciplinary Social Science of Health Studies concentration- Anthropology Michigan State University, E. Lansing, MI
8/2003-5/2005	M.S.	Medical Sciences Indiana University, Indianapolis, IN
8/2005-10/2009	Ph.D.	Biochemistry and Molecular Biology Indiana University, Indianapolis, IN

Employment History

1997-1998	Medical Records Auditor. Perspectives of Troy P.C. Troy, MI
1999-2002	Veterinary Assistant. Mason Veterinary Clinic. Mason, MI
2001-2003	Laboratory Assistant, Department of Physiology, Michigan State University, E. Lansing, MI

Academic Experience

1999	Summer Research Assistantship. Minority Education Program (MMEP). Loyola University Chicago Stritch School of Medicine. Chicago, IL
2000	Summer Research Assistantship. Short Term Training Program for Minority Students in Biomedical Research (T-35). Indiana University School of Medicine. Indianapolis, IN
2001	Research Assistantship. Ronald E. McNair Post-Baccalaureate Achievement Program Michigan State University, E. Lansing, MI
2001	Summer Research Assistantship. Committee on Institutional Cooperation (CIC)/ Summer Research Opportunity (SROP). Michigan State University. E. Lansing, MI

2004 Summer Research Assistantship. Short Term Training Program for Minority Students in Biomedical Research (T-35). Indiana University School of Medicine. Indianapolis, IN

2005 Graduate Student Research Assistant, Department of Biochemistry and Molecular Biology, Indiana University School of Medicine. Indianapolis, IN

Society/Professional Memberships

2003-present Student National Medical Association
2005-present American Association for Cancer Research (AARC)
2007-present American Association of Immunologists (AAI)

Academic and Professional Honors

2000 Diffuse Microvascular Injury of the Lung: Therapeutic Intervention Using Infusion of Vascular Endothelial Cells. Indiana University School of Medicine. P.I. Dr. William Martin. July 2000. Poster Presentation

2001 Influence of Norepinephrine on Apopotosis of Lung Alveolar Epithelial Cells in Vivo. Merit Award. Undergraduate Research and Arts Forum. Michigan State University. Department of Physiology. P.I. Dr. Bruce Uhal. February 2001. Poster Presentation.

2003 Apoptosis-dependent acute lung injury and repair after intratracheal instillation of noradrenaline in rats. University of Wisconsin-Madison. P.I. Dr. Bruce Uhal. April 2003. Oral Presentation.

2004 The Role of Periostin in Bone Growth and Development. Indiana University School of Medicine Department of Anatomy and Cell Biology. P.I. Dr. Janet Hock. June 2004. Poster Presentation.

2005 Grr1-Dependent Ubiquitination and Regulation of Endocytic Trafficking in S. Cerevisae. Annual Biomedical Research Conference for Minority Students. Atlanta, GA P.I. Dr Mark Goebl. September 2005. Poster Presentation.

2006 Different Roles for Matrix Metalloproteinase-2 and Matrix Metalloproteinase-9 in the Pathogenesis of Cardiac Allograft Rejection. *American Journal of Transplantation*. 2005. 5:3 517-528. Indiana University School of Medicine. P.I. Dr. David Wilkes. March 2006. Oral Presentation.

2006 Role of Matrix Metalloproteinases in the Dendritic Cell-Induced T Cell Activation. Indiana University School of Medicine. Department of Biochemistry and Molecular Biology. P.I. Dr. David Wilkes. October 2006. Poster Presentation.

2007 Matrix Metalloproteinase 3 is Present in the Cell Nucleus and is Involved in Apoptosis. American Journal of Pathology. 2006;169:1390-1401. Indiana University School of Medicine. P.I. Dr David Wilkes. February 2007. Oral Presentation.

2007 Harper Scholar Minority Fellowship Award. April 2007.

2007 Gordon Research Conference Travel Fellowship Award: Matrix Metalloproteinases. Ciacco, Italy. June 2007.

2007 Regulatory Role of Matrix Metalloproteinases in T Cell Activation. Poster Award. Indiana University School of Medicine. Department of Biochemistry and Molecular Biology. P.I. Dr. David Wilkes. September 2007. Poster Presentation

2007 Department of Biochemistry and Molecular Biology Student Representative. September 2007.

2008 Matrix Metalloproteinases Regulate Intracellular T cell Activation. ATS May 2008. ATS 2008 Toronto International Conference Program Booklet. P.I. Dr. David Wilkes. October 2008. Poster Presentation.

2008 Matrix Metalloproteinases Regulate Intracellular T cell Activation. Department of Biochemistry and Molecular Biology. P.I. Dr. David Wilkes. October 2008. Poster Presentation.

Publications

Yamada Y, Sekine Y, Yoshida S, Yasufuku K, Petrache I, **Benson HL**, Brand DD, Yoshino I, Wilkes DS. Type V collagen-induced oral tolerance plus low-dose cyclosporine prevents rejection of MHC class I and II incompatible lung allografts. J Immunol. 2009 Jul 1;183(1):237-45.

Li X, Zhuang J, **Rayford H**, Zhang H, Shu R, Uhal BD. Attenuation of bleomycin-induced pulmonary fibrosis by intratracheal administration of antisense oligonucleotides against angiotensinogen mRNA. Curr Pharm Des. 2007;13(12):1257-68.

Li X, **Rayford H**, Shu R, Zhuang J, Uhal BD. Essential role for cathepsin D in bleomycin-induced apoptosis of alveolar epithelial cells. Am J Physiol Lung Cell Mol Physiol. 2004 Jul;287(1):L46-51.

Li X, **Rayford H**, Uhal BD. Essential roles for angiotensin receptor AT1a in bleomycin-induced apoptosis and lung fibrosis in mice. Am J Pathol. 2003 Dec;163(6):2523-30.

Uhal BD, **Rayford H**, Zhuang J, Li X, Laukka J, Soledad-Conrad V. Apoptosis-dependent acute lung injury and repair after intratracheal instillation of noradrenaline in rats. Exp Physiol. 2003 Mar;88(2):269-75.

Published Abstracts

Matrix Metalloproteinases Regulate Intracellular T cell Activation. October 2008. Biochemistry Retreat Program Booklet. IndianaUniversity School of Medicine.

Matrix Metalloproteinases Regulate Intracellular T cell Activation. May 2008. ATS 2008 Toronto International Conference Program Booklet.

Regulatory Role of Matrix Metalloproteinases in T Cell Activation. September 2007. Biochemistry Retreat Program Booklet. Indiana University School of Medicine.

Grr1-Dependent Ubiquitination and Regulation of Endocytic Trafficking in S. Cerevisae. September 2005 Annual Biomedical Research Conference for Minority Students Program Booklet.

The Role of Periostin in Bone Growth and Development. June 2004. Indiana University School of Medicine. T-35 Program Booklet.

Influence of Norepinephrine on Apopotosis of Lung Alveolar Epithelial Cells in Vivo. July 2002. Committee on Institutional Cooperation (CIC) Conference Program Booklet. Ohio State University.

Influence of Norepinephrine on Apopotosis of Lung Alveolar Epithelial Cells in Vivo. February 2002. The McNair/SROP Scholars 2001 Research Abstracts Booklet.

Apoptosis-dependent Acute Lung Injury. February 2001. Committee on Institutional Cooperation (CIC)
Conference Program Booklet. Ohio State University.

Diffuse Microvascular Injury of the Lung: Therapeutic Intervention Using Infusion of Vascular Endothelial Cells. July 2000. University Undergraduate Research and Arts Forum Program Booklet. Michigan State University.

Diffuse Microvascular Injury of the Lung: Therapeutic Intervention Using Infusion of Vascular Endothelial Cells. July 2000. Indiana University School of Medicine. T-35 Program Booklet.

Research Support

NIH NIGMS R25. Edwin T Harper Scholar Fellowship. Hal Broxmeyer. 2006-current. Indiana University Initiative for Maximizing Graduate Student Diversity. David S Wilkes PI. Regulatory Role of Matrix Metalloproteinases in T cell Activation.

HL07802. David S. Wilkes PI. 2004. T35M – NIH-funded Short Term Training for Minority Students. Janet M Hock. The Role of Periostin in Bone Growth and Development.

Am Heart Assoc Grant-In-Aid 250269N. Bruce D Uhal PI. 2001-2003. Roles of Apoptosis and Renin-Angiotensin System on Amiodarone Toxicity.

PHS HL-45136. Bruce D. Uhal PI. 2001-2003. Control of Type II Pneumocyte Proliferation.

HL07802. David S. Wilkes PI. 2000. T35M – NIH-funded Short Term Training for Minority Students. William J. Martin. Diffuse Microvascular Injury of the Lung: Therapeutic Intervention Using Infusion of Vascular Endothelial Cells.